

Department of Mechanical Engineering

**ASSESSMENT OF SEASONAL PERFORMANCES OF AIR SOURCE
CO₂ HEAT PUMP BY DYNAMIC MODELLING**

Author: ROMAIN PETINOT

Supervisor: Paul Tuohy

A thesis submitted in partial fulfilment for the requirement of the degree

Master of Science

Sustainable Energy: Renewable Energy Systems and the Environment

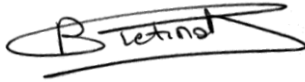
2011

COPYRIGHT DECLARATION

This thesis is the result of the author's original research. It has been composed by the author and has not been previously submitted for examination which has led to the award of a degree.

The copyright of this thesis belongs to the author under the terms of the United Kingdom Copyright Acts as qualified by University of Strathclyde Regulation 3.50. Due acknowledgement must always be made of the use of any material contained in, or derived from, this thesis.

Signed:

A handwritten signature in black ink, consisting of a stylized 'B' followed by the name 'Letford' in a cursive script. The signature is enclosed within a hand-drawn oval shape.

Date: 09/09/2011

ABSTRACT

In order to meet the UK objectives in terms of CO₂ emission reduction, air source heat pumps offer today a promising alternative to conventional systems in order to provide space heating and domestic hot water. However their performances are largely dependent on their environment of operation with important variations from one installation to another. Today in order to be competitive with gas boilers in terms of CO₂ emissions, heat pumps must reach a seasonal performance factor of 2.45. But another environmental impact comes from the leakage of refrigerant gas which can represent from 10 to 20% of the total footprint of the heat pump according to the literature. To cope with this problem, it is possible to use natural refrigerants such as CO₂ but there are still questions about their efficiency.

A group project was realized from February to April 2011 and gathered a lot of data on a new type of CO₂ heat pump which arrived on the UK market a few years ago. The objective was to monitor the systems on real installations in order to get an idea of their actual performances. However the assessment was only carried out over one week of monitoring while the performances throughout the year can vary significantly.

The objective of this project is therefore to develop a dynamic model of a CO₂ heat pump with the data collected from the previous project in order to estimate the seasonal performances of a CO₂ heat pump.

An extensive analysis of the data available on the system was carried out in order to characterize the system behaviour properly. Then, as the focus of the project is not on the thermodynamic cycle of the heat pump but on its operation in a particular environment, a relatively simple model type black box was developed. ESP-r, the integrated energy modelling tool developed at Strathclyde University, was used as the environment of development. It provides the required functionalities to model building and heating systems in different climates.

A model of heat pump had already been implemented in ESP-r by Kelly [1]. If the structure is to be kept, important modifications had to be made to match the case of the CO₂ heat pump. The new equations representing the behaviour of the system were implemented with a new way of modelling the defrost cycles by considering the relative humidity of the outside air. After testing the new heat pump model, it replaced the old component in a complete model developed by Kelly including radiators. It was then shown that the high return water temperature to the CO₂ heat pump penalized its operation.

A whole model, simulating an installation in Oban was then built. It includes a stratified tank designed for the operation of the CO₂ heat pump. After validating the model behaviour against the monitored data collected for the months of March and July, the model was simulated over the whole year. The results then give a seasonal performance factor of 2.15 for the whole system which is in the range of the performances of air source heat pumps in the UK. However this system was not fully optimised and by modifying the structure of the tank and the energy used for the controls, it is shown that the seasonal performance factor can be increased up to 2.54. Being a new technology, this last result highlights that there is a real potential for these system and still some room for improvement.

Acknowledgements

I would particularly like to thank my supervisor, Paul Tuohy, for his advice and support which helped me to go through with this project. In addition, thanks also to Nick Kelly and Aizaz Samuel for their help on the more technical part in ESP-r.

I also want to thank Steven Fortieth, Peter Hamilton and George Russel who allowed me to monitor the different installations in Scotland and provide me with the information that I needed. I also thank Tomi Hakari from Finland who provided me with an incredible amount of data on his installation and who brought a serious contribution to this project.

Finally I want to thank my colleagues from the master for their support in order to go through with this thesis as well as my family.

TABLE OF CONTENTS

COPYRIGHT DECLARATION	2
ABSTRACT	3
ACKNOWLEDGEMENTS.....	5
TABLE OF CONTENTS	6
LIST OF FIGURES.....	8
LIST OF TABLES.....	11
1 INTRODUCTION.....	12
2 LITERATURE REVIEW	15
2.1 AIR SOURCE HEAT PUMP PERFORMANCES	15
2.1.1 <i>Actual heat pump performances.....</i>	15
2.1.2 <i>Required SPF's to be competitive with gas boiler.....</i>	17
2.1.3 <i>Estimation of the SPF (Seasonal Performance Factor)</i>	18
2.2 REFRIGERANT ENVIRONMENTAL IMPACT	19
2.2.1 <i>More and more accurate assessment of this impact</i>	19
2.2.2 <i>Solutions to offset the environmental impact of refrigerant.....</i>	20
2.3 CO₂ AIR SOURCE HEAT PUMP.....	21
2.3.1 <i>The CO₂ cycle specificities.....</i>	21
2.3.2 <i>The recent revival of CO₂ as a refrigerant</i>	23
2.3.3 <i>CO₂ heat pump performances</i>	23
2.4 THE SANYO ECO CUTE SYSTEM	24
2.4.1 <i>Presentation of the system.....</i>	24
2.4.2 <i>What is known about the system</i>	25
2.5 DEFROST CYCLES AND IMPACT ON HEAT PUMP PERFORMANCES	27
2.5.1 <i>Mechanism of frost formation</i>	27
2.5.2 <i>Defrost cycles and air source heat pumps.....</i>	29
2.5.3 <i>Defrost cycle in the Sanyo Heat pump.....</i>	30
3 OBJECTIVES AND METHODOLOGY.....	32
3.1 OBJECTIVES.....	32
3.2 METHODOLOGY	32
4 ANALYSIS OF THE DATA COLLECTED ON THE SANYO SYSTEM.....	34
4.1 ANALYSIS OF THE FINNISH DATA	34
4.1.1 <i>Performances of the Sanyo system</i>	34
4.1.2 <i>Study of the defrost cycle</i>	39
4.2 ANALYSIS OF THE DATA COLLECTED BY THE PREVIOUS GROUP PROJECT ON THE CO₂ HEAT PUMP.....	46
4.2.1 <i>Performances of the system</i>	46
4.2.2 <i>Time of ice formation before defrosting.....</i>	47
4.2.3 <i>Energy used for defrost</i>	48
4.2.4 <i>Electrical Power Consumption of the system</i>	48

4.3	ANALYSIS OF THE INSTALLATION IN OBAN	49
4.3.1	<i>House and system monitored.....</i>	50
4.3.2	<i>Summer monitoring</i>	51
4.3.3	<i>Heat pump operation in March.....</i>	52
4.3.4	<i>Heat pump operation in July</i>	53
5	MODEL OF THE CO₂ HEAT PUMP DEVELOPED IN ESP-R	55
5.1	PURPOSE OF THE MODEL AND COMPLEXITY REQUIRED.....	55
5.2	PRESENTATION OF THE MODEL AND MODIFICATION REQUIRED	56
5.2.1	<i>COP.....</i>	56
5.2.2	<i>Electrical input.....</i>	57
5.2.3	<i>Water mass flow and heat pump thermal inertia</i>	58
5.2.4	<i>Controls of the heat pump.....</i>	59
5.2.5	<i>Defrost cycles</i>	59
5.3	TEST OF THE OF THE CO₂ HEAT PUMP MODEL.....	60
6	COMPARISON WITH THE MODEL OF KELLY.....	67
6.1	DESCRIPTION OF THE MODEL.....	67
6.2	RESULTS OF THE SIMULATIONS.....	69
6.3	DISCUSSIONS.....	71
7	INTEGRATED MODEL OF THE CO₂ HEAT PUMP.....	72
7.1	MODEL OF THE SANYO SYSTEM	72
7.1.1	<i>Model of the Sanyo tank</i>	72
7.1.2	<i>Model realised in ESP-r.....</i>	74
7.1.3	<i>Comparison simulation and experimental data in March.....</i>	76
7.1.1	<i>Comparison simulation and experimental data in July</i>	80
7.2	ESTIMATION OF THE SEASONAL PERFORMANCE FACTOR FOR THE SANYO SYSTEM	81
7.3	DESIGN OF A NEW OPTIMIZED SYSTEM.....	82
8	CONCLUSION.....	83
9	FURTHER WORK	85
	APPENDIX A - EXTRA MONITORED DATA.....	86
	APPENDIX B - PLAN HOUSE IN OBAN.....	87
	APPENDIX C - BUILDING MODEL.....	88
	APPENDIX D - SANYO TANK	92
	APPENDIX E - PLANT FILE MODEL SANYO SYSTEM	93
	BIBLIOGRAPHY	98

LIST OF FIGURES

fig. 1 - Final energy consumption by sector in the UK, 2010 [1]	12
fig. 2 - Domestic Final Energy consumption by end use in the UK, 2009 [1].....	12
fig. 3 - Domestic energy consumption by fuel in the UK between 1970 and 2010 [1]	13
fig. 4 - Air source heat pump powered by renewable sources	13
fig. 5 - Seasonal Performance Factor of the UK field Trial [5]	16
fig. 6 - Comparison CO ₂ emission per unit of heat	17
fig. 7 - Comparison price per unit of heat	17
fig. 8 - Ozone Depletion Potential (ODP) of common refrigerants[16]	19
fig. 9 - Greenhouse Warming Potential (GWP) of common refrigerants [16].....	19
fig. 10 - Footprint and refrigerant contribution with different leak rates [19]	20
fig. 11 - Principle of the transcritical CO ₂	22
fig. 12 - Basic components of the CO ₂ cycle	22
fig. 13 - Illustration of the heat rejection process in the gas cooler for domestic hot water (on the left, high side pressure 10MPa) and for low temperature space heating (on the right, high side pressure 8.5MPa) [21]	22
fig. 14 - The Sanyo Eco-Cute System adapted for the European Market[31]	24
fig. 15 - First Sanyo tank design	26
fig. 16 - Design proposed in the KTH report [33]	26
fig. 17 - Last version of the Sanyo system design.....	26
fig. 18 - Last version of the Sanyo tank design.....	26
fig. 19 - First version of the Sanyo Eco Cute system with heat pump of 4.5kW	27
fig. 20 - Second version of the Sanyo Eco Cute system with heat pump of 9kW.....	27
fig. 21 - Analysis on the frost formation on the pipe on a psychometric chart	28
fig. 22 - Frost thickness and frost thickness growth rate with frosting time under different conditions [41]	29
fig. 23 - Comparison of frost accumulation mass and frost thickness after 35 min operating [41].....	29
fig. 24 - Experimental data used by the previous group project [32] for the regression of the COP	35
fig. 25 - Comparison of the COP calculated with the initial regression and the data from the Finnish installation (27/04/2011)	35
fig. 26 - Comparison of the COP calculated with the initial regression and the data from the Finnish installation (24/04/2011)	36
fig. 27 - Experimental data used for the new regression with 2 extra points considered	36
fig. 28 - Comparison of the COP calculated with the new regression and the data from the Finnish installation (27/04/2011)	37
fig. 29 - Comparison of experimental COP with the calculated one when the system start and after a defrost cycle.....	38
fig. 30 - Comparison of experimental COP at the start of the heat pump after a period of inactivity and after a defrost cycle	38

fig. 31 - Location of the weather station from which the relative humidity data was collected	39
fig. 32 - Graph of the data collected from the Finnish installation on the 9 th and 10 th of February 2010	40
fig. 33 - Graph of the data collected from the Finnish installation on 12th of October 2010.....	41
fig. 34 - Graph of the data collected from the Finnish installation on 16th of March 2010	41
fig. 35 - Graph of the data collected from the Finnish installation on the 22nd of April 2011	41
fig. 36 - Graph of the data collected from the Finnish installation on 26th of April 2011	42
fig. 37 - Time of frost formation in function of the mean outside temperature.....	42
fig. 38 - Time of frost formation in function of the mean relative humidity.....	43
fig. 39 - Energy used for defrost cycles in function of the mean outside temperature during the ice formation	44
fig. 40 - Energy used for the Defrost in function of the ice of frost formation	45
fig. 41 - Comparison of the dynamic fluctuations of the temperature at the outlet of the heat pump in Oban 9kW (left).....	46
fig. 42 - Noise on the relative humidity measurement during the previous project	47
fig. 43 - Comparison of the time of frost formation measured on the Scottish installations with the estimation made with the previous regression	47
fig. 44 - Energy required for the defrost cycles in function of the time of ice formation	48
fig. 45 - Variation of the electrical consumption of the heat pump in function of the outside temperature	49
fig. 46 - House monitored in Oban.....	50
fig. 47- The Sanyo CO ₂ heat pump in Oban.....	50
fig. 48 - Monitoring kit used for the project.....	51
fig. 49 - Main parameters of the heat pump operation in Oban the 18/03/2011	52
fig. 50 - Space heating and domestic hot water consumption in Oban the 18/03/2011.....	52
fig. 51 - Main parameters of the heat pump operation in Oban the 28/07/2011	53
fig. 52 - Domestic hot water draw in Oban the 28/07/2011.....	53
fig. 53 - Suggested road map for finding the required complexity of the sub-models based on the type of analysis[17].....	55
fig. 54 - Estimated COP in function of the outside temperature for different return water temperatures	57
fig. 55 - Schema of the plant used for the test of the model	61
fig. 56 - Model test: temperature at the inlet and outlet of the heat pump and electrical power consumption	61
fig. 57 - Model test: coefficient of performance of the heat pump in correlation with the return temperature and the outside air temperature	62
fig. 58 - Model Test: Defrost status of the heat pump in relation with the outside temperature and air humidity	62
fig. 59 - Model test: comparison of the heat pump start in the model (graph on the left) and in the monitored data(graph on the right)	63
fig. 60 - Energy used for the Defrost in function of the rate of ice formation (time-step 10secondes)	65
fig. 61 - Relative error on the COP induced by the change in the rate of Ice formation	65
fig. 62 - Schema of the house used in Kelly's Model.....	67

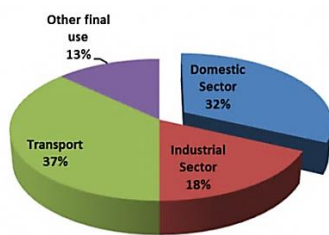
fig. 63 - Table of the U-values of the house model	67
fig. 64 - Schema of the heating system of the model of Dr Kelly	68
fig. 65 - Temperature at the inlet and outlet of the heat pump for the Kelly model (without the consideration of the defrost cycles)	69
fig. 66 – Temperature at the inlet and outlet of the heat pump for the new heat pump model (without the consideration of the defrost cycles)	69
fig. 67 - Comparison of the heat delivered in Kelly model and the CO ₂ model (without defrost cycle consideration).....	70
fig. 68 - Comparison of the COP for the simulation of the Kelly and CO ₂ model including or not defrost	70
fig. 69 - Schema of the Sanyo tank configuration (length given in millimetres)	72
fig. 70 - Schema of the plant used in ESP-r to model the Sanyo system for the Oban case-study	74
fig. 71 - Domestic hot water draw profile used in for the model of the Oban case study.....	75
fig. 72 - Comparison of the monitoring data 18/03/2011 and the model concerning the heat pump parameters	76
fig. 73 - Comparison of the monitoring data 18/03/2011 and the model concerning the heat pump parameters	77
fig. 74 - Comparison of the monitoring data 18/03/2011 and the model concerning the heat pump parameters	78
fig. 75 - Temperature distribution in the tank for the simulation.....	79
fig. 76 - Comparison of the monitoring data 18/03/2011 and the model concerning the heat pump parameters in July.....	80
fig. 77 - Heat pump power consumption in function of the water return temperature to the heat pump for the installations monitored in Scotland.....	86
fig. 78 - Heat pump power consumption in function of the water return temperature to the heat pump for the installations monitored in Scotland.....	86
fig. 79 - Plan of the House in Oban	87
fig. 80 - Schema of the house used in Kelly’s Model.....	88
fig. 81 - Different values used in the Models	88
fig. 82 - Casual gains for the living (top) and non-living (bottom) zone for the Average UK housing model.....	90
fig. 83 - Domestic hot water draw profile in the Kelly Model	91
fig. 84 - Detail schema of the Sanyo tank given by the manufacturer	92

LIST OF TABLES

table 1 - Comparison air source heat pump performance field test in UK, Germany and Switzerland [6].....	16
table 2 - Price and carbon content of the gas and the electricity in 2011 for the UK ([10] and [9]).....	17
table 3 - Critical temperature and pressure of commonly-used refrigerants [16].....	21
table 4 - Regression of the COP in function of the outside temperature and the water return temperature to the heat pump [32]	34
table 5 - New regression of the COP in function of the outside temperature and the water return temperature to the heat pump.....	37
table 6 - Regression of the time of frost formation in function of the relative humidity and the outside temperature	44
table 7 - Regression of the Energy used for the defrost in function of the outside temperature and the Time of ice formation	45
table 8 - Insulation characteristics in the case study in Oban.....	50
table 9 - Parameters used to represent the thermal inertia of the heat pump and the losses with the environment.....	57
table 10 - Table heat pump performance in the test simulation (time-step 10secondes)	63
table 11 - Table heat pump performance in the test simulation	64
table 12 - Controls with set points used in the Kelly model	68
table 13 - Parameters used for the model of the under floor heating system	75
table 14 - Summary of the controls used in the model of the Sanyo system	76
table 15 - Comparison of the energy used and produced for the simulation and the monitored data (one day of March)	80
table 16 - Comparison of the energy used and produced for the simulation and the monitored data (one day of July).....	81
table 17 - Distribution of the glazing area on the House in Oban.....	89
table 18 - U-values finally used in the simulation to model the house in Oban	89

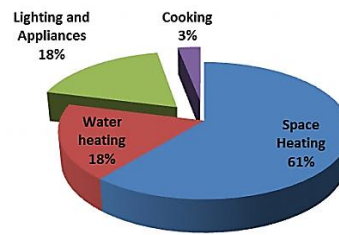
1 INTRODUCTION

With the Climate Change Act of 2008 [2], the United Kingdom has fixed a legally binding target of at least an 80% reduction of their greenhouse gas emission by 2050 and a 34% reduction by 2020 in reference to their 1990 emissions. Considering the distribution of the primary energy consumption by sector and end use in the UK in 2010 (fig. 1 and fig. 2), it can be seen that the domestic sector absorbed 32% of this energy and that 79% of this energy is used for space heating and domestic hot water [1]. Moreover the impact assessment of the Climate Change Act realised in 2009 by the Department of Energy and Climate Change [3] highlighted that financial savings per tonne of carbon saved were found to be greater in the household energy sector than in others. Thus, these figures suggest that improvements in the domestic sector could bring an efficient and significant contribution to the effort of reducing carbon emissions in the country.



Total : 150,071 thousand tonnes of oil equivalent

fig. 1 - Final energy consumption by sector in the UK, 2010 [1]



Total : 48,871 thousand tonnes of oil equivalent

fig. 2 - Domestic Final Energy consumption by end use in the UK, 2009 [1]

In order to reduce the energy use for space heating, keeping the heat through better-insulated houses is probably a first problem to address. However the choice of efficient heating systems, to provide space heating and domestic hot water, can also play a significant role in reducing carbon emissions. Looking at the last trends since 1970 (fig. 3), gas has been more and more used during these last years to provide in 2010 around 70% of the energy in the domestic sector. But the trend of the price gas to increase with the raising stress on the world's resources and its limited but inexorable environmental impact, suggests that viable alternatives will have to be found in the near future.

As biomass resources are limited and solar powered systems are not sufficient in a country like the UK, heat pumps are today more and more seen as an alternative to conventional boilers using fossil fuels or electrical heaters. The advantage of heat pumps is that firstly, they use electricity which is expected to come from more and more renewable sources in the

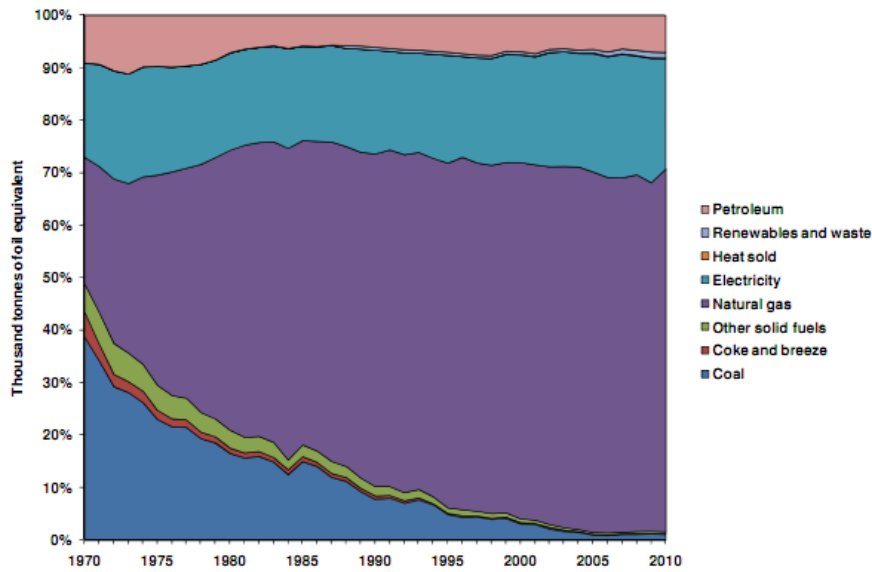


fig. 3 - Domestic energy consumption by fuel in the UK between 1970 and 2010 [1]

future, and secondly, they can potentially produce many kilowatts of heat per kilowatt of electricity by collecting the calories from the surrounding environment (fig. 4). Heat pumps can use different types of heat sources (ground, water) but air source heat pumps present a facility of installation which is particularly promising for their development.

Most of the time heat pumps are considered as a green and sustainable technology. In particular they are integrated (under certain conditions) in the Renewable Heat Incentive (RHI) [4] which has been implemented by the UK government from summer 2011. However the real improvement in terms of environmental impact compared to conventional technologies, in particular gas, is arguable.

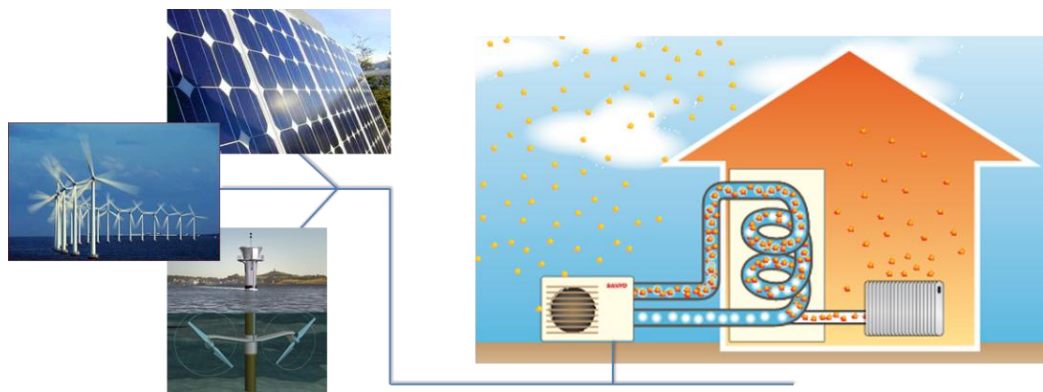


fig. 4 - Air source heat pump powered by renewable sources

The performances of these systems are indeed very variable from one installation to another as highlighted by field trials which have started to be carried out in the UK and in Europe. In addition the common use of HFCs refrigerant, which have a high global warming potential, add an extra environmental impact due to the leakage too often unknown are neglected. To deal with this problem of refrigerant, it is today possible to use natural refrigerants which are much less harmful for the environment. Carbon dioxide is one of them and new systems have been commercialized in Japan from the 2000s and more recently in Europe. The focus of this thesis will be to study more in depth what can be expected from these new heat pumps, which present the advantage of using a natural refrigerant, but still have to demonstrate their performances.

2 LITERATURE REVIEW

This literature review will evaluate the current knowledge and the stakes associated with air source heat pumps. The focus will be first on their actual performances and the methods available to estimate them. Then the impact of HFCs will be discussed before introducing the opportunities offered by natural refrigerants. A particular attention will be given to the use of CO₂ as a refrigerant with the actual development of the technology. Finally, the frost formation, which can appear on air source heat pumps evaporators, is a specific problem that affects the performance of these systems and which needs to be addressed properly.

2.1 Air Source Heat Pump Performances

To characterise their system efficiencies, manufacturers give in general some coefficients of performance (COP) which characterise the ratio of heat produced over the energy consumed in different conditions of operation. The performances of heat pumps are indeed not constant and depend on many parameters: the temperature of the outside air, the temperature of the heat transfer fluid at the inlet and outlet of the heat pump, the electricity used for the controls, the pumps. For air source heat pump the fluctuations of the performances tend to be higher than ground or water source heat pumps because the ambient air temperature varies quite a lot in function of the weather. In addition some defrost cycles are sometime required and reduce the overall performances (cf. paragraph 2.5).

The seasonal performance factor (SPF) of an installation, the COP over one year, give a better idea of the real performance of the system but depend on the characteristics of each installation. Thus, it is in general quite difficult to predict it and not so common to measure it on the installations.

2.1.1 Actual heat pump performances

It can be seen that more and more field trials have been carried out recently and provide better feedback on the device's performances. In particular a field trial realised by the Energy Saving Trust in 2009 [5] included the SPF measurement of 28 air source heat pumps (fig. 5). The mean SPF of the system monitored is around 2.15 with a minimum value of 1.2 and a maximum value of 3.2. There are therefore strong differences between the installations with an important standard of deviation of the SPFs. In their report, the Carbon Saving Trust highlights that the systems design, the system installation and consumer behaviour are the main factors influencing these variations.

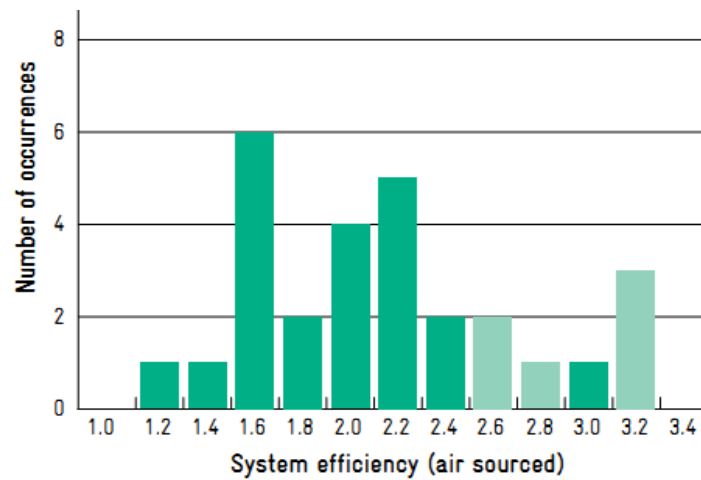


fig. 5 - Seasonal Performance Factor of the UK field Trial [5]

These results have also been compared to other field trial in Swiss and Germany in a report from Delta Energy and Environment [6]. The field tests in Germany and Switzerland were carried out respectively by the Fraunhofer Institute ISE and the Swiss Federal Office of Energy. The comparison shows that 50% of the heat pumps tested in the UK have lower SPFs than in both other countries (table 1). All heat pumps monitored in Switzerland and Germany have indeed a SPF higher or equal to 2.2. This report underlines therefore the margin of improvements for the heat pumps installed in the UK since the difference in the performances should be that high.

	UK	Germany	Switzerland
Air source	<ul style="list-style-type: none"> ▶ 60% of installations: SPFs 1.7 – 2.2 ▶ 30% of installations: SPFs 2.3 - 3.2 	<ul style="list-style-type: none"> ▶ Range of SPFs 2.3 – 3.4 ▶ Cluster of SPFs around 2.5 - 2.6 (retrofit) and 2.9 (new build). 	<ul style="list-style-type: none"> ▶ Range of SPFs 2.2 – 3.0 ▶ Half the units in the range 2.5 – 2.8

table 1 - Comparison air source heat pump performance field test in UK, Germany and Switzerland [6]

Manufacturers also start understanding that more transparency in the performances of their devices is required to convince new customers but also authorities on the quality and the potential of their product. Thus Fujitsu General is now displaying online [7] the live performances of 6 of their air/water heat pumps in Belgium and the Netherlands. The measurements started in January 2011 and now reveal SPFs between 2.5 and 3.7 (the results were checked by M. J Bobbaers, expert appointed by the Court, and the counters are under bailiffs' supervision). If the choice made by Fujitsu General of showing these installations might not have been random, it nevertheless illustrates that heat pumps, at least in certain conditions, can really work efficiently.

The industry has also started being more organised, in particular around the European Heat Pump Association [8] which represents the majority of the European actors involved in this sector. Its key goal is to “promote awareness and proper deployment of heat pump technology in the European market”. They have also developed a quality label for heat pumps which guarantee minimum efficiencies in standard conditions and quality customer services. More and more manufacturers are following this label which is delivered in many countries including since quite recently the UK.

2.1.2 Required SPF's to be competitive with gas boiler

The higher the SPF is, the better the system is, in terms of both environmental impact and economics for the owner. The SPF characterizes indeed the electrical energy consumed to meet the load. Knowing this parameter, the environmental impact of the device and the energy costs during its operation can be then calculated and compared with other type of systems like gas boilers. The carbon content [9] and the price [10] of common fuel (electricity and gas in particular) are given by the Department of Energy and Climate Change for the UK (table 2) and enable to calculate the CO₂ emissions and running costs according to of the SPF of the heat pump (fig. 6 and fig. 7). It can then be compared to a gas boiler whose efficiency is taken at 0.9 which is among the best performances of the current boiler for the SAP2009 annual efficiency [11].

	Gas	Electricity
Price (p/kWh)	4.15	12.27
Carbon content (kg CO ₂ /kWh)	0.20	0.55

table 2 - Price and carbon content of the gas and the electricity in 2011 for the UK ([10] and [9])

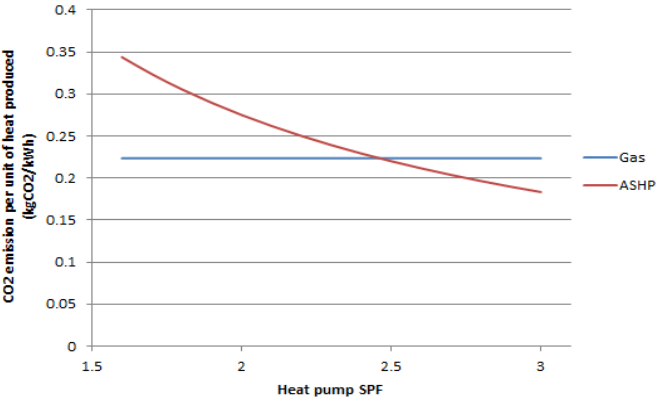


fig. 6 - Comparison CO₂ emission per unit of heat produced for a gas boiler and an ASHP

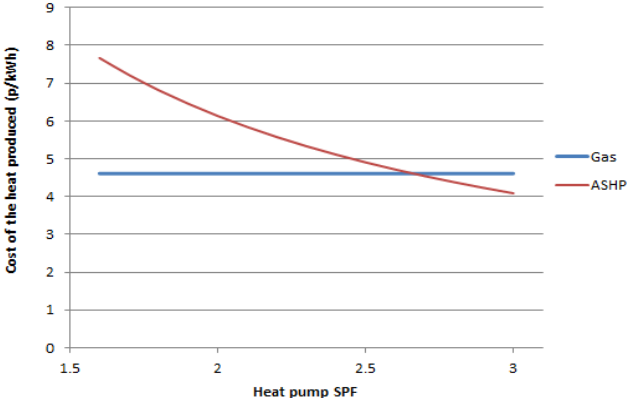


fig. 7 - Comparison price per unit of heat produced for a gas boiler and an ASHP

Then the graphs (fig. 6 and fig. 7) show that heat pumps have to reach a COP of **2.45** to achieve lower CO₂ emissions than a state of the art gas boiler and a COP of **2.67** to be more profitable. These figures are quite high but achievable as shown in the previous field trial. Furthermore, there is still room for improvement of heat pumps performances and the carbon content of electricity is expected to decrease. In opposition, gas boiler characteristics are expected to stay similar. These indications allow us to believe that the future will be to the advantage of heat pumps.

2.1.3 Estimation of the SPF (Seasonal Performance Factor)

The previous part showed the importance of the SPFs of heat pumps from an economical and environmental point of view. That is why today, it is crucial to develop methods to predict the performance of a heat pump in a particular environment of operation. Two main methods can be used today in order to predict the SPF. The first one is in the appendix Q of SAP 2009 and the second possibility is to realize a dynamic model of a heat pump over one year.

The method proposed in the appendix Q of SAP 2009 is based on the European standard 15316-4-2 [12]. It estimates the SPF considering the performances of the heat pump tested under the European standard 14511 [13, 14]. It takes into consideration the climate data for one year, the mode of operation of the heat pump (space heating, domestic hot water or combination of both) and some adjustable parameters to represent the losses, the electric back-up and the design of the installation. The method has been fitted to monitored data with an relative error of around 6% [12]. This method provides a reasonable estimate for use in calculations such as energy rating calculation. However it doesn't allow detailed investigations of site-specifics parameters. In particular, the defrost cycles are directly included in the standard European test 14511 but for standard levels of relative humidity. High humidity regions close to the sea could be a reason for a drop in performances. In addition the dynamic behaviour of the heat pump and the components of the system (tanks, pumps...) and the controls of the system cannot be properly analysed with this method.

The other possibility is to model dynamically the behaviour of the heat pump throughout the year. Dr Kelly [15] realised in ESP-r, a model of a heat pump which can be integrated in a dynamic building model to estimate the SPF. The model is also semi empirical and based on monitored data from a specific heat pump, but it enables to represent the dynamic behaviour of the system in diverse environments of operation. The key element of the model is the COP which is expressed in function of the outside air temperature and the return water temperature

to the heat pump. This COP regression is however specific to the heat pump considered. It can also be noticed that the consideration of the defrost cycles in the model is approximate.

If the study aims to analyse more in depth a particular component of the heat pump, more detail models including the thermodynamic cycle of the heat pump can also be realised. For example Madani et al. [17] address the problem of capacity control in ground source heat pump systems and use both EES and TRNSYS in a co-solving technique to achieve the required level of detail in their model.

Thus, dynamic modelling enables to study in more detail the behaviour of a heat pump in integration within other systems and its surrounding environment. The level of complexity of the model has to be adapted to the specific objectives of the study.

2.2 Refrigerant environmental impact

The refrigerants used in air conditioning systems and heat pumps have been raising questions throughout the year in the 20th century. While CFCs (like R11) brought a revolution for refrigerants in terms of efficiency and safety in the 1960s, it has been noticed that they tend to deplete the ozone layer. Then appeared HCFCs (like R22) whose ozone depletion potential (ODP) was significantly reduced and finally HFCs with a totally negligible ODP. However with increasing concern about global warming, HFCs are now criticised for their relatively important Greenhouse Warming Potential (GWP) compared to that of carbon dioxide.

2.2.1 More and more accurate assessment of this impact

The fig. 8 and fig. 9 illustrate the ODP and GWP values of the main refrigerants which have been used in heat pumps. It can be seen that HFCs enabled to cancel out the ODP problem but their GWP is a thousand time higher than the CO₂ which is taken as a reference. Although the

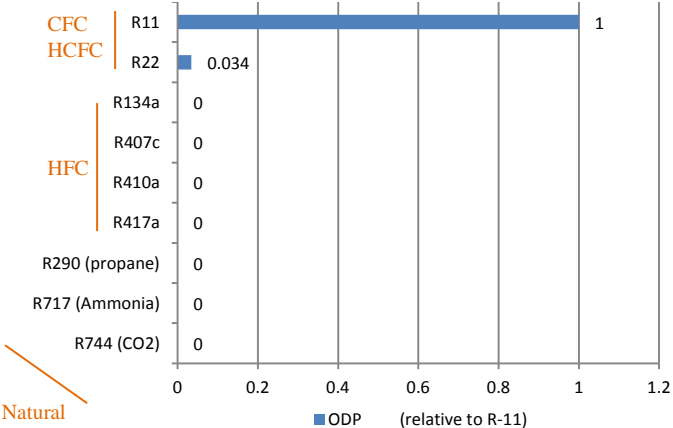


fig. 8 - Ozone Depletion Potential (ODP) of common refrigerants [16]

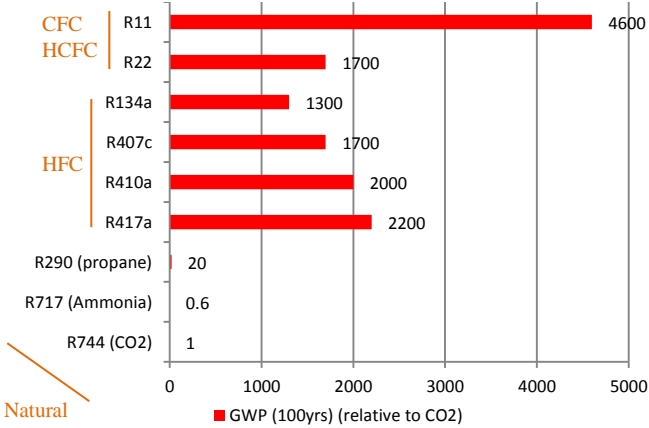


fig. 9 - Greenhouse Warming Potential (GWP) of common refrigerants [16]

refrigerants are operating in a closed cycle, a report made in contribution to the fourth assessment report of the IPCC in 2007 [18] highlights that the leakages of refrigerant can have a non-negligible impact on the environment.

In the case of residential heating and cooling devices, leakages stay limited during the system operation (1 to 5%) but there are still questions about the recovery of the refrigerant at the end of the life of the system. Without recovery, refrigerant emission in the atmosphere represents around 15% of the carbon footprint device during its lifetime. Indeed, the release of 2kg of HFC with a GWP of 1500 in the atmosphere represent 3,000kg of CO₂ or the equivalent carbon footprint of 30,000 km of a car trip (assuming an emission of 100 gCO₂/km).

Another paper [19] from Johnson study the carbon footprint of air source heat pump. Considering a leakage of 6% per year and a leakage of 55% of the refrigerant at the end of the life of the heat pump (base case), the refrigerant represents 16 to 18% of the total carbon footprint which confirm the figures of the IPCC. Moreover, the impacts of different leakage rate were also studied and they are presented in fig. 10. The importance of the refrigerant recovery at the end of life is then highlighted along with the sensibility of the operating leakage. On most installations, the refrigerant is likely to represent 10% to 20% of the total carbon footprint.

Table 18
Footprints and refrigerant contribution thereto over a range of leak rates.

Case	Operating leakage %/ year	EoL leakage % of charge	Footprint kg CO ₂ e/kWh	Refrigerant % of total footprint
Highest leak rate	8	155 ^a	0.21-0.24	24-28
Higher leak rate	8	55	0.20-0.23	18-20
Base case	6	55	0.19-0.22	15-18
Lower leak rate A	4.5	55	0.19-0.22	13-15
Lower leak rate B	6	15	0.18-0.22	12-14
Lower leak rate C	4.5	15	0.18-0.21	10-11
Lowest leak rate	2	15	0.17-0.20	6-7

^a Includes one full venting during servicing per lifetime, as described in section 7.2.

fig. 10 - Footprint and refrigerant contribution with different leak rates [19]

2.2.2 Solutions to offset the environmental impact of refrigerant

Considering this extra environmental impact of 11% to 25%, heat pump using HFCs have to be still more efficient to be equivalent to a gas boiler. A SPF of 2.45 is not sufficient and the requirements increase to a SPF of 2.75 to 3.27. Only 18% of the installations monitored by the EST field trial reach these performances.

In order to cope with this problem, special attention could be accorded to the recovery of refrigerant and the minimization of leakages. However the control of the installations is really difficult and it is obvious that leakage will always occur. Otherwise, natural refrigerants like ammonia (R717), propane (R290) or CO₂ (R744) present another alternative.

These potential refrigerants which are not new were abandoned for safety and efficiency reasons at the beginning of the 20th century. However, with a better harnessing of the refrigerant and the development of the technology, these new refrigerants are more and more considered as replacements of HFCs. In particular, **carbon dioxide** presents interesting properties to be used in heat pumps and will be the focus of this project.

2.3 CO₂ Air Source Heat Pump

2.3.1 The CO₂ cycle specificities

Carbon dioxide is characterized by a low critical temperature of 31.1°C and a high critical pressure of 73.78 bar [16]. In comparison, HFCs will have a temperature 2 to 3 time higher and lower critical pressure (table 3).

Refrigerant	Critical Temperature (°C)	Critical Pressure (bar)
CO ₂ (R744)	31.1	73.8
R134a	101.1	40.6
R407c	81.9	44.9
R410a	72.5	49.5

table 3 - Critical temperature and pressure of commonly-used refrigerants [16]

Consequently, in order to achieve sufficient temperatures, CO₂ heat pumps will operate at pressure which will be 5 to 10 times higher than for HFCs systems and the cycle will be transcritical (fig. 11). However the principle of the thermodynamic cycle stays quite similar (fig. 12). On process 1-2, there is compression of the CO₂ which reaches a temperature of around 70 to 100°C. The specificities of the CO₂ cycle appear on process 2-3 where the useful heat is transferred to the heat sink. As the cycle is transcritical, there is no condensation of the refrigerant at constant temperature but a heat transfer through a gas cooler with a temperature glide. Finally a valve enable to expand the CO₂ (process 3-4) before the classic evaporation process (4-1) to collect the heat from the outside air. The COP of the system is then the ratio of the heat transfer through the gas cooler over the energy used for the compression (fig. 11). In the case of the CO₂ cycle, as the heat transfer is not made at constant temperature, the

outlet temperature of the gas at the outlet of the gas cooler is critical (point 3 on the fig. 11). At constant work in the compressor, the CO₂ in the gas cooler must be cooled down as much as possible in order to extract a maximum of heat from the refrigerant and maximize the COP. In fig. 11, the point 3' show a less favourable situation than the point 3 with a lower COP.

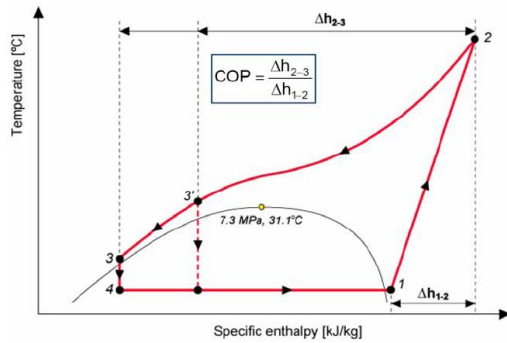


fig. 11 - Principle of the transcritical CO₂ heat pump cycle [20]

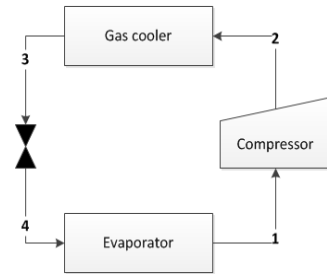


fig. 12 - Basic components of the CO₂ cycle

This specificity of the CO₂ cycle will induce a better efficiency when the fluid heated in the gas cooler arrives at a low temperature. That's why CO₂ heat pumps are more efficient in providing domestic hot water than for space heating. The following graph (fig. 13) from Stene's thesis [21] illustrates it with the characteristics of the heat rejection in the gas cooler for the different mode of operation. It can be noticed that the CO₂ temperature profile in the gas cooler matches the heating of domestic water from a low temperature and up to 70°C quite well. However for space heating, even at low temperature 35/30°C, the return temperature limit the heat rejection in the gas cooler and the global efficiency of the cycle. For HFCs cycle, as the heat transfer is made at a constant temperature in the condenser, the situation is reversed: the heat pump struggles to provide high temperature for domestic hot water but they are more suitable for space heating.

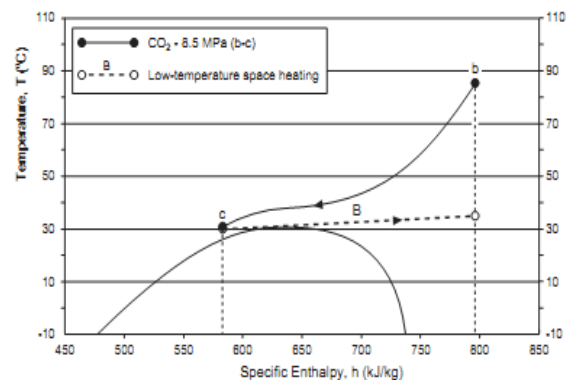
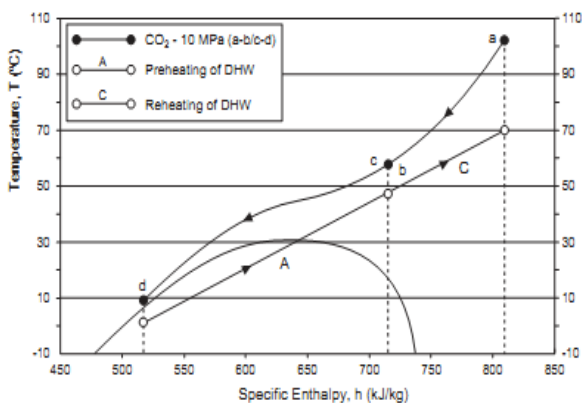


fig. 13 - Illustration of the heat rejection process in the gas cooler for domestic hot water (on the left, high side pressure 10MPa) and for low temperature space heating (on the right, high side pressure 8.5MPa) [21]

2.3.2 The recent revival of CO₂ as a refrigerant

The first problems encountered in early ages, high pressure of operation and low efficiency, can be now overcome by new knowledge and technology in thermodynamic cycles. Thus, in 1994, Gustave Lorentzen spoke about the revival of carbon dioxide as a refrigerant [22]. Denouncing this trend of trying to find new chemicals, Lorentzen reminded engineers that the “COP of any reversible (loss free) process, working between given temperature limits, is exactly the same and completely independent of the properties of the working medium used”. He highlights the potential of CO₂ as a refrigerant and the proven possibilities of using it for motor-car air conditioning or domestic hot water. In 2002, Neksa [23] confirmed the competitiveness of CO₂ systems with synthetic working fluids if they are properly designed. But it is mainly in Japan that CO₂ heat pumps have started to be commercially available since the early 2000s. The market is indeed particularly adapted for the development of the technology due to a high domestic hot water demand, especially because of their traditional habit of hot bathing, Onsen. Thus, more than 2.5 Million of these units were sold at the end of September 2010 [24]. More recently, Japanese manufacturers started to propose their systems in Europe. In addition, as space heating represents the main heating load in Europe, some manufacturers like Sanyo developed systems to provide both space heating and domestic hot water heating (paragraph 2.4).

2.3.3 CO₂ heat pump performances

A lot of the papers in the literature ([25], [26], [27], [28]) study the possibilities to improve the thermodynamic efficiency of the CO₂ cycle with better designs, more efficient components or controls. However, much less studies focus on the actual seasonal performance factor of CO₂ heat pumps in real operating conditions.

Reports and feedback about the heat pump water heater “Eco Cute” are however available with the development of the Japanese market. In particular, a field trial on 36 units in Japan reports an average seasonal performance factor of 3.16 when producing hot water at 40°C, according to a report of Staffel in 2009 [29]. But for the new systems providing both domestic hot water and space heating in Europe, there is much less information available at the moment and very few studies on their performances. The work of Jorn Stene must however be cited with an interesting thesis [21] which study different CO₂ system designs and their performances. In particular, he underlines the potential of a tripartite gas cooler to provide both space heating and domestic hot water efficiently and the importance of the ratio of domestic hot water demand. Such a system could become more performing than high

efficiency HFC system when this ratio reaches 45-55% of the heat demand in the case study of a water (brine) source heat pump. CO₂ system could therefore be efficiently used in passive house which are characterized by a low energy demand as mentioned by Stene in a more recent paper [20]. However, the system with a tripartite gas cooler is only today an experimental device which is not commercially available.

A lot of research is however still going on concerning CO₂ system. The last congress of refrigeration for sustainable development assembled between the 21st and 26th of August 2011, included two technical sessions on “Heat pumps and Natural refrigerant”. The output of some of the very last studies on the performances of CO₂ water heaters and the performances of water/water CO₂ heat pump for residential application were in particular presented. The website R744 [30] which reports about these last researches, must be mentioned as the platform which gathers most of the latest development and evolution concerning the used of CO₂ as a refrigerant.

All this current research on the subject highlights the fact that CO₂ heat pumps are still a new technology. If the efficiency of the system has been proved in Japan with the Eco-Cute Water Heaters, the performance of currently commercialised systems for both domestic hot water and space heating has still to be demonstrated. There are still a lot of questions on the systems, especially concerning the capability of the system to efficiently provide some space heating.

2.4 The Sanyo Eco Cute System

2.4.1 Presentation of the system

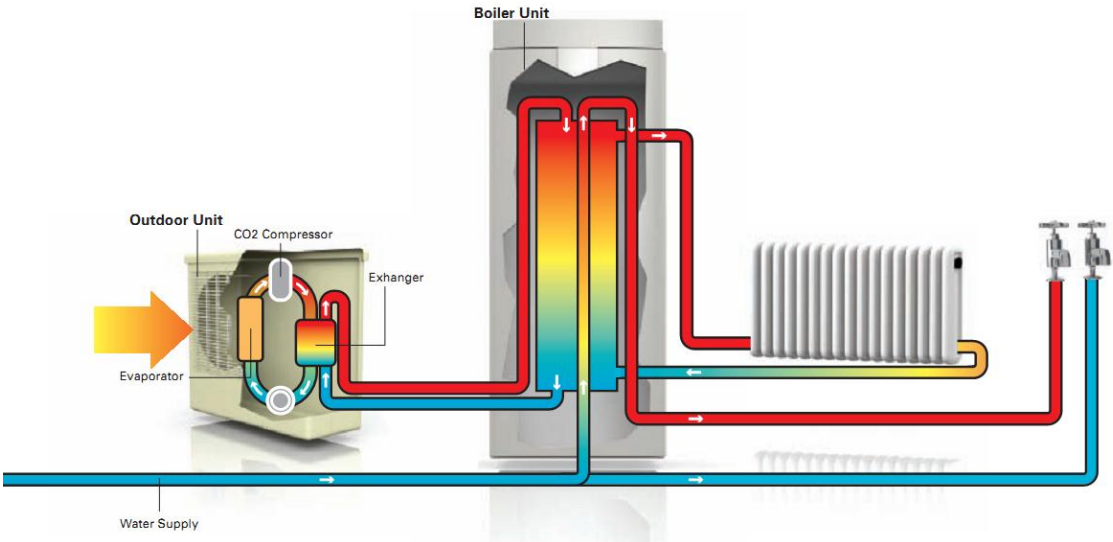


fig. 14 - The Sanyo Eco-Cute System adapted for the European Market[31]

The Sanyo Eco Cute system adapted for the European market combines a 9kW CO₂ heat pump unit, similar to the one used for the “Eco Cute” water heater in Japan, with a special tank and adapted controlled designed in Sweden to provide both space heating and domestic hot water (fig. 14). It started to be installed in the UK a few years ago and the manufacturer claims promising performances with a COP of 4. There are however still questions about the real efficiency of the system in the British environment.

This system will be the focus of this project which ensues from a previous master group project realised in spring 2011 [32] in which this author participated. The project was realised in partnership with an installer and a housing association which were both interested by knowing a bit more about the efficiency of the Sanyo System. Thus, the performances of 3 of these installations in Scotland were analysed during the project. It was concluded that the performances of the whole system in operation were moderate and SPF_s were expected to be between 1.7 and 2.2 even though some improvement might be easily achievable. Nevertheless the project made these predictions based on monitored data of the systems over a few weeks in March. To properly estimate the seasonal performances of an installation, a specific method taking into consideration the dynamic variations of the environment must be considered.

2.4.2 What is known about the system

An extensive description and analysis of the Sanyo Eco Cute system has already been made by the previous project with different sources of data. This section will only summarize the important point which will be useful in this project.

The Sanyo system has already been studied by KTH University in 2007 and the report [33] highlights that the performances of the heat pump itself match the expectations and the figures given by the manufacturers. Many tests have been realised in different conditions of operation and the results have been used by the previous project at Strathclyde University [32]. It was shown that a regression of the coefficient of performance could be made in function of the outside air temperature and the return water temperature with a correlation coefficient of 0.99.

The KTH report questions also the tank design which doesn't seem to minimize the return water temperature to the gas cooler (fig. 15). The Sanyo tank is relatively complex with partition plates, many water outlets at different height for the space heating, a heat exchanger coil for the hot water and 2 back-up electric heaters. All the stakes of this design in association with proper controls are to meet the heating load while minimizing the temperature at the bottom of the tank.

Many suggestions have been made to improve the performances of the system by modifying the design of the tank (fig. 16). These remarks led to a second version of the system in 2008 which follows some of the recommendation but not all of them (fig. 17). The study of this new system by the project at Strathclyde University found that the modifications didn't bring a real change. In particular the inlet of the cold water from the city is still in the middle of the tank while it should be at the bottom to cool it down. It is also the inlet of the hot water coming from the heat pump which is also located in the middle of the tank and not at the top, as it would be expected to keep the stratification.

During the previous group project, a lot of data have also been collected from an Finnish installation whose live performances are available online [34]. The system is the previous version of the system now installed in Scotland with a CO₂ heat pump of only 4.5kW (fig. 19

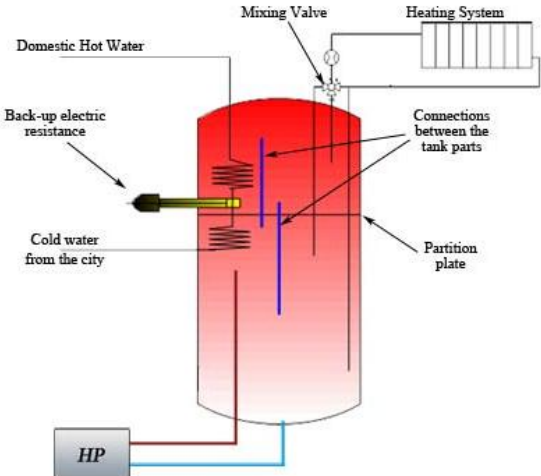


fig. 15 - First Sanyo tank design

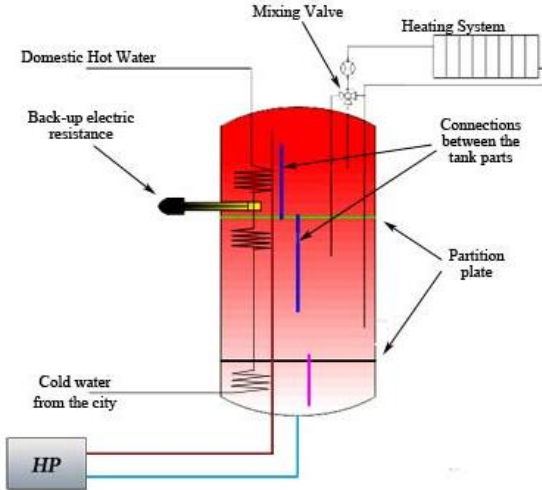


fig. 16 - Design proposed in the KTH report [33]

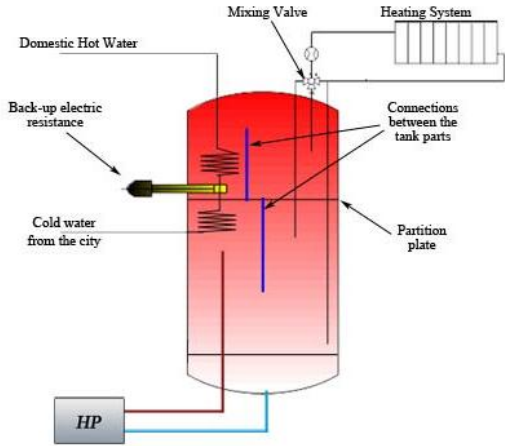


fig. 17 - Last version of the Sanyo system design

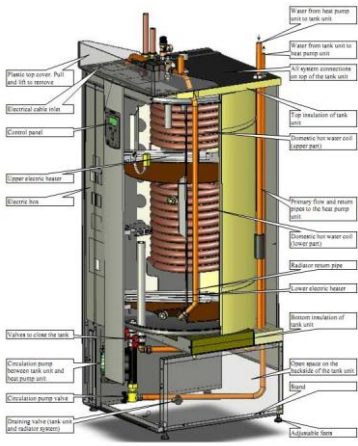


fig. 18 - Last version of the Sanyo tank design (bigger picture in appendix D) [31]

and fig. 20) but accredited with the same performances by the manufacturer. The seasonal performance factor of the system is relatively low which is due to the cold and humid climate in Finland and most of the data collected during last winter were too low due to a sensor calibration problem. A more extensive analysis of the installation is given in the website of the previous project [32].



fig. 19 - First version of the Sanyo Eco Cute system with heat pump of 4.5kW



fig. 20 - Second version of the Sanyo Eco Cute system with heat pump of 9kW

2.5 Defrost cycles and impact on heat pump performances

The defrost cycles are required in air source heat pump to remove the ice which can form on the pipes of the evaporator in certain conditions and tend to reduce the efficiency of the device. This is a relatively complex problem of heat transfer and psychometrics, which is not easy to model. The mechanism of frost formation and the impact on impact on the heat pump performances are the focus of this section.

2.5.1 Mechanism of frost formation

The ice formation on the pipe of the evaporator is a problem of psychometrics and heat transfer. The air passing through the evaporator is cooled down and the energy is collected by the refrigerator. In certain cases, the air temperature will be decreased beyond its dew point and the extra humidity that cannot be held in the air will condense on the pipes.

This is a problem that can be described on a psychometric chart (fig. 21). Assuming the outside air at 5°C and 80% of relative humidity, the air is cooled down and its absolute humidity content will stay constant. At the dew point, the air reaches the limit of the humidity that it can hold. If the temperature keeps decreasing, there will be condensation of the humidity and freezing if the pipes are cold enough. Thus this phenomenon depends on the initial point (air temperature and relative humidity) and on what extent the air is cooled down.

But the problem is not that simple to be modelled. Firstly, the air is not cooled down evenly in the evaporator in function of the distance to the pipes and the heat transfer. In addition the heat transfer is dynamically affected by the changes of state (condensation, solidification) and the ice formation which adds solid external layer on the evaporator's pipes and impacts the air mass flow.

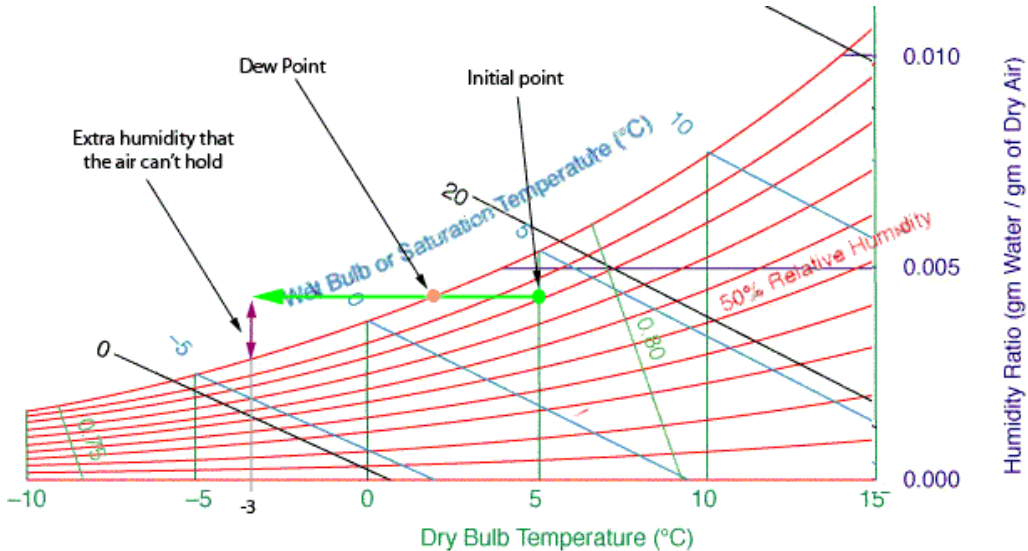


fig. 21 - Analysis on the frost formation on the pipe on a psychrometric chart

In the literature, a lot of models have been suggested in order to predict ice formation and the impact on the heat exchange in different configurations: on flat surfaces [35], on fin and tube heat exchangers [36], on fan supplied tube-fin evaporators [37]... These models, using fundamental equation with sometimes empirical results, in general present results which are within a 12% error dead band in comparison with experimental measurements. Similar trends are also highlighted concerning the influence of different parameters such as the air temperature, humidity and velocity. Some models gain in complexity to provide a more detailed analysis of the phenomena, like for example this model of Cui et al. [38] which consider both time and space dependencies of the frost formation and use a CFD tool.

Some experimental studies have also been conducted to analyse the ice formation at very detailed level including local variations and morphology [39] or a microscopic analysis [40]. These works underline the characteristics of the ice formation as a non-regular process which include different steps with different crystal shape and frost growth patterns. These local variations are identified as responsible for fluctuations in the heat transfer and the speed of the ice formation.

2.5.2 Defrost cycles and air source heat pumps

When the ice forms on the pipes of the evaporator, the heat transfer tends to decrease because the air mass flow falls and the ice act as an insulating layer. As soon as 1987, Tassou and Marquand [42] analyse this phenomenon which leads to a temperature and pressure decrease in the evaporator to maintain a sufficient heat transfer and then a loss of efficiency for the heat pumps.

More recently, some interesting papers focus on the impact of the frost formation on the performances of heat pumps. For example Guo et al. [41] studied experimentally in 2008 the frost growth pattern on a heat pump evaporator and the impact on the performances. 3 steps in the growth pattern of the ice are in particular highlighted. The first stage led to the formation of a column shaped ice crystal layer which tended to improve the performances of the heat pump due to an increase of the heat performances due to an increase of the heat transfer surface area. In the second stage the ice layer growth in its radius more than in its length which started affecting slightly the heat pump performances. In fig. 22, this step is characterized by a stagnation of the frost thickness growth rate. Finally in the third stage, the ice layer starts growing quickly in its length and significantly reduces the heat pump efficiency.

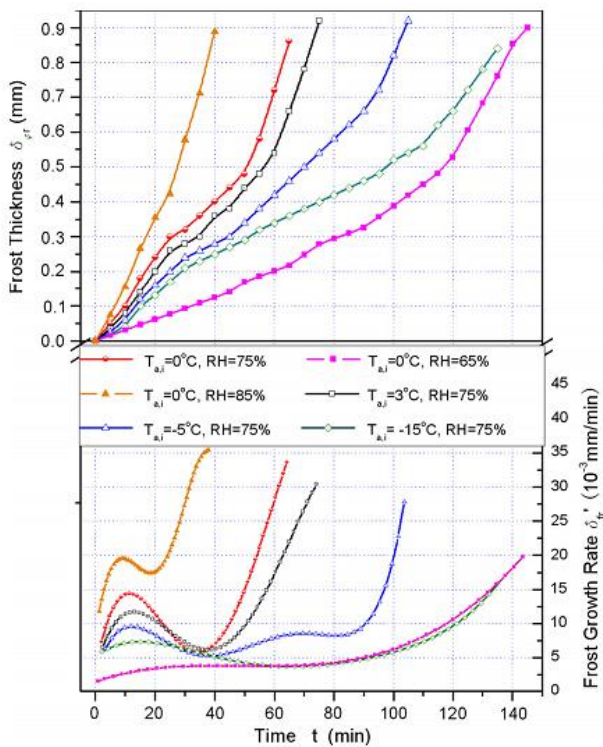


fig. 22 - Frost thickness and frost thickness growth rate with frosting time under different conditions [41]

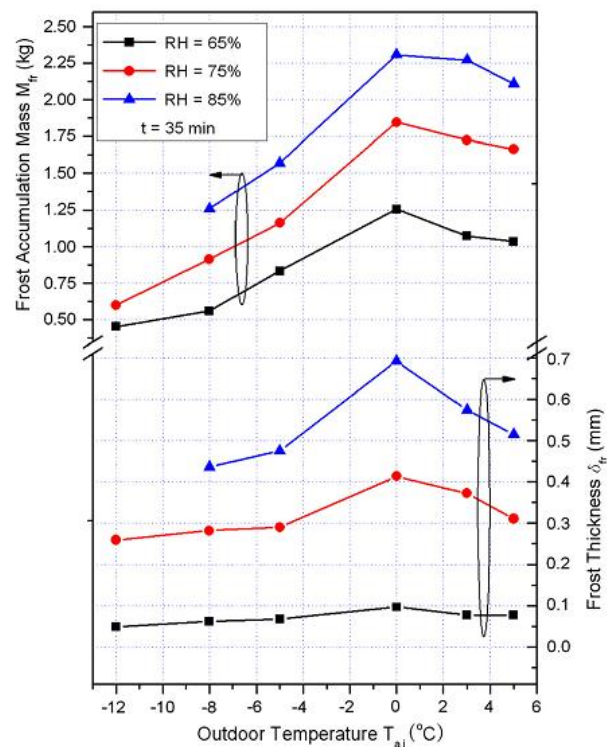


fig. 23 - Comparison of frost accumulation mass and frost thickness after 35 min operating [41]

Air temperature and relative humidity, as illustrated previously influence frost formation. The higher the air inlet relative humidity and temperature is, the faster the frost formation is when the temperatures are lower than 5 to 6°C (fig. 22 and fig. 23). There is indeed a temperature limit when the pipes of the evaporator are not cold enough to freeze the condensed humidity.

Different strategy like reverse defrost cycle, a hot gas bypass method or even direct electric heating can be used to remove the ice formed on the evaporator. But one of the important points highlighted by Wand et al. [43] is the control of these defrost cycles. It is indeed necessary to properly detect the ice formation and growth on the evaporator to trigger the defrost cycle at the right moment. With field tests realised on certain systems, Wand et al. highlight that a lot of mal-defrost problems occur in heat pumps and contribute to a further degradation of the system performances.

More specifically, a paper from Chen et al. [44] studies the reverse-cycle defrosting characteristics of an air source heat pump. In particular they show that the energy required for the defrost cycles is higher at lower outside air temperatures and low relative humidity. They also use the concept of total COP which directly includes the possible occurrence of defrost cycles. The variations of the total COP are then analysed in function of the air temperature and relative humidity. It is important however to remember that frost formation and defrost cycles are specific to each heat pump and depend on the design of the evaporator, the difference of temperature between the refrigerant and the outside air and also on the defrost method chosen.

In the European standard 14511 [13, 14] which provide a method to test heat pumps, the defrost cycle are directly taken into consideration in the COP given in the different operation. However standard humidity levels are considered.

2.5.3 Defrost cycle in the Sanyo Heat pump

In the case of the Sanyo Heat pump, a system of bypass valves has been chosen in order to bring hot gas to the evaporator and defrost the evaporator when it is required. The report from KTH University analysed the defrost cycle on the 4.5kW heat pump. It showed that the starting point for the defrosting mode is controlled by difference of temperature between the evaporator air inlet temperature and evaporator temperature. During the defrost cycle, the fan and the water pump stop while hot CO₂ is sent to the evaporator until it reaches a certain temperature.

From the data collected on the Finnish installation, the previous project at the University of Strathclyde highlighted some trend some and correlation between the defrost cycles, the outside air temperature and relative humidity. As the heat pump is almost operating in permanence in Finland, it is indeed quite easy to identify the defrost cycles and the period of ice formation.

3 OBJECTIVES AND METHODOLOGY

3.1 Objectives

As highlighted in the literature review, CO₂ heat pumps are now available in the United Kingdom but their seasonal performance factors can only be roughly predicted. The first objective of this project is then to develop an operational model of a CO₂ Heat pump in ESP-r, the integrated energy modelling tool developed at the University of Strathclyde. A dynamic model, rather than a method similar to SAP appendix Q will be used since it provides more possibilities for a detail analysis of the system. The Sanyo system providing both domestic hot water demand and space heating will be the particular case study of this project.

Once the model defined, it will be then possible to estimate the seasonal performance factor of a specific installation in Scotland used as a case-study. But the KTH report and the previous group project highlight that improvements are quite easily achievable by modifying the tank design and the controls. Considering these modifications another simulation will be run to study to what extent the seasonal performance factor will be enhanced.

3.2 Methodology

A first project on the Sanyo system has already been realised at Strathclyde University [32] and enabled to understand a bit more about the behaviour of the system. The output of this first project with a further analysis of the data collected on the system will be used to characterize the heat pump behaviour.

From this analysis, a new component modelling the behaviour of the CO₂ heat pump will be implemented in ESP-r. ESP-r is a dynamic simulation tool for integrated building which will be used in this project. A model of non CO₂ heat pump has already been developed in this software by Kelly at the University of Strathclyde [15]. Thus, using this model as a starting point, it will be modified to match the case of the Sanyo CO₂ heat pump and improved to get in particular a better model of the defrost cycles. The new heat pump component will be then tested to be sure that it behaves as expected.

Once the model is validated, the heat pump component can be integrated in a complete model of a house with a hydronic heating system. In particular Dr Kelly already made such a model with the previous heat pump component connected to radiators and a domestic hot water tank. By replacing the heat pump by the new component, a comparison and analysis of both systems will be realised.

Finally, a particular installation located in Oban will be used as a case study and the dwelling with the Sanyo system will be modelled in ESP-r. The new CO₂ heat pump will be connected to a stratified tank and integrated in a house model including an under-floor heating system and a characteristic domestic hot water draw profile. The global model will be then validated against monitored data collected from the previous project. In addition, some extra monitoring realised in summer will enable to check the validity of the model during a summer operation, with domestic hot water only. Finally an optimized configuration of the heating system will be proposed to see to what extent it can improve the performances of the whole system.

4 ANALYSIS OF THE DATA COLLECTED ON THE SANYO SYSTEM

In this part, the monitored data which are available on the Sanyo system will be carefully analysed. The information on the system behaviour will be indeed used to define the model of the CO₂ heat pump and the installation in Oban that will be used as a case-study.

The analysis will focus on the variations of the coefficient of performance, the defrost cycles and the electrical energy consumption of the heat pump. The data from the KTH report [33], the Finnish installation and the monitoring realised on two Scottish installations by the previous group project will be used.

4.1 Analysis of the Finnish Data

A lot of data from the **Sanyo Eco Cute installation (4.5kW)** monitored in Finland [34] were given by M. Hakari, the landlord. It included the power consumption, the heat output of the heat pump and the outside air temperature. A first analysis of the data have been made by the previous project and highlighted in particular a problem of sensor calibration (cf. previous project website for more information [32]). The measurements of the COP were therefore not valid before the calibration, realised on the 7th of April 2011. For this project all the data from October 2010 to April 2011 have been collected and a more extensive analysis will be realised concerning the performances (for the month of April) and the defrost cycles (whole period).

4.1.1 Performances of the Sanyo system

Analysis of the previous project output

The previous project realised a regression of the CO₂ heat pump COP based on laboratory tests realised at KTH University [33]. The COP was expressed in function of the outside temperature (T_{out}) and the water return temperature to the heat pump (T_{wr}) (table 4). 30 points (fig. 24) were used in the regression and a coefficient of correlation of 0.99 was found. It was however difficult to compare this regression with the data from the Finish installation because of the calibration problem mentioned previously.

Parameter	T_{wr}	T_{out}	T_{out}^2	Cst
Coefficient	-0.036	0.0469	0.000610	3.627
Error	0.00124	0.00123	0.0000863	0.0401
Correlation	0.992			

table 4 - Regression of the COP in function of the outside temperature and the water return temperature to the heat pump [32]

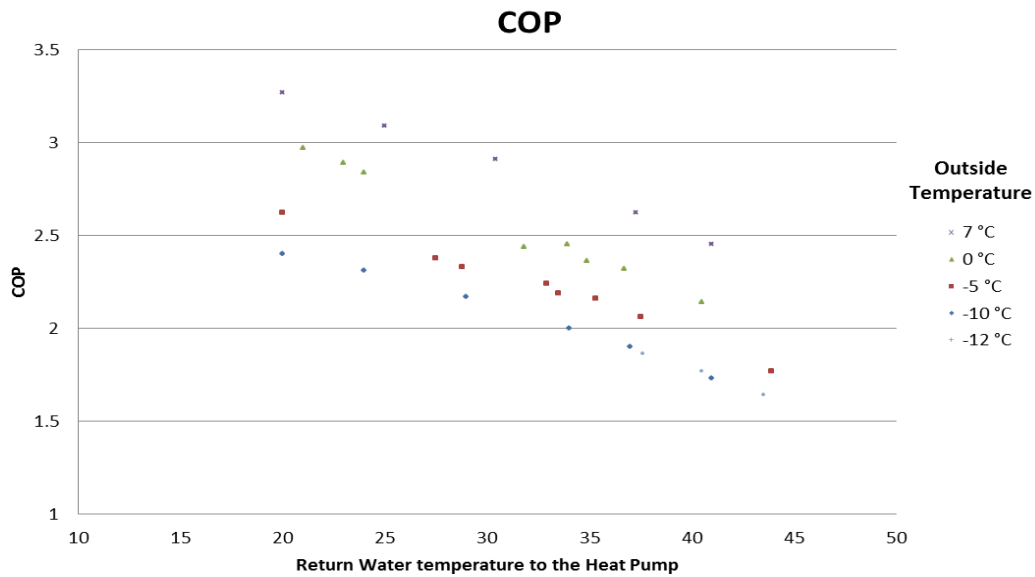


fig. 24 - Experimental data used by the previous group project [32] for the regression of the COP

With the new monitored data collected from the 7th of April, the direct comparison with the regression is now possible (fig. 25). It can be then noticed on the graph that the predicted COP follow the same trend that the measurements realised on the system. Considering the data from the 8th to the 30th of April 2011, the average relative error between the calculated COP and the data is however still of 9.3% and the average COP is 5% higher. More specifically, it can be seen that the regression tends to overestimate the COP at high temperature and high return water temperature.

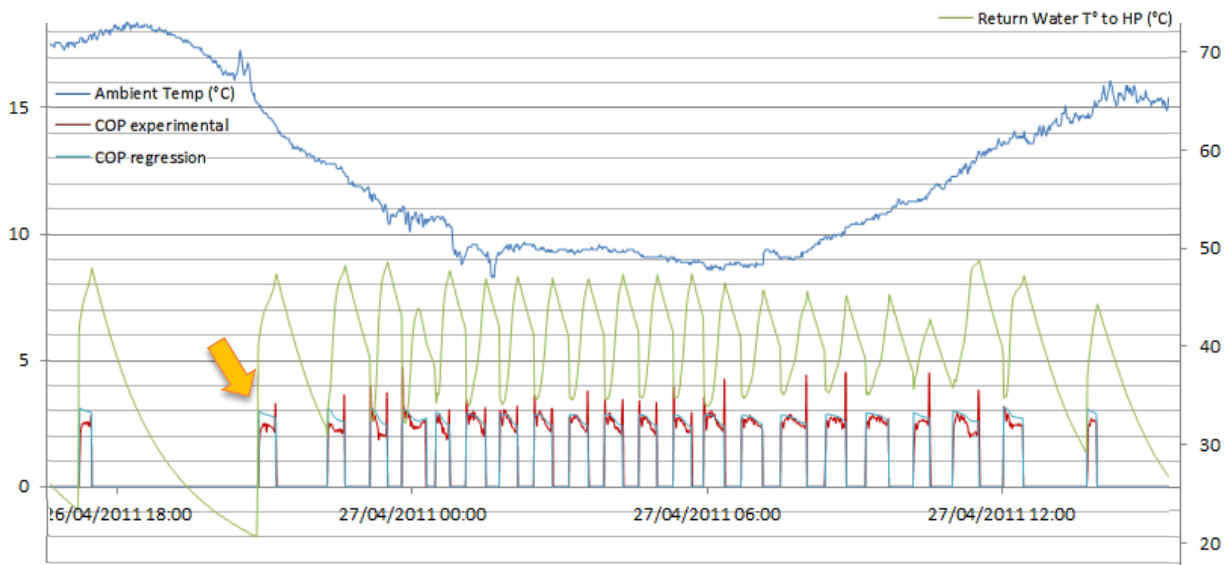


fig. 25 - Comparison of the COP calculated with the initial regression and the data from the Finnish installation (27/04/2011)

As illustrated more precisely on the next graph (fig. 26), when the return water temperature to the gas cooler is higher than 40 - 45°C (at high outside air temperature of 13°C), the system presents a drop in the performances which doesn't appear in the estimated COP. This range of temperature is indeed out of the range for the regression realised by the previous project whose main operating points for the return water temperature are between 20 and 40°C (fig. 24).

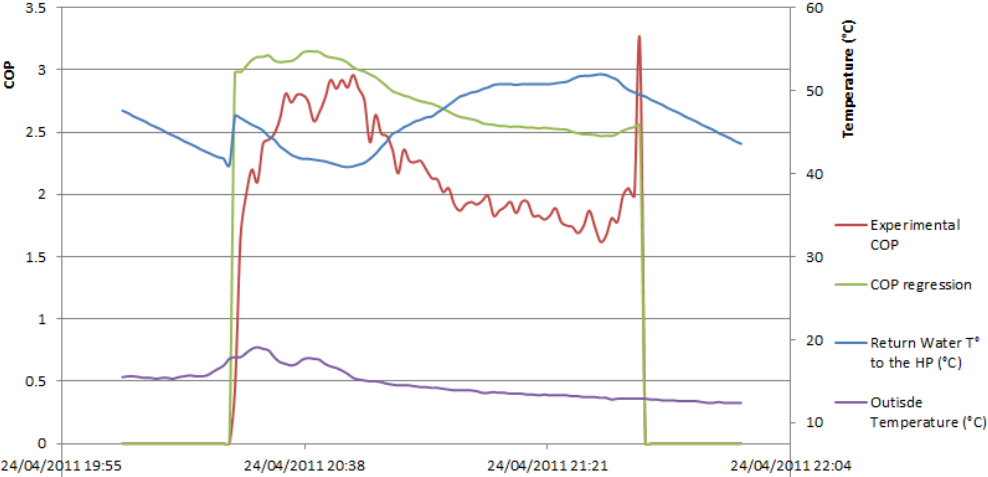


fig. 26 - Comparison of the COP calculated with the initial regression and the data from the Finnish installation (24/04/2011)

Proposition of a new Regression

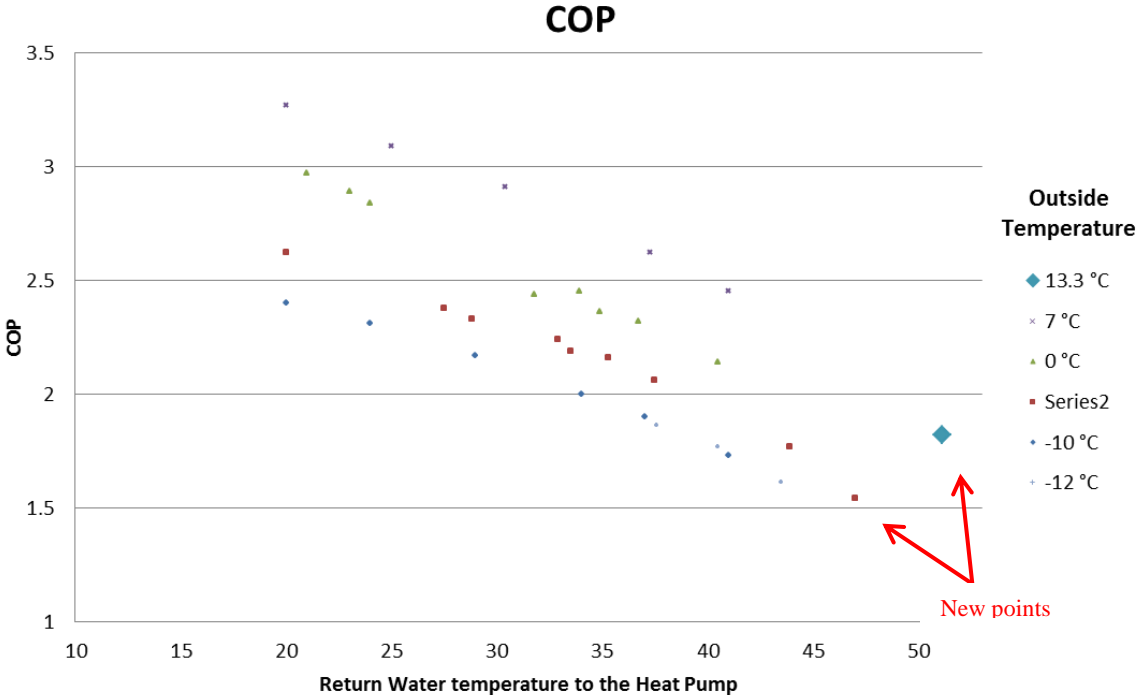


fig. 27 - Experimental data used for the new regression with 2 extra points considered

To be sure that the regression stays valid in a sufficiently wide range of temperature, another regression is realised by considering 2 other points at higher return water temperature. One comes from the report from KTH University which was initially considered as marginal and the second one from the data above (fig. 26). At 51°C of average return temperature, the system is indeed operating at a near steady state during 20 minutes at a mean outside temperature of 13.3°C and with a COP of 1.81.

As the variations of the COP in function of the return water temperature (T_{wr}) is not linear anymore, a new regression is then done with a polynomial of order 2 in function of both temperatures. The new regression is presented below and has a similar coefficient of correlation (table 5).

Parameter	$T_{out} * T_{wr}$	T_{out}^2	T_{out}	T_{wr}^2	T_{wr}	Cst
Coefficient	-0.00102	0.000482	0.0787	-0.000712	0.00371	3.12
Error	0.000136	0.0000868	0.00488	0.000124	0.00842	0.137
Correlation	0.993					

table 5 - New regression of the COP in function of the outside temperature and the water return temperature to the heat pump

Doing the comparison with the experimental data, the correspondence between the curves is now enhanced (fig. 28). From the 8th to the 30th of April 2011, the average relative error is now a bit lower, at 8.4%. The improvement is not very significant since most of the time the return temperature stays between 30 and 45°C, i.e. in a range where the previous regression is still valid. It is however important to do this modification so that the regression stays valid in a wide range of temperature.

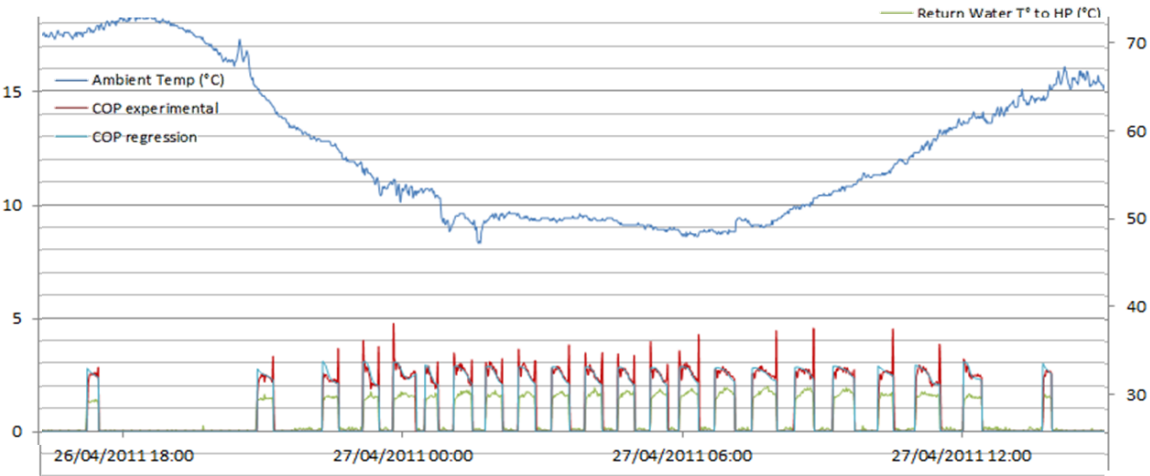


fig. 28 - Comparison of the COP calculated with the new regression and the data from the Finnish installation (27/04/2011)

COP fluctuations when the heat pump start

Concerning the accuracy of the regression, an important relative error can be noticed when the heat pump starts. In fig. 29, the graph shows that it takes 10 to 20 minutes at 4 -5 °C of outside temperature so that the system actually reaches the COP that is expected. This effect seems to be more important at cold outside temperature and still worse after a defrost cycle. The fig. 30 shows the heat pump is more reactive after a defrost cycle since the pipes of the evaporator are still hot from the defrost cycle operation. However the heat pump reaches quickly 80% of its performances and struggles after during around 20 minutes to reach the expected COP in the conditions considered.

A possible explanation to this phenomenon could be that it takes time to the system to reach the optimal operation point characterized by a certain pressure in the gas cooler. This effect could be more important at lower temperature since the compressor has to reach higher pressure. During the defrost cycle, a bypass valve is used in order to send hot gas to the evaporator and the good operation of the thermodynamic cycle might be therefore a bit disturb, in such way that it requires more time to come back to a normal and optimal operation.

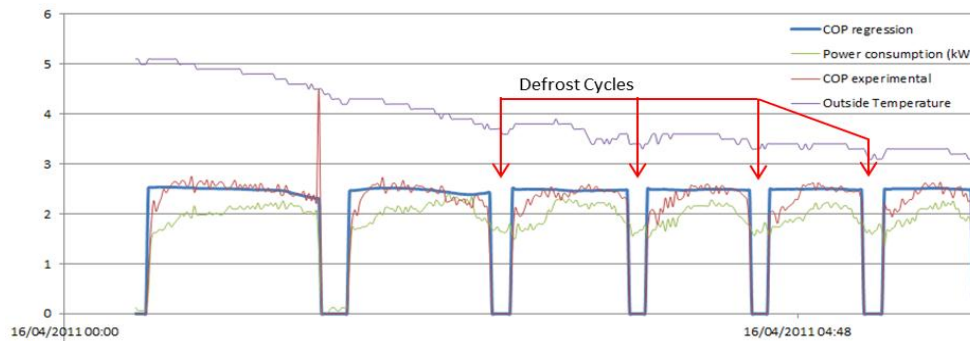


fig. 29 - Comparison of experimental COP with the calculated one when the system start and after a defrost cycle

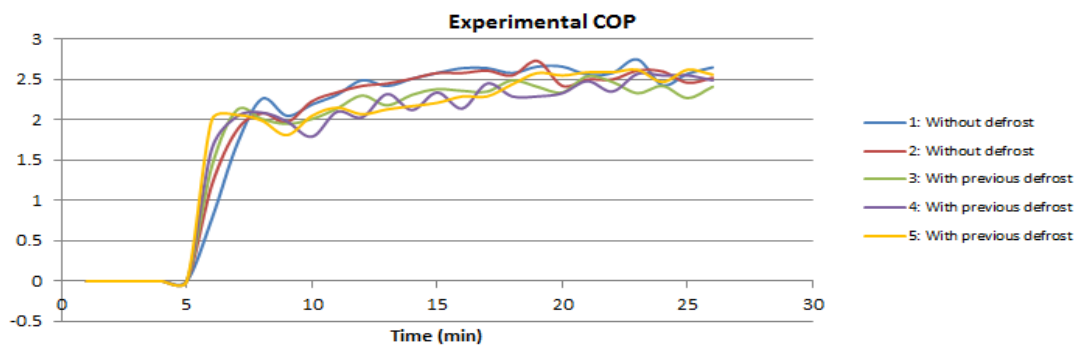


fig. 30 - Comparison of experimental COP at the start of the heat pump after a period of inactivity and after a defrost cycle

If the first 6 minutes at the heat pump starts are not considered, the mean relative error goes down to 5.4% and an average value 1.7% lower than the experimental data. These values seem acceptable and within the range of the precision of the measurement realised on the Finnish installation.

Otherwise, no important losses in efficiency are noticed when the heat pump operates with ice on the evaporator, before the defrost cycles. The system must indeed trigger the defrost cycle at the right moment in most of the cases, or one can wonder if it is not a bit too early.

4.1.2 Study of the defrost cycle

For the dynamic model, it will be required to model the defrost cycles of the heat pump which impact its performances. From the monitored data, it is therefore necessary to identify the time of frost formation and the energy required for the defrost operation in function of the outside air conditions.

The data collected from the Finish Installation

The air relative humidity is not monitored on the Finnish installation but was collected from a weather station located at around 8km from the installations (fig. 31). The measurements are available thanks to the project Helsinki Testbed [45]. They are realised at 4 meters height above the ground and are collected every 5 minutes.



fig. 31 - Location of the weather station from which the relative humidity data was collected (From Google Map)

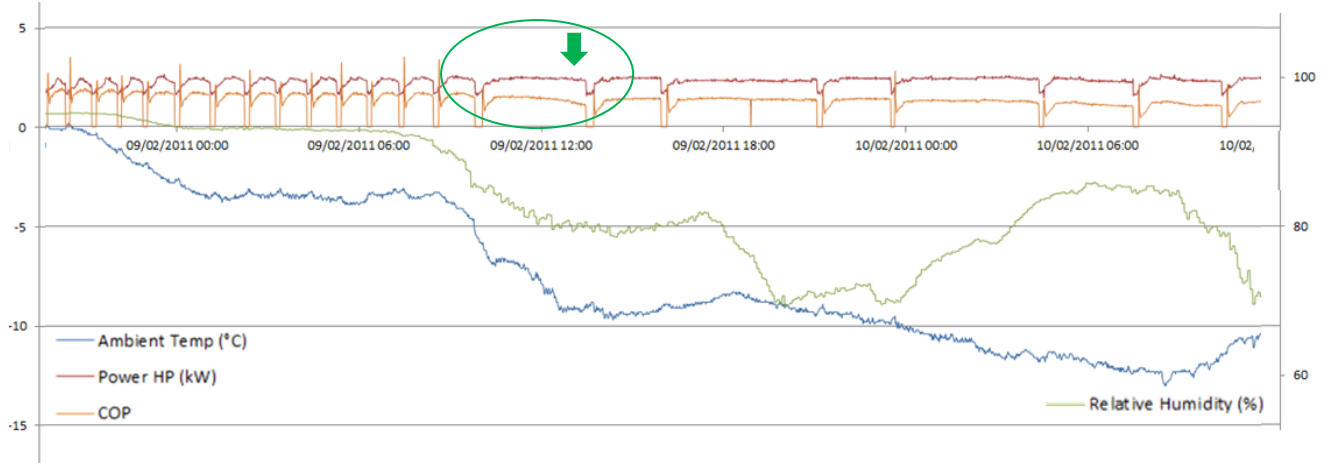


fig. 32 - Graph of the data collected from the Finnish installation on the 9th and 10th of February 2010

The data were then processed to repair the damaged measurement and make match the time-step between the two sources. The fig. 32 shows a sample of the data for the month of February 2011. The graph highlights the influence of the temperature and the relative humidity on the frequency of the defrost cycles. The lower the temperature and the relative humidity are (but below 5°C), the more time is required for the ice to form on the pipes.

Conditions of frost formation

It is first required to find in which conditions (air temperature and relative humidity) it can be considered that some ice starts forming on the pipes of the evaporator. This task is difficult since the data collected enable to know when the system starts a defrost cycles but not when the ice starts forming. The dynamic variations of the outside air parameters and the heat pump capacity as well as the occasional stops of the compressor don't help to identify these particular conditions. In addition, as underlined in the literature review, there is no guarantee that the heat pump detects properly the frost formation. For example in fig. 32, it can be seen that a defrost cycle (green circle) is carried out later than expected in comparison with other defrost cycles. A significant decrease of the COP is therefore occurring.

A priori, it should be considered that the limit air temperature and relative humidity are both interrelated. However, with the limited precision of the data, it can only be shown that:

- ✓ When the relative humidity decreases below 60%, it tends to induce long periods without any defrost cycles required (fig. 33 and fig. 34).
- ✓ At high humidity, when the outside air temperature is above 5.5°C (fig. 35), it can be seen that no defrost cycles are required.

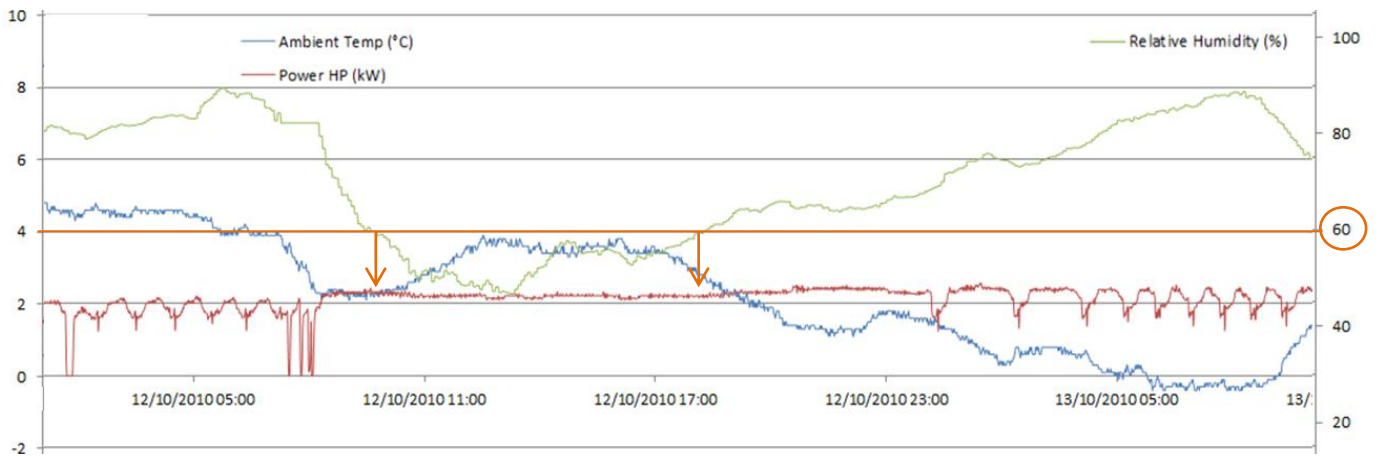


fig. 33 - Graph of the data collected from the Finnish installation on 12th of October 2010

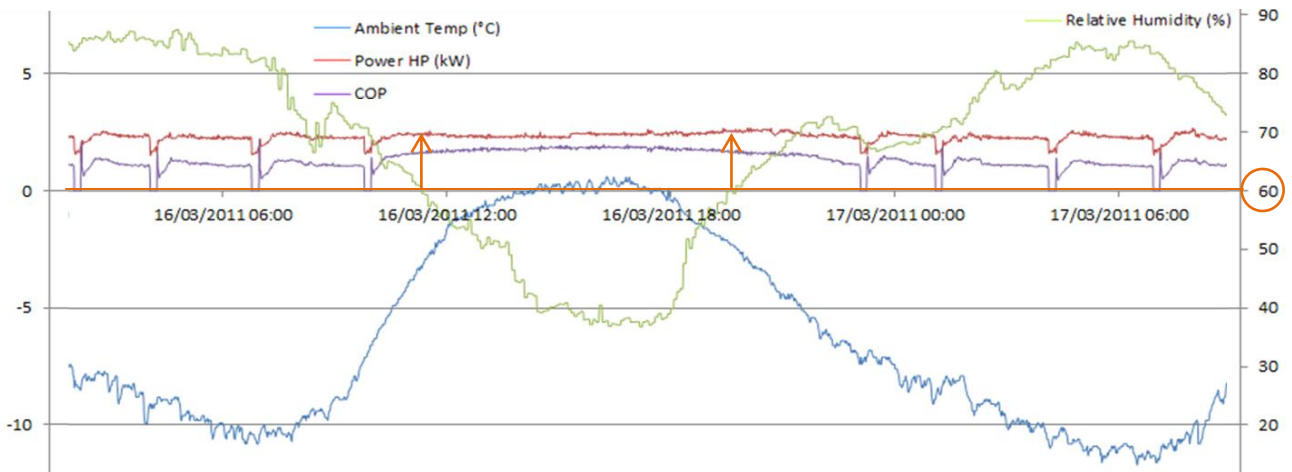


fig. 34 - Graph of the data collected from the Finnish installation on 16th of March 2010

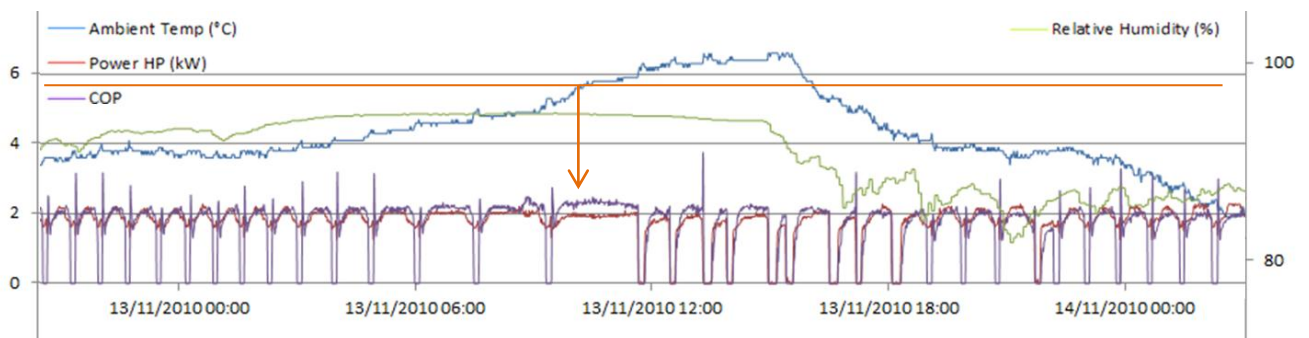


fig. 35 - Graph of the data collected from the Finnish installation on the 22nd of April 2011

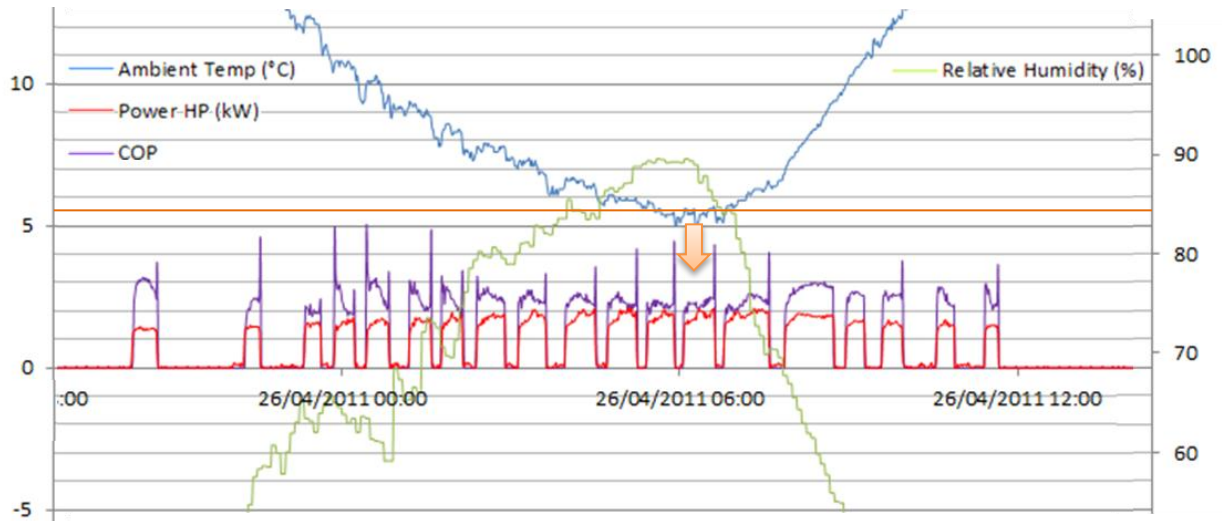


fig. 36 - Graph of the data collected from the Finnish installation on 26th of April 2011

Analysis of the time of ice formation

An excel spread sheet was then used to realise a more systematic analysis of the data. When the heat pump is in operation at an outside temperature lower than 5.5°C and a relative humidity higher than 60%, it is considered that the ice starts forming on the pipes of the evaporator. It is then possible to calculate the length of the ice formation and analyse it in function of the mean outside temperature and relative humidity over the period. Over the 7 months of monitoring, more than 2800 cycles are identified and are represented on the following graphs (fig. 37 and fig. 38).

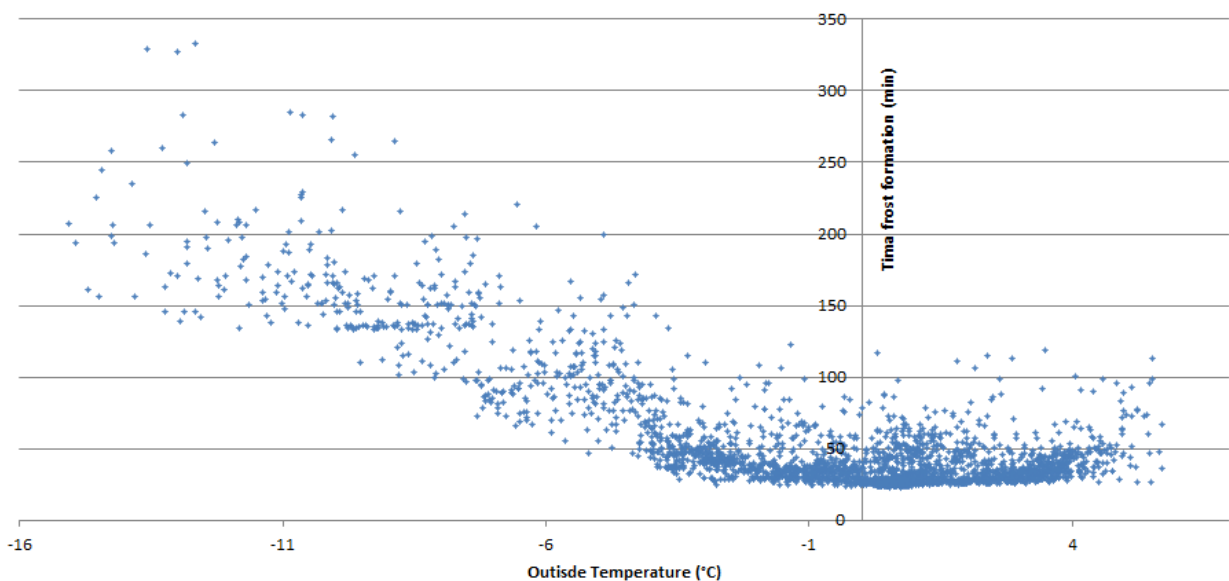


fig. 37 - Time of frost formation in function of the mean outside temperature

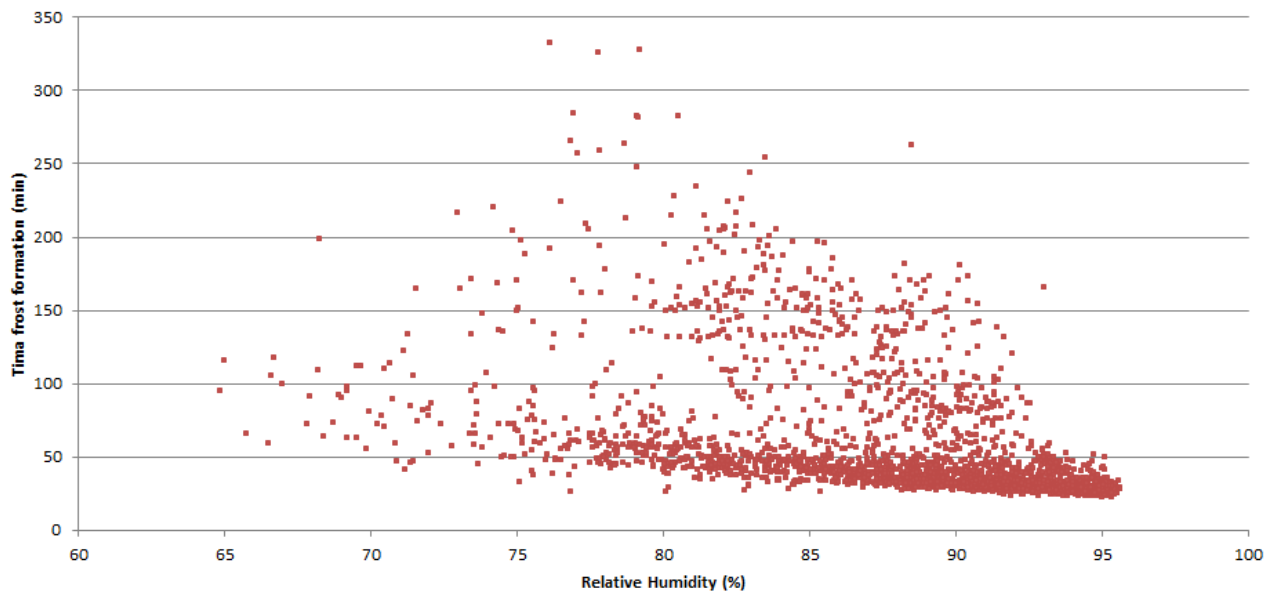


fig. 38 - Time of frost formation in function of the mean relative humidity

The trends highlighted in the literature review are confirmed by the data collected. When the air temperature and relative humidity increase, the ice formation is faster on the pipes of the evaporator.

For every heat pump, the time of ice formation depends on the outside air temperature, the relative humidity and the heat transfer through the evaporator. But normally, the heat pump tries to maintain if possible its heating capacity. The heat absorbed through the evaporator should stay therefore relatively constant assuming an operation at full capacity (although some fluctuation can occur in function of the actual thermodynamic cycle and when the system reaches the limits of the devices).

In this study, the ice formation is assumed to depend mainly on the outside air temperature and relative humidity. A regression (table 6) is therefore realised in function of these 2 variables similarly to the one realised during the previous group project. The best correlation is obtained by expressing the time of frost formation in function of the parameter presented in the table below (table 6). In comparison with the regression made in the previous project, 2 other coefficients (RH^2 and $RH * T_{out}$) have been added to avoid short length of ice formation at high relative humidity.

The correlation coefficient of the regression is not perfect but reaches 0.89. The error can be explained by the assumption realised, but also by the imprecision in the ice detection that occurs in most of heat pump as mentioned previously in the literature review.

Parameter	$RH * T_{out}$	RH^2	RH	T_{out}^3	T_{out}^2	T_{out}	Cst
Coefficient	0.234	0.0551	-11.6	0.06	1.23	-25.1	629.6
Error	0.014411	0.006454	1.102922	0.002796	0.032106	1.278004	46.92115
Correlation	0.89						

table 6 - Regression of the time of frost formation in function of the relative humidity and the outside temperature

A remark should also be made concerning the fact that it is the average values of the outside temperature and the relative humidity that are considered to characterize the ice formation. These parameters are however most of the time fluctuating. The dependency of the time of frost formation in function is almost linear (fig. 38) and is therefore not too problematic. However for the outside temperature, the relation is clearly non-linear. In these conditions the time of frost formation at the average temperature considered is not equal at the real time of frost formation considering the temperature fluctuations. Nevertheless, the temperature fluctuations during the periods of ice formation, which last between 25 to 150 minutes for 90% of the cases, stay limited.

Energy used for the defrost cycles

The energy used for the defrost cycles can also be calculated and analysed in function of the outside temperature and the time of ice formation. Chen et al. [44] highlighted that the energy required for the defrost cycles are higher at lower temperatures and low relative humidity in

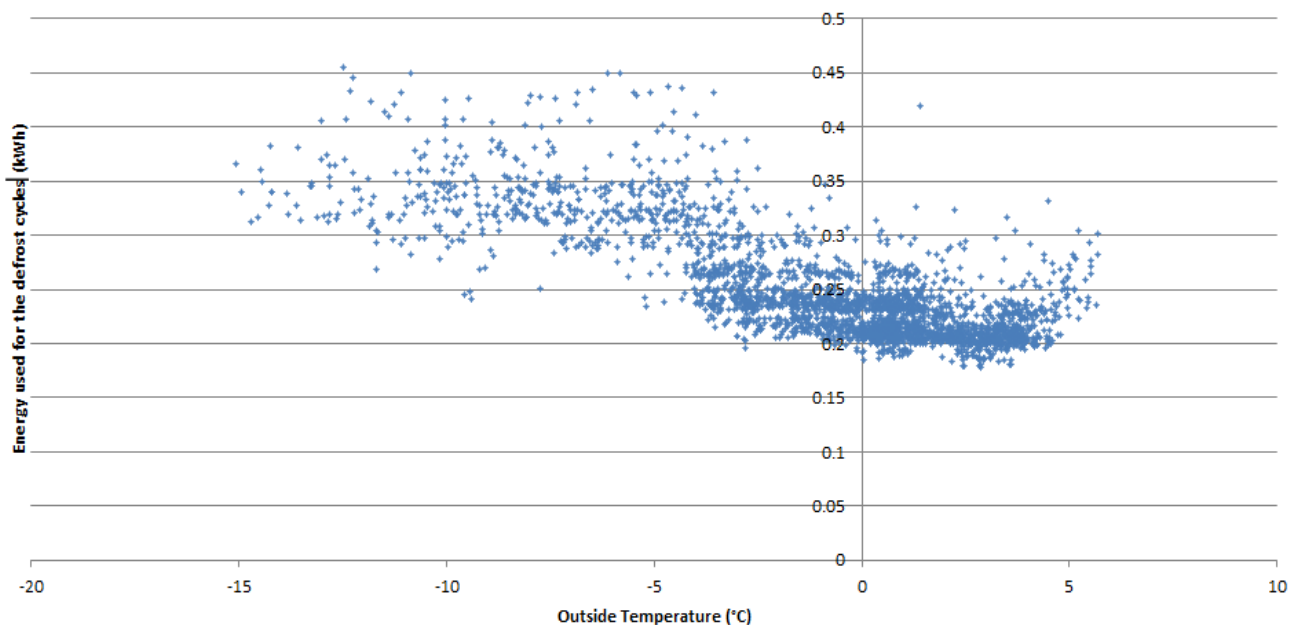


fig. 39 - Energy used for defrost cycles in function of the mean outside temperature during the ice formation

the case of a reverse-cycle to defrost the evaporator. Even if the defrost mode is different (hot gas bypass), the trend is similar in the Finnish data collected. In particular, it is more difficult with a lower outside temperature to defrost the evaporator (fig. 39). However these parameters alone give a regression of order 3 whose correlation is not higher than 0.73.

Actually the same level of correlation can be given by considering the energy required in function of the time of frost formation (fig. 40). It could be explained by the fact that, when the ice forms more slowly, its density is higher since the ice crystals have more time to be properly arranged. Then an ice of higher density will require more energy to be melted.

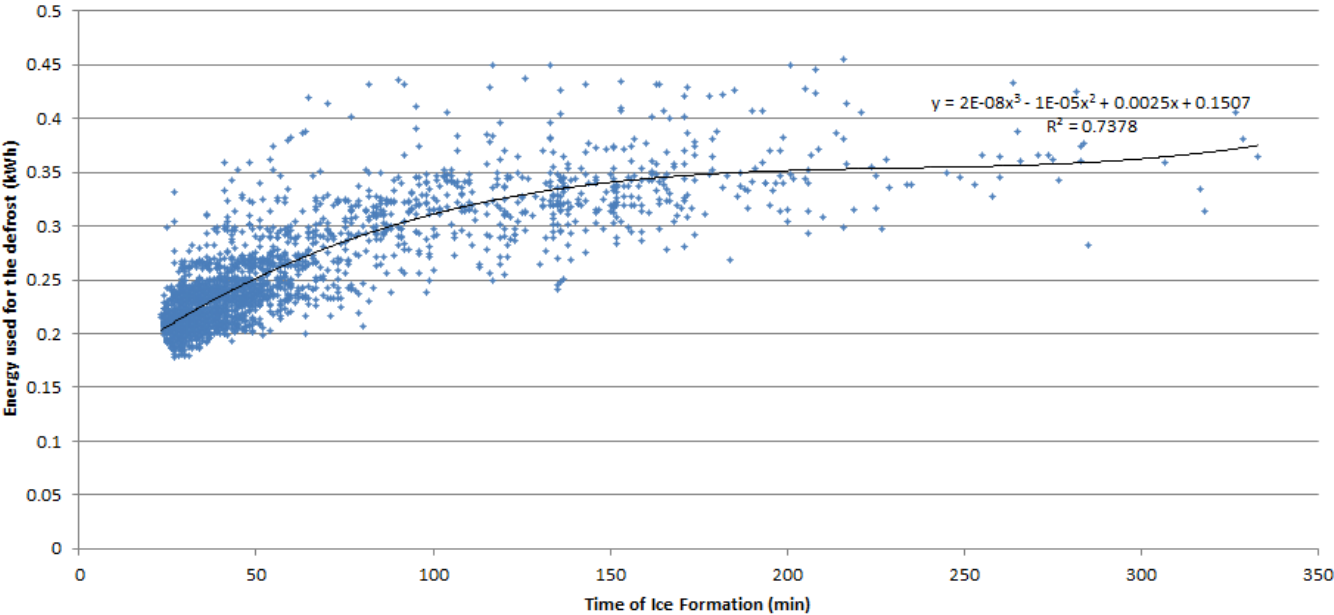


fig. 40 - Energy used for the Defrost in function of the ice of frost formation

In addition, the correlation can be a bit improved by considering both the time of frost formation and the outside temperature as presented on the table 7. The imperfections in the correlation (0.79) can be partially justified by the random behaviour of heat pump whose control is probably imperfect.

Parameter	T_{out}^2	T_{out}	T_f^3	T_f^2	T_f	Cst
Coefficient	-0.000311	-0.00489	1.65E-08	-1.03E-05	0.00226	0.163
Error	0.0000307	0.000189	1.72E-09	7.29E-07	8.01E-05	0.00222
Correlation	0.79					

table 7 - Regression of the Energy used for the defrost in function of the outside temperature and the Time of ice formation

4.2 Analysis of the data collected by the previous group project on the CO₂ heat pump

The monitoring data collected by the previous group project on two installations in Scotland are also considered in this analysis. It is in this case **the more recent version of the Sanyo Eco Cute system**, with a capacity twice as high (9kW), which is concerned. As it was not possible on these systems to measure the heat output of system for technical reasons, the analysis of the performances are limited and the focus will be mainly on the defrost cycles and the electrical power consumption.

4.2.1 Performances of the system

The system monitored in this case was the more recent Sanyo heat pump of 9kW. According to the manufacturer, the performances of the system (the 3 COP given) are the same than for the smaller heat pump of 4.5kW. The temperature ranges during the system operation are very similar and it is only the mass flow in the gas cooler which double to carry the 9kW of heat produced by the system.

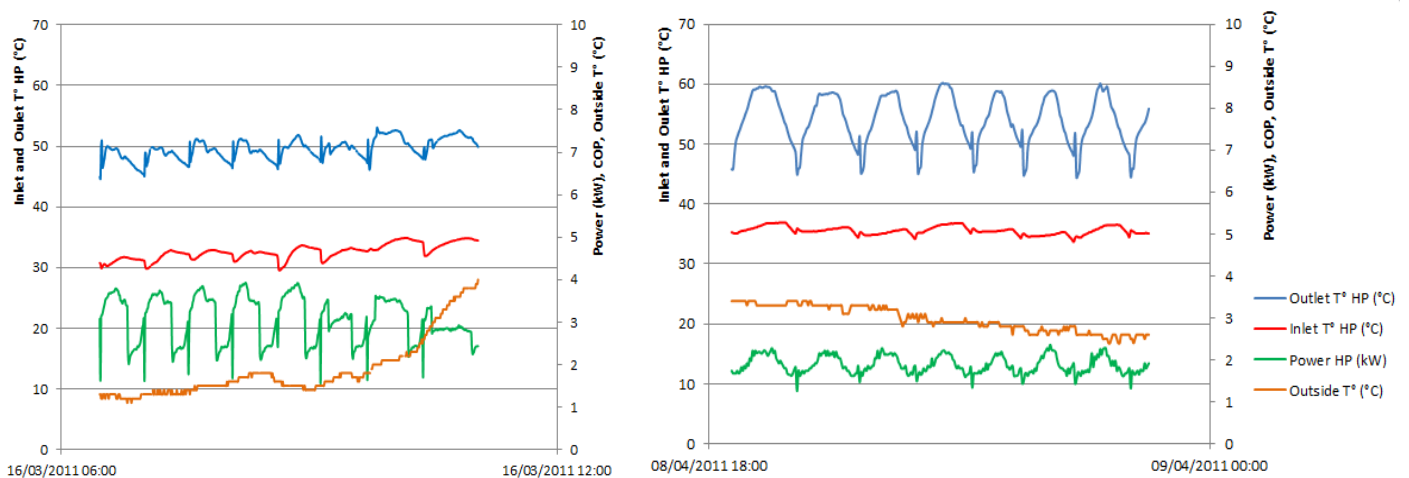


fig. 41 - Comparison of the dynamic fluctuations of the temperature at the outlet of the heat pump in Oban 9kW (left) and in Finland 4.5kW (right) in similar conditions of operation

Concerning the temperature at the inlet and outlet of the heat pump, while the small system of 4.5kW seems to present some inertia before reaching its nominal point of operation, the 9kW heat pump looks a bit more reactive after the defrost, as highlighted by the fig. 41. Within 3 minutes, the system of 9kW stabilizes its outlet temperature while the 4.5kW system in Finland requires 15 to 20 minutes. The more recent system seems to have better controls which enable to reach more quickly the optimal operation point of the heat pump.

4.2.2 Time of ice formation before defrosting

During the 2 weeks of monitoring on the 2 Sanyo installations monitored, 27 defrost cycles were recorded at certain air temperature and relative humidity. However the measurement from the relative humidity sensors doesn't seem very reliable. It is probable that the sensor was sometime receiving direct solar radiations or maybe rainfall since there is a lot of noise on the measurements during the day (fig. 42).

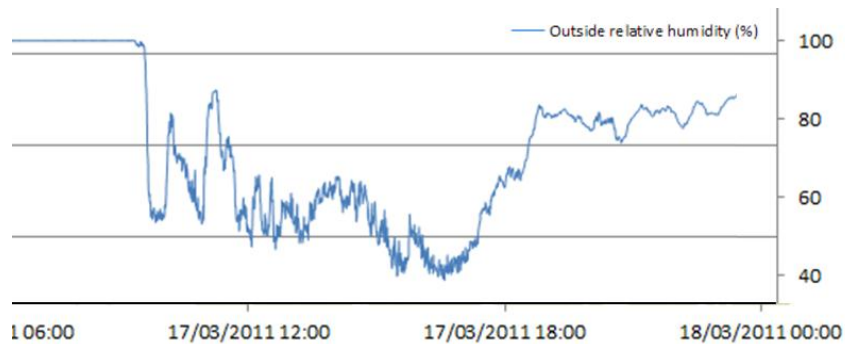


fig. 42 - Noise on the relative humidity measurement during the previous project

Finally 19 defrost cycles, for which the measured relative humidity seem reasonable, are compared with the Finnish installation behaviour. The time of ice formation can be calculated with the mean outside temperature and mean outside relative humidity during the ice formation. The comparison of the measurement and the estimation from the regression (paragraph 4.1.1) is presented in fig. 43.

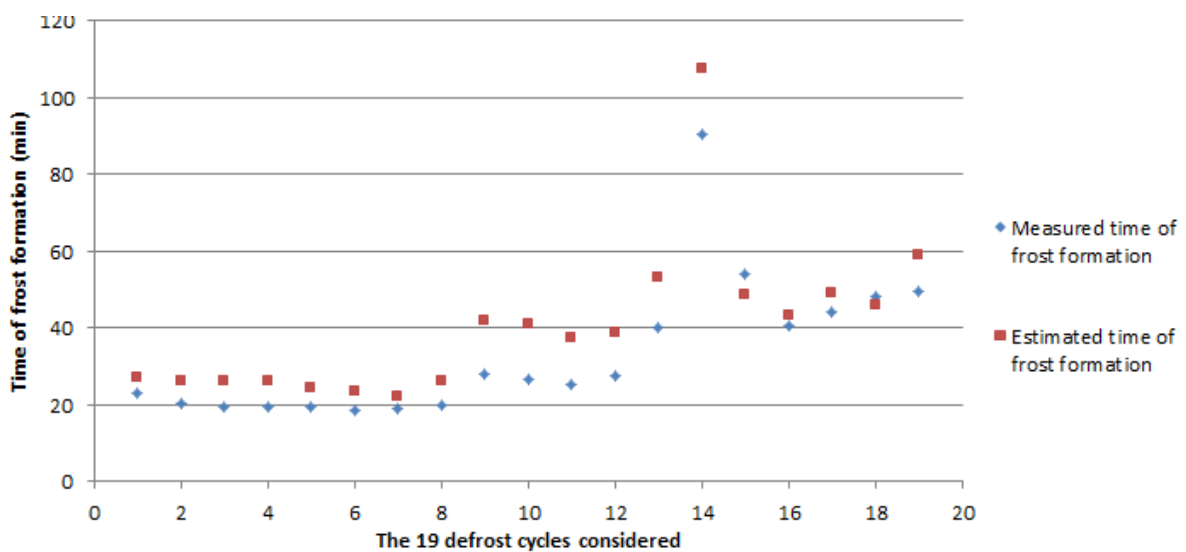


fig. 43 - Comparison of the time of frost formation measured on the Scottish installations with the estimation made with the previous regression

It can be seen that the time of frost formation measured and predicted follow the same trend. However the regression tends to be overestimating a bit the real time of ice formation. In particular, the Sanyo system installed in Scotland can form the ice in less than 20 minutes while the minimum noticed on the previous system was 24 minutes. The new system is characterized by a power twice as much important (9kW) than the old one (4.5kW). But the size of the heat pump has also double to provide a higher capacity. Thus, there is a priori no reason that the ice form faster on the evaporator and it might be the controls which spark the defrost cycles or the way of detecting the ice may be different.

4.2.3 Energy used for defrost

The energy required for each of the 27 defrost cycles was recorded in function of the time of ice formation (fig. 44). As shown on the graph, the points representing the energy used for the defrost cycles are still relatively scattered, similarly to the data collected from the Finnish installation. It seems also that the energy required for the defrost cycles has doubled with a bit more than 0.4kWh for a quick ice formation to around 0.6kWh for an ice formation of 100 minutes. This behaviour can be explained by the size of the evaporator which has double in comparison with the system in Finland since the power is twice as high (cf. fig. 19 and fig. 20). During the defrost cycles, the average power used is 2.4 kW between 10 to 15 minutes.

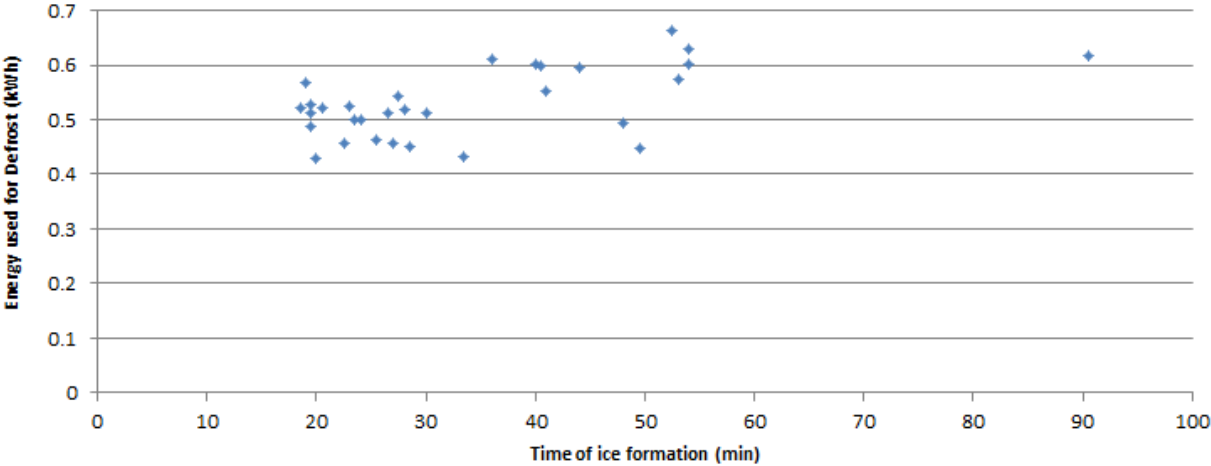


fig. 44 - Energy required for the defrost cycles in function of the time of ice formation

4.2.4 Electrical Power Consumption of the system

For the model of the heat pump, it is also required to characterize the electrical consumption of the heat pump. The main energy consumption is due to the compressor which has to compress the refrigerant to assure the operation of the thermodynamic cycle. In particular, it

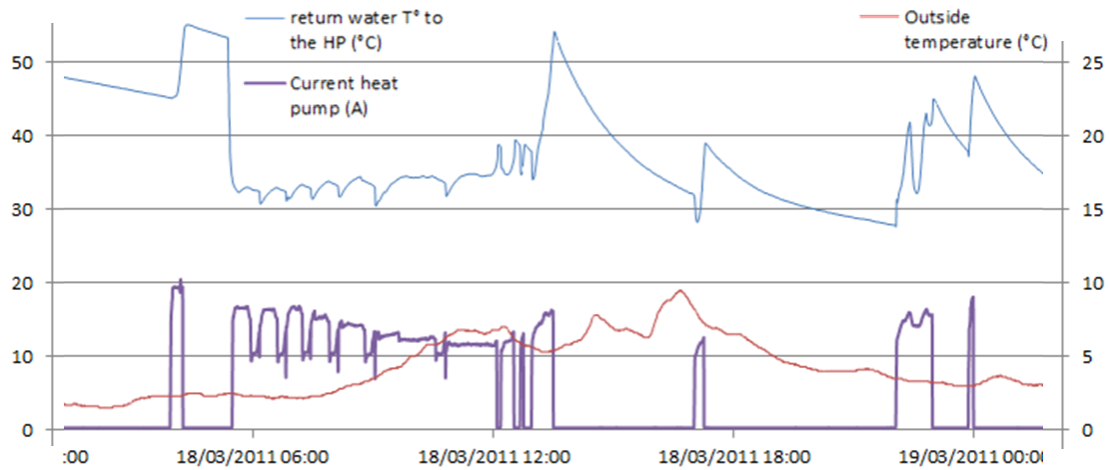


fig. 45 - Variation of the electrical consumption of the heat pump in function of the outside temperature and the return water temperature to the heat pump

tends to consume more energy at colder outside temperature and at higher return water temperature to the gas cooler since the compression rate is higher. This relation is verified on the monitored data as illustrated in the fig. 45.

Considering all the points of operation from the installation in Oban and Haddington, the graph of the electrical power in function of the outside temperature and return water temperature to the heat pump can be drawn (graphs given in appendix A). However a regression in function of these 2 parameters doesn't give a better correlation than 0.7. There might be hence to some extent a capacity control of the compressor to produce more or less heat in function of the needs.

It is also important to specify that the system has a maximum electrical input power. At low temperature, the compressor can reach its limit and the heating capacity can be reduced. For the Sanyo system monitored in Scotland (single-phased), the maximum power (as visible on the graph in appendix A) of the device is 4.5kW.

Finally, it can be noticed from the monitoring data that the power required for the control is around 60W for the heat pump and that the circulation pump used between the outside unit and the tank consume a power of around 90W.

4.3 Analysis of the installation in Oban

A particular attention is given to the installation of Oban which will be considered as a base case for the modelling work. A description of the house and monitored data is already presented in the website of the previous project. The main points are however reminded in

this section and the extra summer monitoring realised on the installation during this project is presented. These monitored data will be indeed used to validate a model of this installation.

4.3.1 House and system monitored

The house monitored in Oban is a new build detached house of 135m² occupied by 2 retirees. The house was built with significant amount of insulations and the windows are double glazed (the U-values are given in the table 8). A plan of the house is presented appendix B and its orientation is North-West (-55° from the North direction). A Sanyo Eco Cute system adapted for the European market with a heat pump of 9kW has been installed in 2010 and provides both space heating and domestic hot water for the occupants.

	Wall	Floor	Ceiling
Thickness (mm)	140	150	340
Conductivity (W/mK)	0.035	0.022	0.044

table 8 - Insulation characteristics in the case study in Oban

The system has been set up to run from 6am in the morning to 11pm in function of the demand. The house is totally heated with an under-floor heating system which is fed at a water temperature varying between 35 and 40°C. One sensor is located at the back of the house control the temperature with a set point of 22°C. The whole house is heated on the same way everywhere. The domestic hot water consumption of both occupants is relatively high since they take baths almost every day.



fig. 46 - House monitored in Oban



fig. 47- The Sanyo CO₂ heat pump in Oban

The 2 occupants are in general quite happy of the system performances. However they noticed that certain days, the system struggles to provide enough hot water for the bath.

Some monitoring of the installation has been realised during one week in March 2011 by the previous group project. The data and their analysis are presented on the website of the previous group project [32]. But another monitoring has been realised for this project during 2 weeks in July in order to study the behaviour of the system providing only domestic hot water in summer.

4.3.2 Summer monitoring

The same monitoring kit than for the previous project was used. With a main logger connected wirelessly to different sensors placed on the strategic points of the installation (fig. 48), 9 measurements were collected and stored every 30 seconds during the 14 days:

- ✓ 2 measurement of the ambient air temperature outside and inside the house.
- ✓ 3 measurements of the current consumption for the heat pump, the tank (including the controls) and the water circulation pump between the heat pump and the tank.
- ✓ 4 measurement of water temperature at the inlet and outlet of the heat pump and for the domestic hot water. The measurement were realised on the water pipes by using some thermal compound to optimize the thermal contact. A small error and a delay might be induced by the copper used for the pipes, especially when there are quick changes of the water temperature. But it won't fundamentally modify the interpretation of the results.



fig. 48 - Monitoring kit used for the project

4.3.3 Heat pump operation in March

The fig. 49 and fig. 50 present the characteristics of the system operation during one day of the month of March. It shows that the heat pump operates mainly in the morning to heat the under-floor heating system. Once heated, the inertia of the heating system in combination with internal gains and heat gains is sufficient to provide the heat to the house during the whole day. The temperature in the house reaches 22.5°C around 6pm before decreasing.

The water that is sent to the under-floor heating system is at a temperature of 35 to 40°C. This temperature is controlled in function of the outside temperature. The blue curve represents the temperature of the cold water inlet to the tank. When there is no domestic hot water draw, the temperature increases because of the tank proximity.

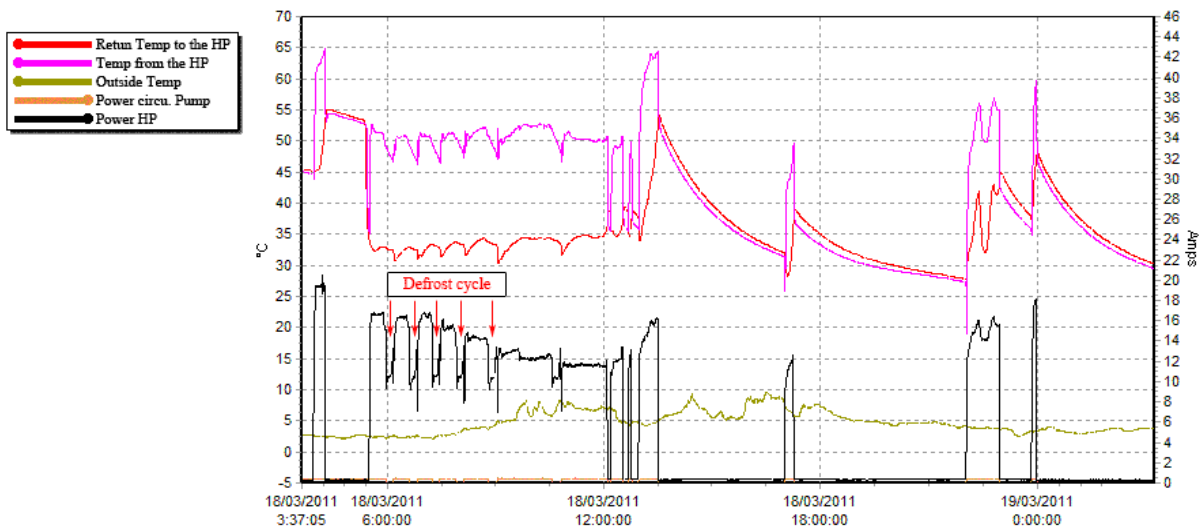


fig. 49 - Main parameters of the heat pump operation in Oban the 18/03/2011

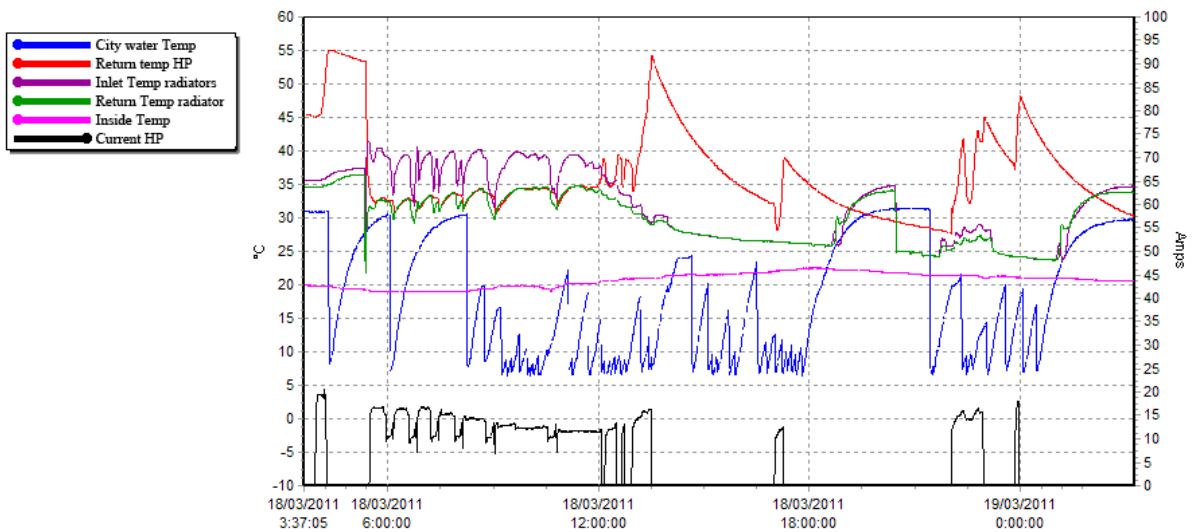


fig. 50 - Space heating and domestic hot water consumption in Oban the 18/03/2011

4.3.4 Heat pump operation in July

The system operation in July is reduced since there is no space heating and only domestic hot water required in the dwelling. In addition the heat pump seems to work at reduce capacity since the electrical consumption is rarely higher than 2kW. So even assuming a COP of 3, the heat output is not higher than 6kW.

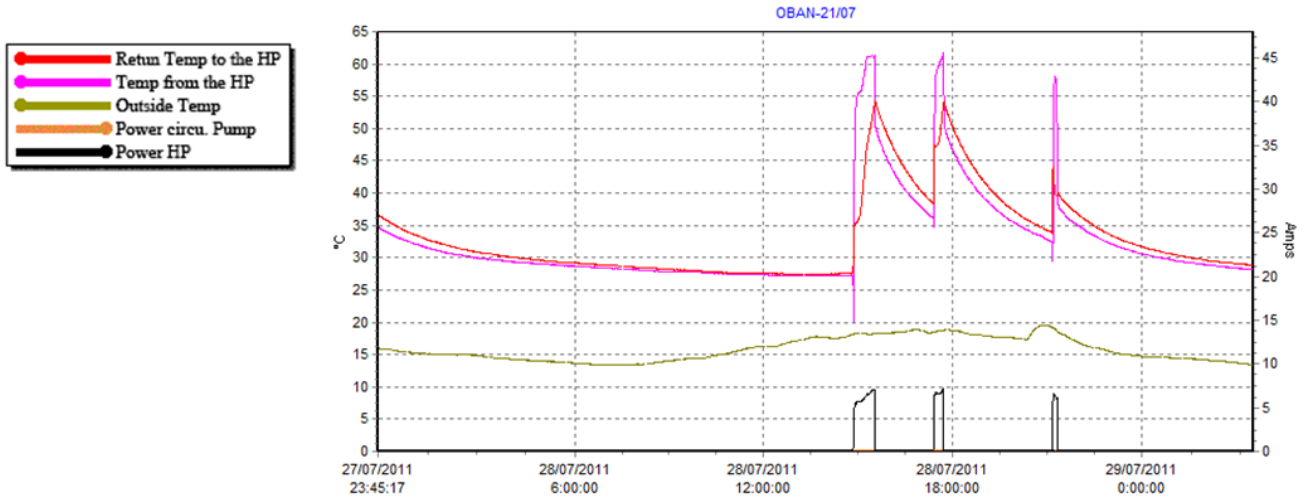


fig. 51 - Main parameters of the heat pump operation in Oban the 28/07/2011

Concerning the performances of the system, it can be seen that the return water temperature to the heat pump tends to rise very quickly when the heat pump start operating. It comes from the fact that the tank design is not really optimized with the hot water flow from the heat pump arriving in the middle of the tank as mentioned in the literature review.

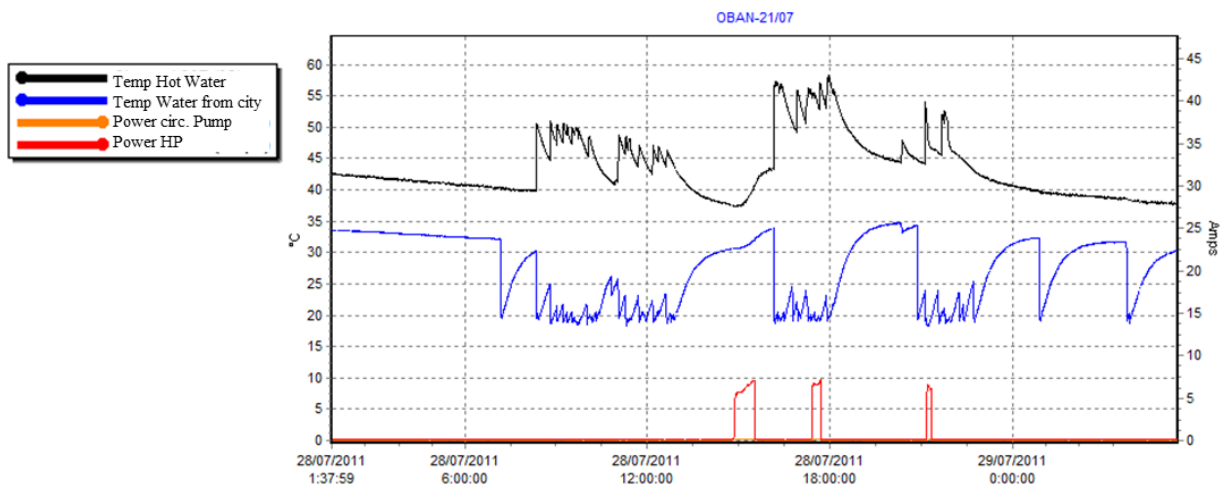


fig. 52 - Domestic hot water draw in Oban the 28/07/2011

The fig. 52 characterizes the domestic hot water draw for a typical day of July. The cold inlet of the city is at a temperature of around 19°C and is heated up to a temperature of 47 to 57°C. The analysis of one week of monitoring from the 22nd to the 28th of July give a total electric consumption is 20.5kWh knowing that 35W are used for the stand-by controls when the heat pump is not operating.

Using the previous regression of the COP in function of the outside temperature and the water return temperature to the heat pump (paragraph 4.1.1), the heat output from the heat pump is estimated at 39.7kWh. The COP is only of 1.93 because 25% of the energy is consumed for the controls since the heat pump doesn't operate very often.

The heat generated is therefore only used for the domestic hot water including some additional losses. The domestic hot water draw per day can be therefore estimated considering a calorific capacity of 4200J/kg.K and a density of 1 kg/L:

$$V = \frac{39700 * 3600}{4200 * 31} * \frac{1}{7} = 156 \text{ l}$$

Considering that there are some losses in the system, the domestic hot water consumption is therefore estimated at around 150 litres of water at 50°C.

5 MODEL OF THE CO₂ HEAT PUMP DEVELOPED IN ESP-R

This part will present the model of the CO₂ heat pump developed in ESP-r. ESP-r has been chosen as the environment of development since this software, developed at the University of Strathclyde, enables to realise dynamic building simulations. The tool also includes a module to simulate plant such as hydronic heating system which fit the needs of this project. A model of a CO₂ heat pump will be therefore added to current library of component. The assumptions and simplifications realised will be discussed and analysed.

5.1 Purpose of the model and complexity required

The aim of this model is to simulate the heat pump operation in order to predict its SPF in a particular environment of operation. The heat pump environment for a specific installation is the climate in which the heat pump operates but also the type of house, the structure of the heating system, the controls of the systems and the occupants' behaviour. The model developed must therefore be adapted to this particular objective.

In the model that they developed, Madani et al. [17] insisted on the importance of choosing an appropriate degree of complexity for their model and suggest a road map for finding the required complexity of the model based on the type of analysis (fig. 53). An adapted complexity is indeed important to achieve relevant results while minimizing the calculations required.

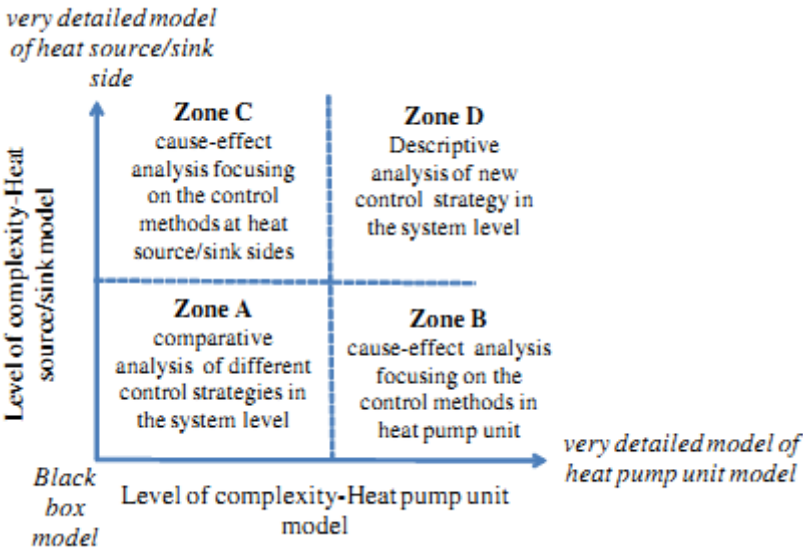


fig. 53 - Suggested road map for finding the required complexity of the sub-models based on the type of analysis[17]

In this project, there is no interest in the thermodynamic cycle of the heat pump since it is not the object of this study. As the focus is on the heat pump environment, a simple black box model will be then sufficient by considering an electrical consumption and a heat production depending on the heat source and sink characteristics. A detailed model will be therefore required for the sink and source model. The heat source will be the outside air. Some climate data are available in ESP-r and will be used in the simulation. The heat sink is the building through the heating system which can be modelled in ESP-r. Hence, this software is totally adapted to develop this model. Considering the road map of Madani (fig. 53), this model will be located in the zone C.

5.2 Presentation of the model and modification required

A first model of an air to water heat pump has already been developed by Dr. Kelly from ESRU at the University of Strathclyde [15]. Modifications will therefore be implemented to adapt the model to the specificities of a CO₂ heat pump with new equations and in particular a new way of considering the defrost cycles.

The model is semi-empirical, type black box. It doesn't represent the fundamental equations of the thermodynamic cycle but is based on monitored data. It is a one node model which can be connected to a hydronic plant circuit in ESP-r. With internal equation specified, the heat pump transfers heat to a hydronic circuit which will be integrated in a building model in ESP-r.

5.2.1 COP

To estimate the amount of heat delivered to the heat pump at each time step, the key element of the model is to determine the COP of the system in function of the conditions operation.

In most of air source heat pump, the COP of the system depends mainly on the outside temperature and the return water temperature to the heat pump. For systems with conventional refrigerant, the COP can most of the time be expressed in function of the difference of these two temperatures. For the Sanyo system, the regression presented in the previous part (paragraph 4.1.1) is implemented. When this type of regression is used, it is important to be sure that the regression is valid in the range of value that will be used in the model. The regression is assumed to be valid for outside temperature in a range of -15 to 25°C and return water temperature in a range of 20 to 50°C. Beyond these limits, the regression can still be used but the results will have to be treated with caution.

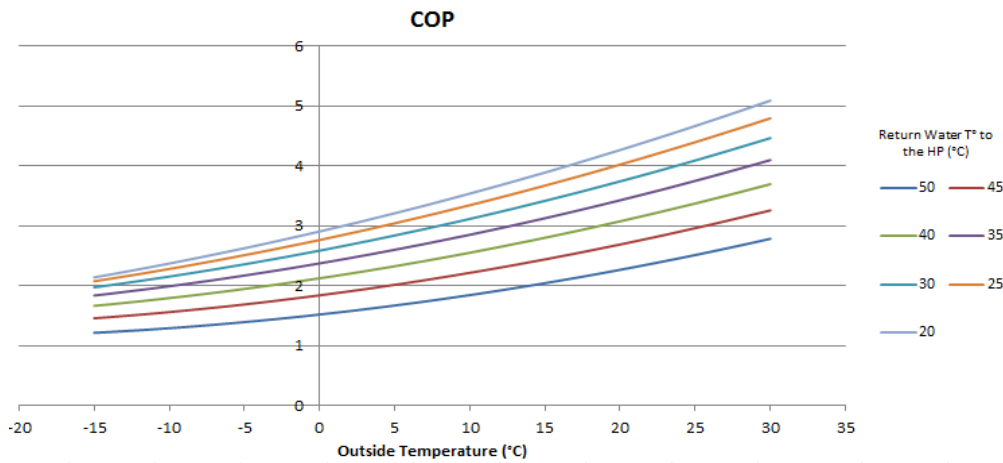


fig. 54 - Estimated COP in function of the outside temperature for different return water temperatures

It was noticed previously that there is some inertia when the heat pump starts operating. In ESP-r, a certain mass and specific heat can be associated to the plants components. Physically it would represent the inertia of the gas cooler at the starts of the heat pump. A certain U-value is also associated to the heat pump in order to express the losses with the environment. The values considered (table 9) have been calibrated with the monitored data in order to get a similar inertia and temperature variations when the heat pump starts operating.

Parameter	Mass of component (kg)	Mass weighted average specific heat (J/kgK)	UA modulus (W/K)
Value Used	14	2000	1.6

table 9 - Parameters used to represent the thermal inertia of the heat pump and the losses with the environment

5.2.2 Electrical input

The COP alone is not sufficient to express the heat output of the system and the electrical input power has also to be specified. In real systems, the electrical consumption is not a constant since the compressor will tend to work more at colder outside temperature or at higher return water temperature in order to compensate a decrease of the COP and maintain the heating capacity. That is why the Kelly model calculates the power consumption as a function of these 2 temperatures.

With the data collected during the previous project, the same trends than in real systems are observed but the variations of power cannot be always explained by the outside temperature and the return water temperature fluctuations. The internal control of the Sanyo system is

indeed not really known and it is possible that the heating capacity of the system is controlled to a certain extent in function of the needs.

In the model, the COP is already calculated in function of these parameters and the heat pump is normally controlled and dimensioned to provide a nominal output power of 9kW. Instead of giving an approximate equation for the power consumption, it is considered that the heat generated is 9kW at a certain COP. The power consumption is then calculated by dividing the nominal power by the COP. If the electrical power exceeds the maximum power of the compressor (4.5kW), the power consumption is fixed at 4.5kW and the heating capacity is reduced accordingly.

On the real system, it can be sometimes noticed that the system can exceed its nominal heat output at high outside temperature. It is here neglected in the model. The difference that could occur in the heat output in comparison with the real system is not too problematic. It would just mean that the heat generated is partially shifted in time, but the performances of the system are still assessed properly.

Finally, when the heat pump starts, it is considered that the power consumption increases progressively to reach at the end of the first minute the nominal power consumption.

5.2.3 Water mass flow and heat pump thermal inertia

In the model of Nick Kelly, the water mass flow through the gas cooler is controlled by the heat pump component. With a certain heat output from the heat pump, the mass flow determines the ΔT in the gas cooler. The lower the flow is, the higher will be the ΔT . It is however important to limit the outlet water temperature to be coherent with this the system behaviour. The mass flow is otherwise assumed to be constant when the heat pump is operating.

The default mass flow is fixed at 0.11 kg/s to make it fit the monitoring data concerning the CO₂ system. With a heat output of 9kW, the ΔT of the water in the gas cooler is around 20°C which is characteristic of the CO₂ heat pump. It can be more in certain situations and can be adapted if required.

In addition, a modification in the code enables to maintain the mass flow for a chosen amount of time (2 minutes by default) when the heat pump stops. It enables to get all the heat that the heat pump has by inertia, as it is made on the real system.

5.2.4 Controls of the heat pump

Concerning the controls, the model of Kelly has 2 parameters controlling the heat pump behaviour. Firstly, a control is implemented on the return water temperature to the heat pump, as it is generally done on real systems. The heat pump stops when the return temperature is too high. The set point of water return temperature can be fixed or can vary in function of the outside temperature to consider a system of temperature compensation.

In the Sanyo system, the heat pump won't be controlled by the return water temperature. However, the set point for the return temperature will be fixed at 48°C since it is a limit of operation for the heat pump which reaches an outlet temperature of 68°C. In the real system, when the inlet temperature becomes high, the mass flow in the gas cooler tends to increase and the ΔT decreases. In the monitoring data collected, the Sanyo system doesn't produce water at higher temperature than 65 - 70°C.

Secondly, the heat pump can also be controlled by another parameter external to the heat pump. It can be a tank temperature or directly the temperature of the room. Only an On-Off control can be implemented since no capacity control is considered in the model.

5.2.5 Defrost cycles

It is also possible to consider the defrost cycles during the dynamic simulations. In his model, Kelly considers that a defrost cycle is triggered when the ambient temperature becomes lower than 5°C. For a certain period that can be fixed or determined in function of the outside temperature and relative humidity, the heat pump is considered in defrost with no heat output while maintaining the same electrical consumption. A constant amount of time is after considered between each defrost to model the time of frost formation as long as the outside temperature stays below the limit defined at 5°C.

The way of modelling the defrost cycle is modified for the Sanyo system since quite a lot of data have been collected and analysed (paragraph 4.1.2) and the behaviour of the system proved to be relatively different from the Kelly model. The conditions of frost formation are first identified in function of the outside temperature and the relative humidity. The set points are fixed at a maximum of 5.5°C and a minimum of 60% of relative humidity. If the system meets these conditions, a period of ice formation is first considered. Its length depends on the temperature and relative humidity of the outside air. Then a certain energy is required to realise the defrost cycle. To estimate the time of ice formation and the energy used, the previous regressions established for the installation in Finland will be used (paragraph 4.1.2).

The energy used for the defrost cycle is however doubled as highlighted by the monitored data. The size of the heat pump and in particular the evaporator has indeed doubled which suggest that twice as much energy will be required for the defrost cycles.

The time of ice formation is calculated in function of the mean air temperature and relative humidity during the frost formation. In the model, progressing step by step, it is assumed that at each time step, a percentage of the ice formation process is realised in function of the air parameters. It is then considered that the speed of the process at the different step of the ice formation is always proportional to the average speed.

Another issue is that, the ice is not necessarily removed when the heat pump stop operating. It is therefore considered in the model, that, firstly the ice stays on the evaporator if the air temperature is below 0°C, and secondly that the ice will melt at a speed proportional to the outside air temperature if positive. The energy is indeed mainly required to melt the frost at a constant temperature (change of state) of around 0°C. The thermal resistance between the frost and the air is taken at 0.04 Km²/W, i.e. the value usually used for external surface resistance in building calculations (EN ISO 6946). Assuming a frost layer of 2mm just before the defrost with a density of 150kg/m³ (value taken from Zhiqiang work [46] and in a range confirmed by Hermes [35]) and a latent heat of 334kJ/Kg, the time of natural defrost of the evaporator is:

$$\Delta t (s) = \frac{h_{latent} * T_{thickness} * \rho_{frost}}{\frac{1}{R_{thermal}} * \Delta T} = \frac{334000 * 0.002 * 150}{25 * T_{out}} = \frac{4008}{T_{out}}$$

Then, the percentage of the frost removed per minute and °C is 1.5%. If the outside temperature is 5°C, the frost is therefore assumed to melt in 13.4 minutes.

A lot of approximations have been used in this calculation method of the ice formation. That is why a sensibility analysis will be conducted on this parameter. In particular, the speed of ice formation will be increased or decreased to study the impact on the performances and estimate to what extent it affects the performances of the system.

5.3 Test of the of the CO₂ heat pump model

Most of the equations in the model are directly reflecting the behaviour of the real system. Hence, the results will depend mainly on the quality of the equations used. A model including a house with the Sanyo System will be presented and analysed in detail in the paragraph 0. But firstly, the behaviour of the new heat pump component alone has to be checked.

The heat pump is tested with a model of an average UK house including a simple stratified tank and radiators with relatively high thermal inertia. The heat pump is controlled in function of the temperature in the tank and operates from 6am in the morning to 11pm. The simulation is realised with the climate data of the uk-temperate between the 15th and 17th of January at a time step of 10 seconds. The whole model is not presented in detail since the focus is only on the behaviour of the heat pump.

It can be seen on the previous graphs (fig. 57 and fig. 58) that the model behaves according to description given on the previous part.

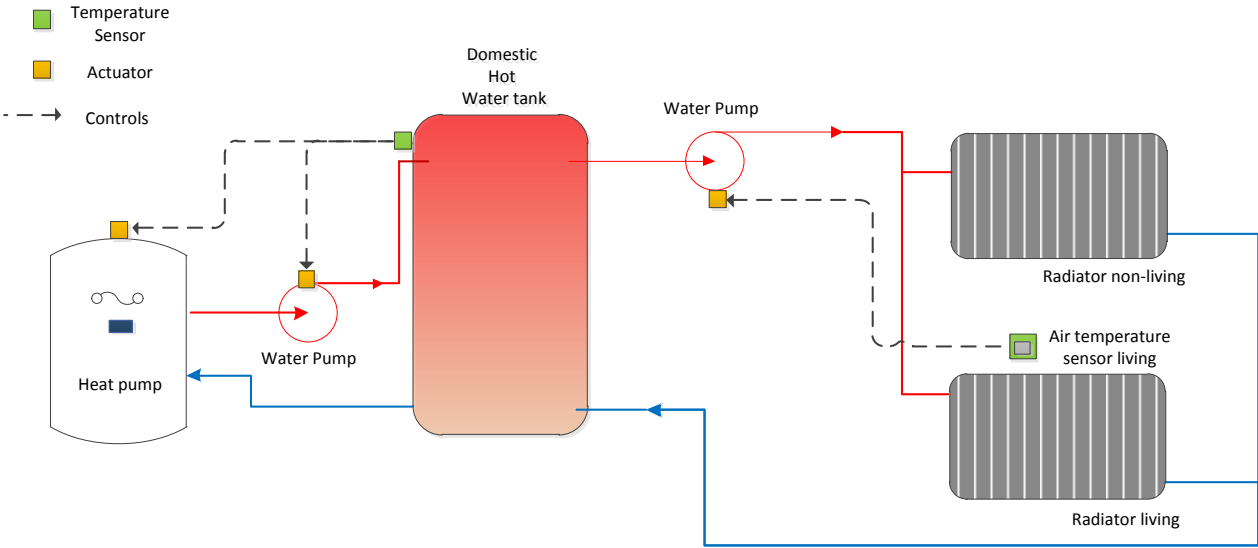


fig. 55 - Schema of the plant used for the test of the model

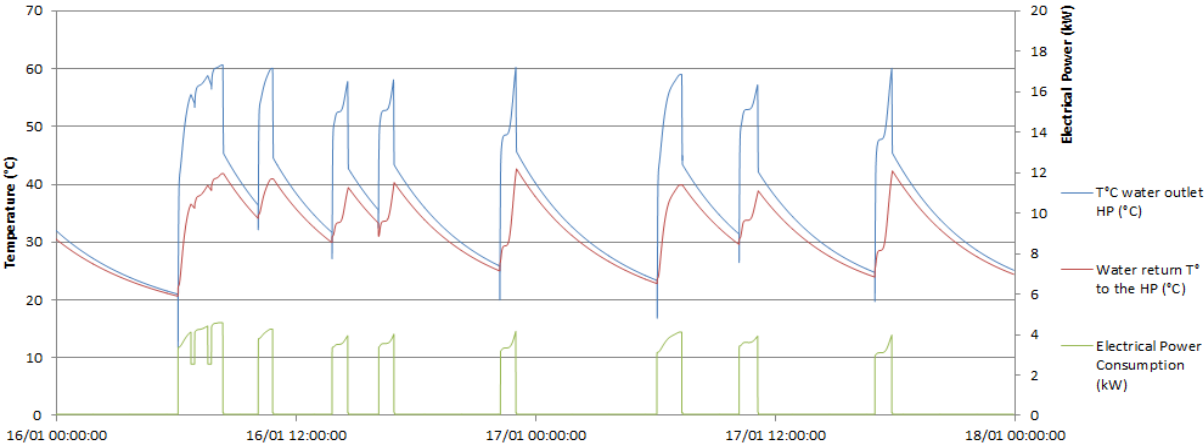


fig. 56 - Model test: temperature at the inlet and outlet of the heat pump and electrical power consumption

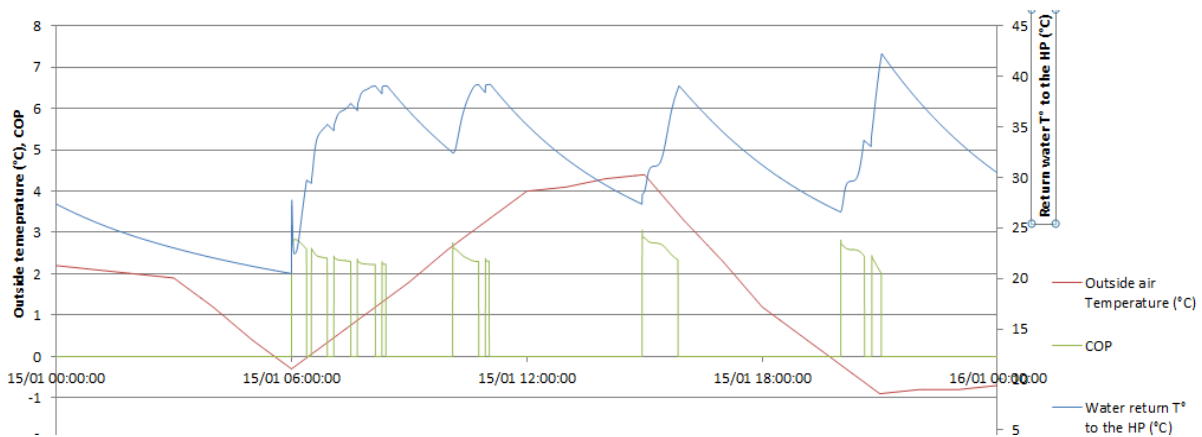


fig. 57 - Model test: coefficient of performance of the heat pump in correlation with the return temperature and the outside air temperature

When the heat pump is in operation, the component transfers heat to the fluid at a rate of 9kW if the capacity of the compressor is not exceeded. When the outside temperature is high and the return water temperature is low, the COP is maximized according to the equations implemented. The power consumed is calculated in function of the COP of the system. The higher the COP is, the lower will be the electrical consumption.

In addition it can be seen that some defrost cycles occur during the period. The fig. 58 shows the periods of ice formation and defrosting of the heat pump. At the beginning of the simulation, the system is in the conditions of ice formation. The time of ice formation is not constant and depends on the outside temperature and air relative humidity, as well as the energy used for the defrost cycles. Thus in the morning of the 15th of January, the ice form faster than on the 16th of January since the temperature is higher. But around 1pm on the 16th, the relative humidity decreases below 60% and the model doesn't consider any frost formation anymore.

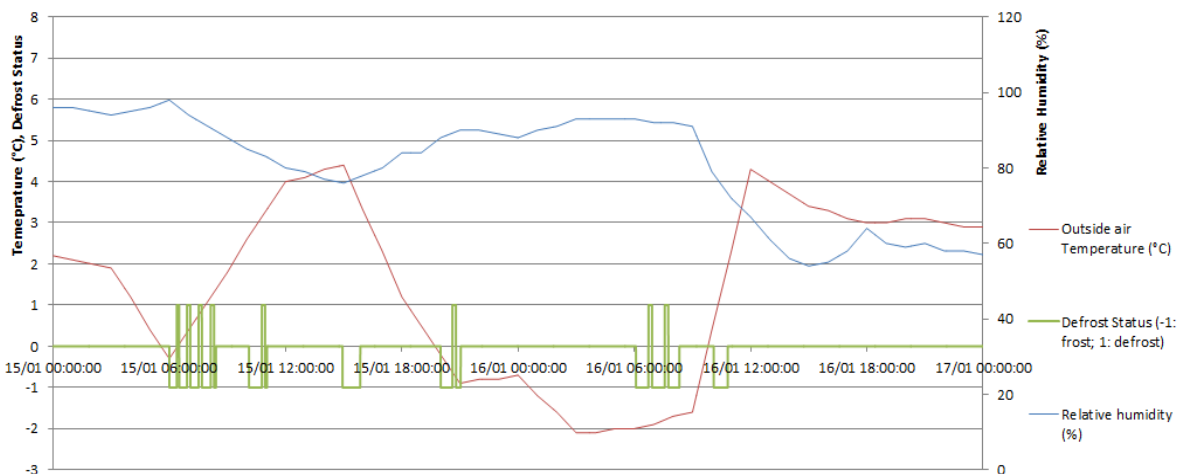


fig. 58 - Model Test: Defrost status of the heat pump in relation with the outside temperature and air humidity

As it is a dynamic model, a particular attention is given to the starts and stops of the system. It was previously noticed a certain thermal inertia at the heat pump start that is represented on the fig. 59. In particular, the circulation pump starts operating while the gas cooler is not hot yet. To represent this behaviour in the system, the power consumed by the heat pump is not considered as instantaneous but a little slope is implemented over the first minute. In term of inertia, the model is adapted to produce the required temperature within 2 minutes (fig. 59).

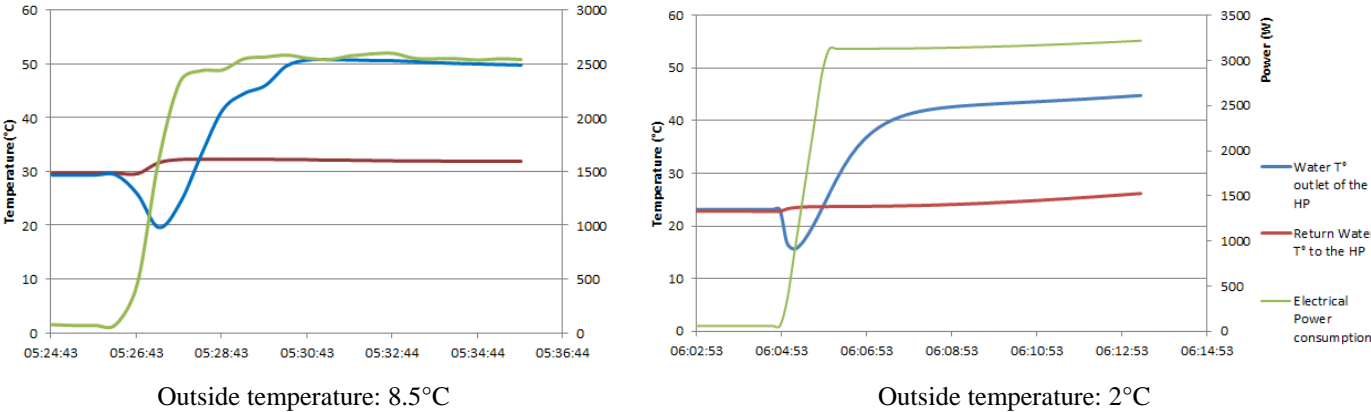


fig. 59 - Model test: comparison of the heat pump start in the model (graph on the left) and in the monitored data (graph on the right)

At the stop of the heat pump, the mass flow is maintained during 2 minutes to bring back the temperature of the heat pump outlet close to the inlet. During the three days of the simulation, the system heat pump performances are presented on the table 10. The heat produced by the heat pump can be considered for the COP. Otherwise the heat entering the tank can be considered and will include the heat losses with the outside environment and the effects of thermal inertia (table 10).

	Total electrical energy consumed	Heat produced by the heat pump	Heat entering the tank
	52.9 kWh	109.7 kWh	105.9 kWh
COP over the period		2.07	2.00

table 10 - Table heat pump performance in the test simulation (time-step 10seconds)

The average COP of this simulation is 2.07 by considering the heat produced by the heat pump. If the losses with the external environment are considered, the COP becomes 3.4% lower. In this case, it is important to underline that the COP is underestimated of 1% because some heat transfer occur between the pipes coming from heat pump and the house.

The performances of the system are relatively low due to the fact that 8 defrost cycles are triggered by the system and the return water temperature is relatively high (30 to 40°C). These conditions, in addition of the quite low outside air temperature are relatively unfavourable for the CO2 heat pump operation.

Different simulations have been also realised to study the influence of certain model parameters. In particular, the impact of maintaining the mass flow when the heat pump stops, simulating a progressive start of the compressor and using a higher time step are investigated. The results are presented in the table 11.

	Total electrical energy consumed	Heat produced by the heat pump	Heat entering the tank
Without maintaining the mass flow during 2 min after the heat pump stop	53.0 kWh	110.1 kWh	105.2 kWh
COP over the period		2.08	1.98
Without simulating a progressive start of the compressor	53.1 kWh	110.4 kWh	106.5 kWh
COP over the period		2.08	2.00
With a time-step of 1min (without maintaining the mass flow and starting progressively the compressor)	53.5 kWh	110.8 kWh	105.7 kWh
COP over the period		2.07	1.99

table 11 - Table heat pump performance in the test simulation

These figures show that the details used in the model for the starts and stops of the system don't impact seriously the system performances. In particular, maintaining the mass flow after the heat pump stops enables to increase of 1% the COP. Concerning the time-steps of the simulation, the results with the 1 minute time-step simulation are very similar to the 10 seconds time-step in term of COP and the energy values are slightly higher due to the lower resolution. A time step of 1 minute is therefore sufficient for the simulations.

With this first model, the sensibility of the parameters used in the model to define the defrost cycles can be analysed. However it must be underlined that the defrost cycles will have an impact more or less important in function of the characteristics of the installation considered. During the previous project, the first installation monitored was characterized by a lot of starts and stops of the heat pump which was operating on short periods. Less energy was then used to defrost of the evaporator than for the second installations where the system was running one long period in the morning.

For this model an intermediate situation were chosen with an average inertia for the system which require that the heat pump operates on more or less long periods in function of the weather. A sensibility analysis of the time of ice formation can be therefore realised. The energy used for the defrost cycles is calculated for different rates of ice formation as well as the relative error on the COP in comparison with the simulation of reference. But the impact on the COP depends also on the proportion of energy used for the defrost cycles. During the 3 days of simulation, the 15th of January concentrate 75% of the defrost cycles. It means that if the period had been less favourable more energy could have been required for the defrost cycles. To take it into consideration, an unfavourable case with twice as much energy used for the defrost cycle is also considered.

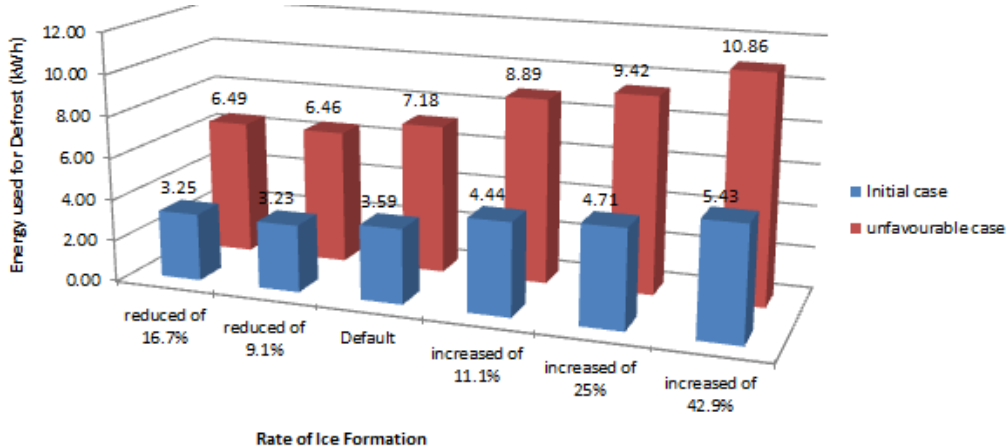


fig. 60 - Energy used for the Defrost in function of the rate of ice formation (time-step 10seconds)

The results of the simulation (fig. 60) show that the energy used for the defrost cycle can be increased by a factor similar to the one applied on the rate of ice formation. There is however a threshold effect in the phenomenon which is not directly proportional.

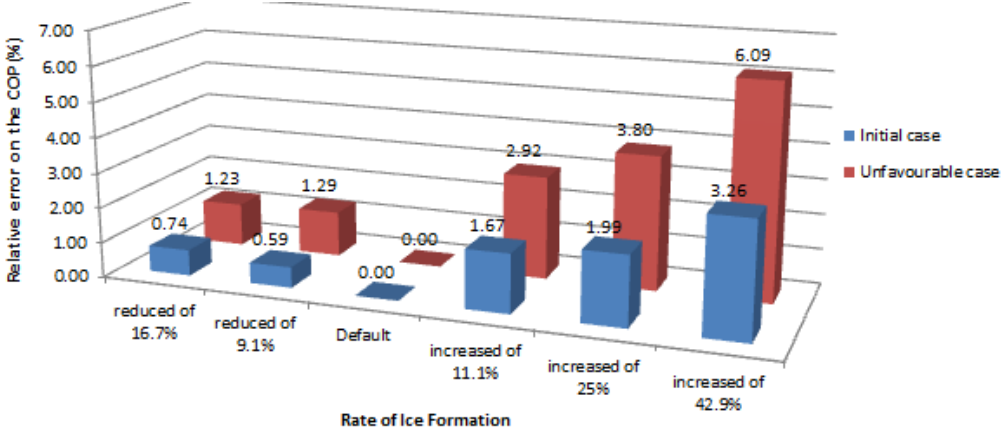


fig. 61 - Relative error on the COP induced by the change in the rate of Ice formation

In the initial case, 6.8% of the total energy consumed by the system is used for the defrost cycles. With a variation within 25% of the rate of ice formation, the relative error on the COP is lower than 2% (fig. 61). Considering the unfavourable case, where twice as much energy is assumed to be required for the defrost cycles, 12.6% of the energy consumed is used for the defrost cycles. With a similar behaviour in function of the rate of ice formation, the relative error on the COP is lower than 4% for a 25% variation of the rate of ice formation.

The general error on the COP stays limited but logically depends on the actual impact of the defrost cycles on the COP.

6 COMPARISON WITH THE MODEL OF KELLY

A complete model, including a detached house and its heating system, has been realised by Dr Kelly to run its heat pump model. This model will be used to implement the new CO₂ plant component developed and the results will be then compared with the Kelly model.

6.1 Description of the model

The building modelled is a 2 storey detached house of 135m² with 3 zones: living, non-living and loft. The characteristics of the house represent the average UK housing with the main U-values presented on the table below (fig. 63). The operational details considered simulate a full occupation of the house by four people during the day. The casual gain due to the people, the electrical equipment and lighting represent a total of 8W/m². The infiltration rate is fixed at 0.5 ac/h and increases if the temperature in the room rises. It enables to avoid overheating in summer and simulates the windows opening. More information about the building model are given in appendix B.

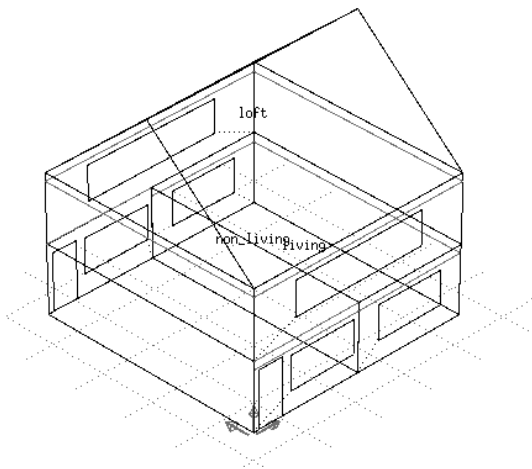


fig. 62 - Schema of the house used in Kelly's Model

	U-value
Walls	0.45
Glazing	3.3
Roof	0.25
Ground Floor	0.6

fig. 63 - Table of the U-values of the house model

The heating system structure is presented in fig. 64. The heat pump feeds the radiators and/or the domestic hot water tank with a double control on its operation: the temperature in the living area and the temperature in the tank. The valve on the pipe going to the domestic hot water tank is also proportionally controlled by the tank temperature. The priority is given to the supply of the domestic hot water. The controls with the set points are summarized on the table 12.

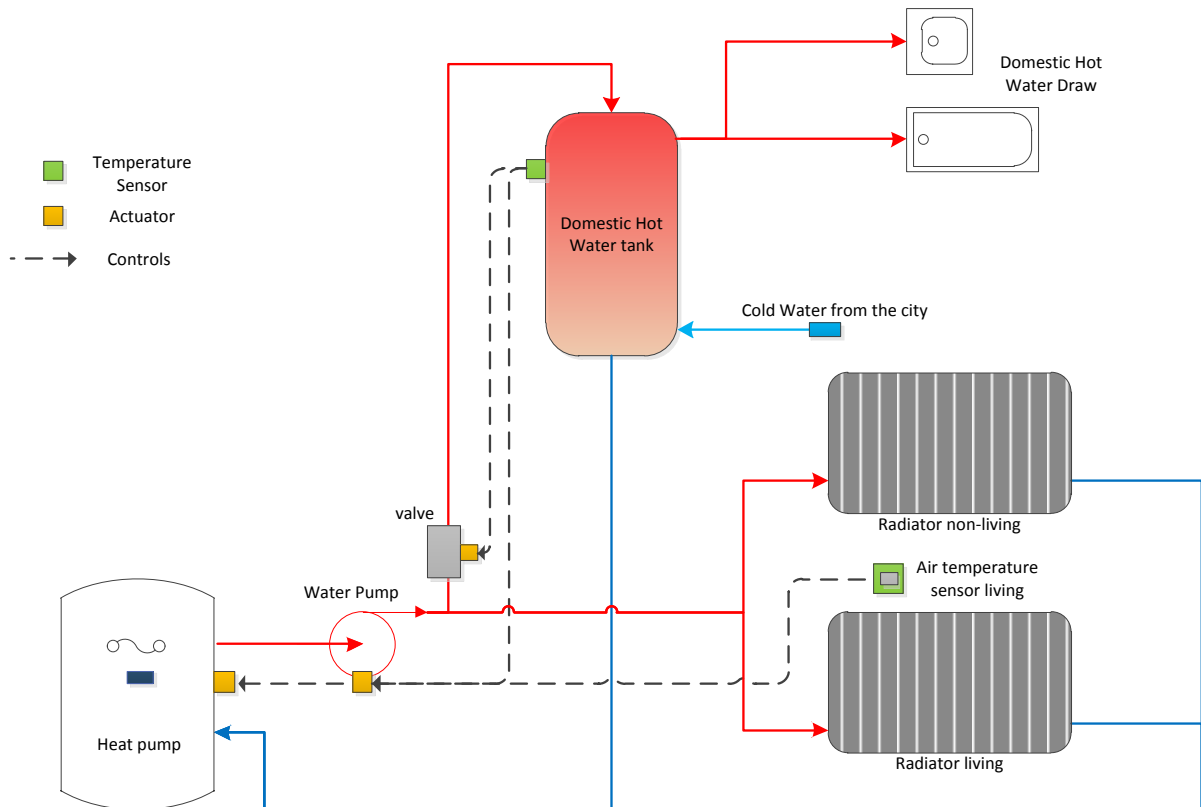


fig. 64 - Schema of the heating system of the model of Dr Kelly

Sensor	Actuator	Type of control	Setpoints	Period operation
Tank temperature	Pump	ON-OFF control	40 – 43 °C	6am – 23pm
	Valve : diversion ratio	Proportional control	40 – 45 °C	6am – 23pm
Room Temperature	Pump	ON-OFF control	20.5 – 21.5 °C	7am – 23pm

table 12 - Controls with set points used in the Kelly model

The domestic hot water draw in the model is taken at 122 litres per day, assuming a family of 4 persons, in correspondence with the IEA/ECBCS Annex 42.

This model is used to simulate both the heat pump of Kelly and the CO₂ heat pump with the average UK-climate for 1 week of January (7th to 15th of January 2011). During this period, the ambient air temperature fluctuates between -1 and 8°C for a mean value of 4.87°C. The relative humidity varies between 68 and 98% for a mean value at 81.8%. The time-step used is the minute and the results for different simulation are compared.

6.2 Results of the simulations

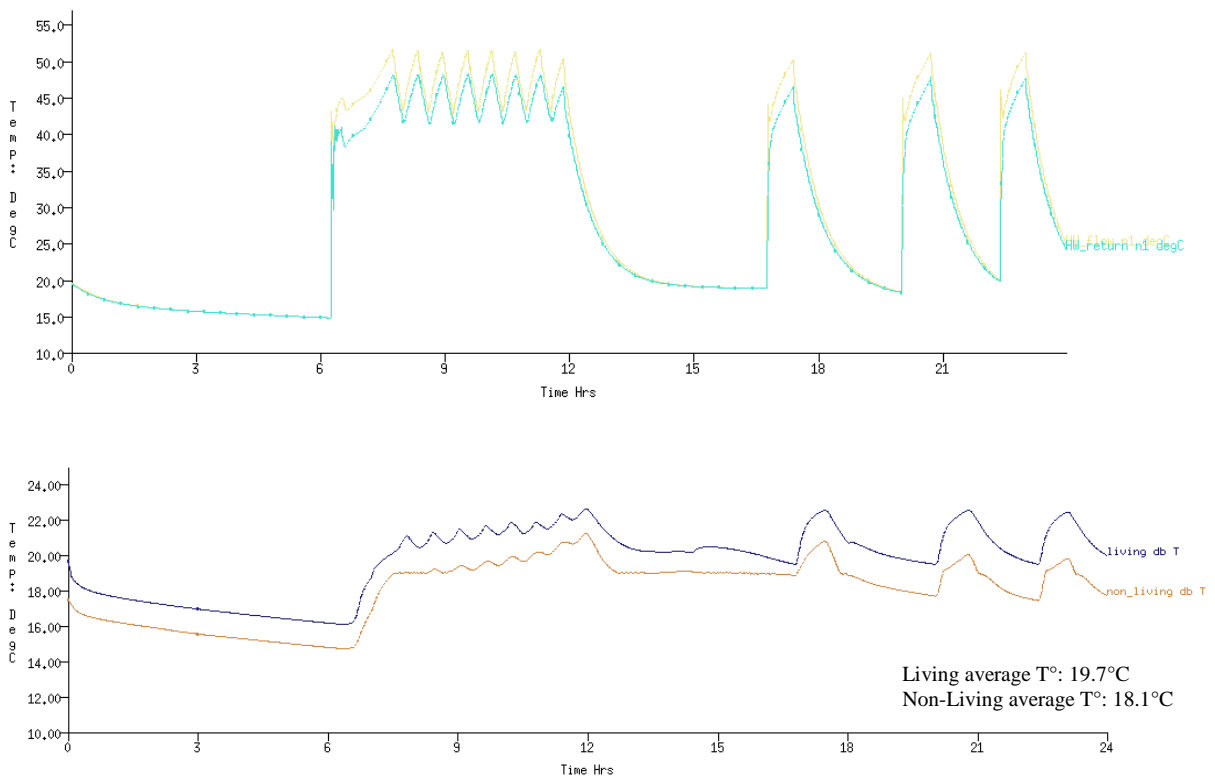


fig. 65 - Temperature at the inlet and outlet of the heat pump for the Kelly model (without the consideration of the defrost cycles)

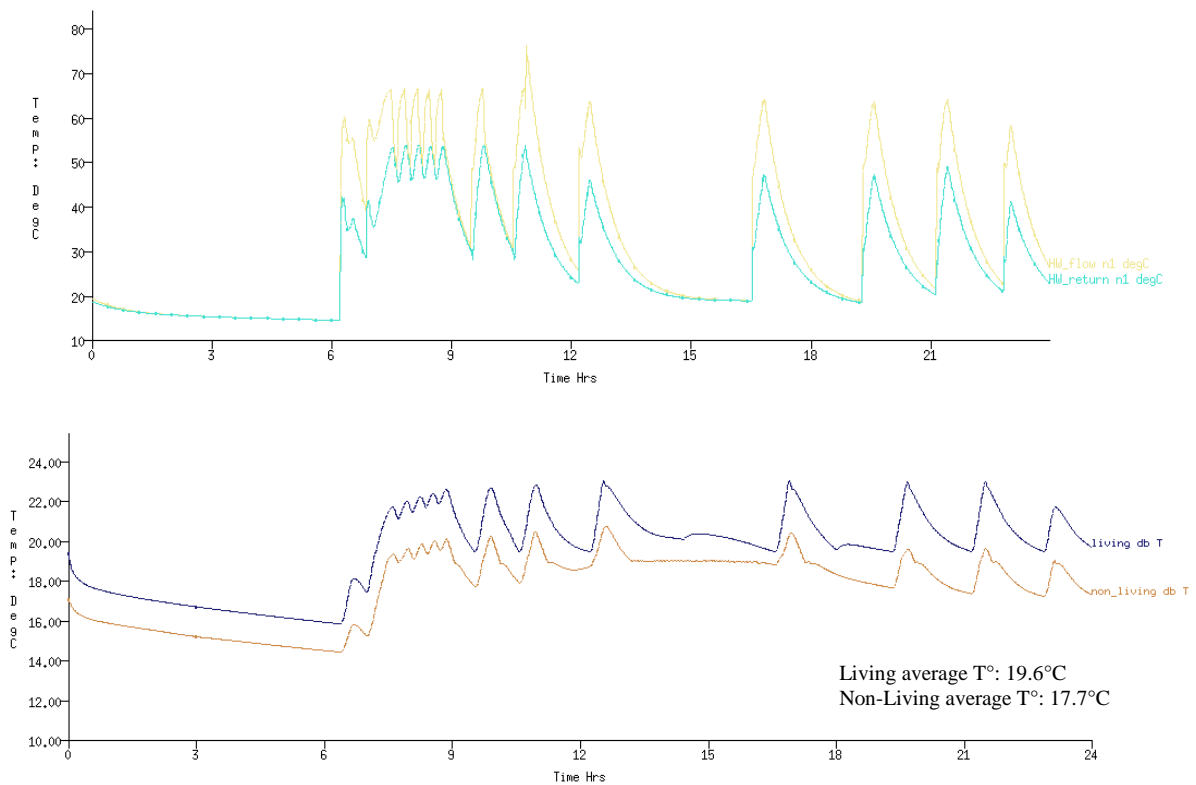


fig. 66 - Temperature at the inlet and outlet of the heat pump for the new heat pump model (without the consideration of the defrost cycles)

The graphs (fig. 65 and fig. 66) give the temperature profile at the inlet and outlet of the heat pump as well as the ambient temperature in the house for the Kelly Model and the new heat pump model.

It can be seen that for the CO₂ heat pump, the ΔT in the heat pump is much important and the system reach temperature of 60-65°C. With higher temperature, the system is more efficient to raise the temperature in the tank or in the zones. The average temperature for the 7th of January is however lower for the simulation with the CO₂ heat pump.

The return water temperature to the heat pump is relatively high at 40 - 48°C for Kelly model and still higher for the CO₂ model at 40 to 52°C.

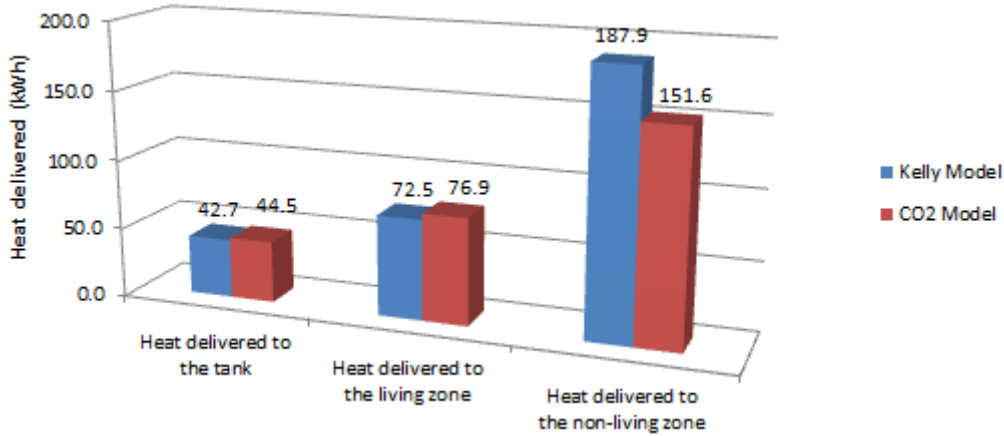


fig. 67 - Comparison of the heat delivered in Kelly model and the CO₂ model (without defrost cycle consideration)

In term of heat delivered (fig. 67), it can be noticed that a similar amount of heat is provided to the tank and the living zone for the CO₂ and the Kelly model. However the heat delivered to the non-living zone, for which there is no control, is almost 20% lower for the CO₂ model.

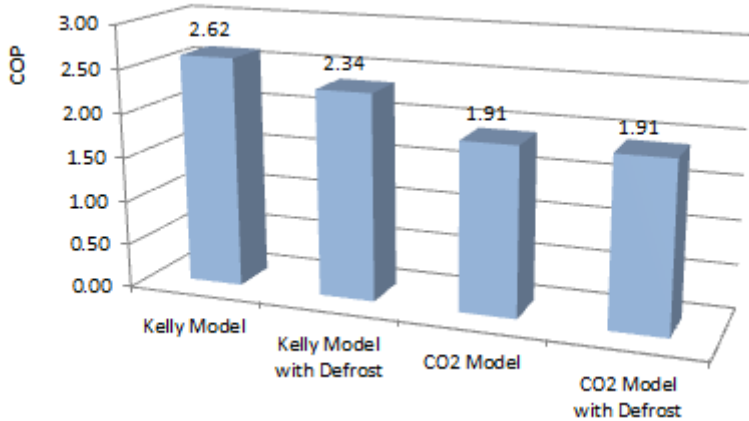


fig. 68 - Comparison of the COP for the simulation of the Kelly and CO₂ model including or not defrost

The COP of the installations for the simulations including or not the defrost cycles can be then compared (fig. 68). Over the week considered in the simulation, the Kelly heat pump present a COP 37% higher than the CO₂ heat pump model for the simulation without the defrost cycles. If the defrost of the evaporator is considered, the COP of the Kelly model drops of 11% while the COP of the CO₂ model stays exactly similar.

6.3 Discussions

As the model includes radiators and a fully mixed tank for the domestic hot water, the return temperature to the heat pump is relatively high. This phenomenon is still more important for the CO₂ heat pump which feed the radiators at higher temperature 60-65°C. The configuration is therefore quite unfavourable for the CO₂ heat pump whose performances drop significantly when the return temperature exceeds 40°C. The average COP for the system is therefore significantly lower at 1.91 while the model of the Kelly heat pump displays a COP of 2.62. A test was also made to replace the fully mixed tank by a stratified tank and the COP was then a bit increased to 1.96. The performance of the CO₂ model could be also increased by reducing the set point for the return temperature which was fixed at 53°C for this simulation.

The heat delivered to the living zone and the tank is similar in both models since the controls directly apply to them. However the heat delivered to the non-living area drops with the CO₂ heat pump model. The reason lies in the structure of the heating system. The hot water mass flow for space heating is indeed divided equally for the radiators in the living and non-living room. As the controls apply on the living zone only, the radiators of the non-living zone were dimensioned to provide enough heat to this area during the time that the living zone reach it set point. With the CO₂ heat pump model, as the temperature of the water going to the radiators is much higher, the living zone heats quickly and stops the heat pump operation while the second zone, much bigger has less time to heat. The controls of the system could be optimized to take also in consideration the temperature of the non-living area.

Concerning the defrost cycles, the performances of the Kelly model are significantly reduced when the defrost cycles are considered while the CO₂ model is not affected. This result comes from the way of modelling the defrost cycles. In the Kelly model, a defrost cycle is directly triggered when the outside air temperature go below 5°C and the next one is triggered after a fix period. In the CO₂ model, when the outside air temperature go below 5.5°C, it is first considered that the ice start forming on the evaporator. As in the simulations the system doesn't operate for long period, the ice on the evaporator is assumed to melt each time the system stops since the outside air temperatures are in general between 3 and 5°C.

7 INTEGRATED MODEL OF THE CO₂ HEAT PUMP

Sanyo developed a particular tank which enables to provide both domestic hot water and space heating in combination with a CO₂ heat pump. This system, designed to optimize the performances of the CO₂ heat pump, will be modelled in this part. The seasonal performances of the system will be the assessed.

7.1 Model of the Sanyo System

The Sanyo system is characterized by the combination of a CO₂ heat pump with a particular tank. It is therefore required to model this tank which is a key component of the system in order to simulate the operation of the full system.

7.1.1 Model of the Sanyo tank

A detailed schema of the Sanyo tank given by the manufacturer is presented in appendix D. The tank has a total water volume of 223 litres for a height of around 1 meter. A separate coil is used to heat the domestic hot water through the tank. The water for space heating is mainly taken in the middle of tank and if necessary at the top of the tank to feed the heating system at the required temperature. The following graph (fig. 69) shows the height of the different water inlet and outlet in the tank. Two partition plates are also used to improve the stratification and limit the mixing while 2 electric heaters guarantee the heat supply to the house. One electric heater is located in the middle of the tank and used only if a problem occurs to the heat pump. The second one is at the top of tank to adjust the temperature of the domestic hot water.

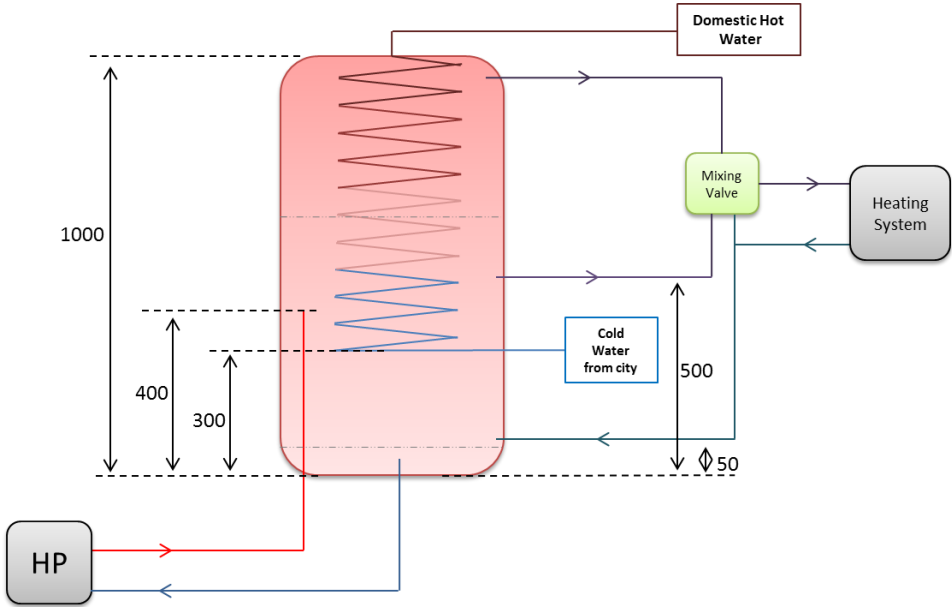


fig. 69 - Schema of the Sanyo tank configuration (length given in millimetres)

The temperature of the tank is controlled both in the middle and at the top. The temperature in the middle controls the heat pump operation. The set point is determined by the system in function of an internal algorithm also considering the outside temperature. The temperature at the top of the tank controls the heat pump operation and also, after a delay, the upper electric back-up if the heat pump cannot provide enough heat to follow the set point.

Different model of water storage tank are available in ESP-r. For CO₂ heat pumps, the return water temperature is relatively critical and must be minimized as much as possible to optimize the performances of the heat pump. It is then crucial to consider a stratified tank with a distribution of the water temperature along its height. In ESP-r, a model of a stratified tank has been recently included in the plant database. It is characterized by one fluid inlet and outlet with the possibility of adding 1 or 2 heat exchangers in the system. These models have been developed by Didier Thevenard and integrated in 2010 in ESP-r but they have not been so far used a lot and their validity is questionable. Looking at the source code, the model is a relatively simple one dimension model which divides the tank in up to 100 nodes and calculates successively the mass and thermal transfer in each layer. As underlined by Han et al [47], a one dimension stratified tank can give relatively accurate results, in particular if some empirical mixing coefficient are used. However since the 90s, many models developed are 2 or 3 dimensional to have a better representation of the tank behaviour. For this study, the model available is used with the default parameters.

Even with this model, it is not possible to model in detail the Sanyo tank, with the partitions plates and the back-up heater. These elements will be therefore neglected and a stratified tank with 2 heat exchangers will be considered. One heat exchanger will represent the coil which enables to heat the domestic hot water, and the other one will represent the heat taken from the tank to feed the heating system. The heat transfer through the second coil is taken at a very high value to represent a direct fluid connection as it is the case in the system. The inlet and outlet of each flow are fixed to match the tank configuration (fig. 69).

It can be noticed that the temperature of the water going to the radiators won't be controlled as precisely that in the real system since it is draw taken at only one height of the tank and without mixing valve. It is indeed still not possible with the current model to reach this degree of detail. The control of the tank will be made at both the top of the tank and the outlet for heating system but no temperature compensation will be considered.

7.1.2 Model realised in ESP-r

The house model is realised according to the specifications given by the owner in terms of insulations and dimensions (paragraph 4.3.1). The details concerning the building model are given in appendix C.

The plant used to model the Sanyo system integrated in the house in Oban is presented in fig. 70. The CO₂ heat pump model is used in combination with the stratified tank previously described. Most of the components for the pipes and the pumps are taken with their defaults parameters. The input file used in ESP-r for the plant is given in appendix E and give all the information on the plant. The following description will focus on the domestic hot water draw and the heating system.

A similar domestic hot water draw profile to the Kelly model is used but the main hot water draw is displaced from the morning to the afternoon in order to simulate at 6pm the bath that the occupant used to take every day (fig. 71). In addition, it was deduced from the summer monitoring that the domestic hot water consumption is estimated at 150 litres of hot water at 50°C per day. The profile is therefore equally increased by 23%. For the temperature of the water from the city, the monitored data highlighted some fluctuations during the year (7°C in March and 19°C in July). In the model, only a fixed value of 10°C will be considered. The water at the top of the tank is controlled to be between 50 and 53°C.

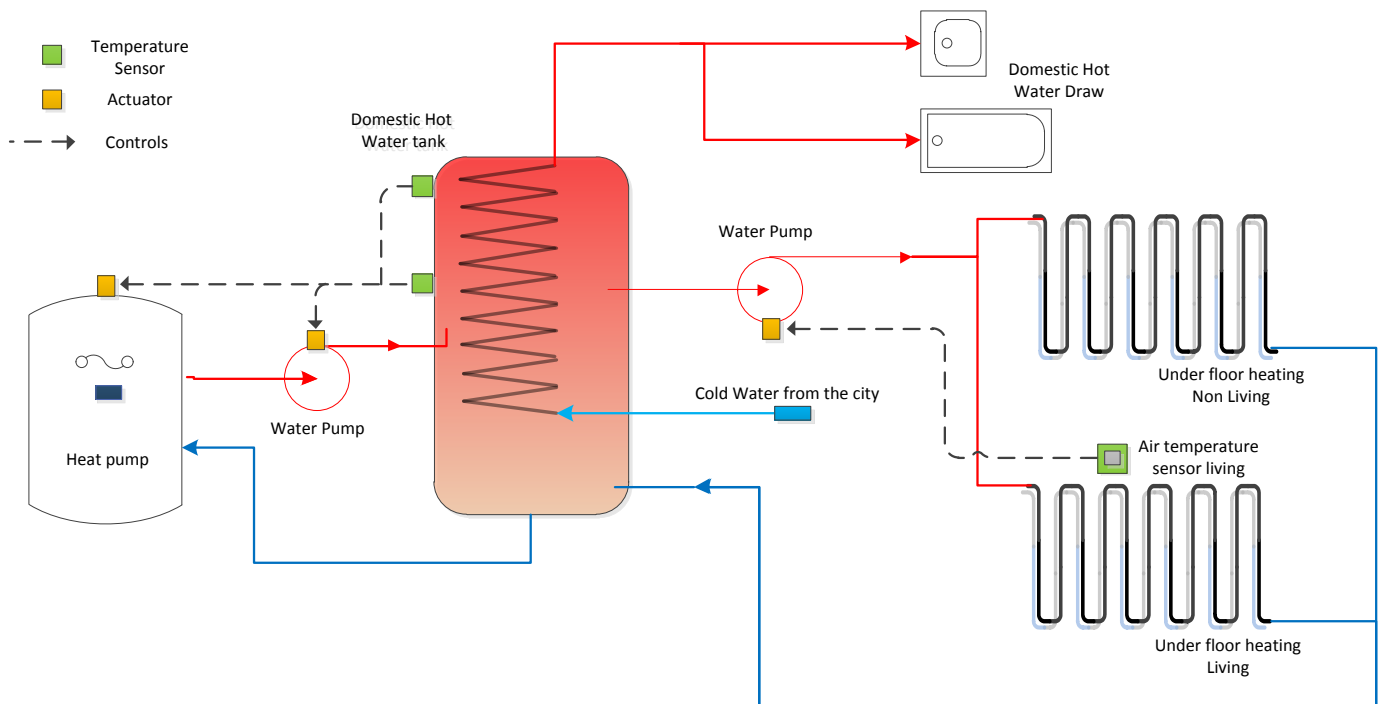


fig. 70 - Schema of the plant used in ESP-r to model the Sanyo system for the Oban case-study

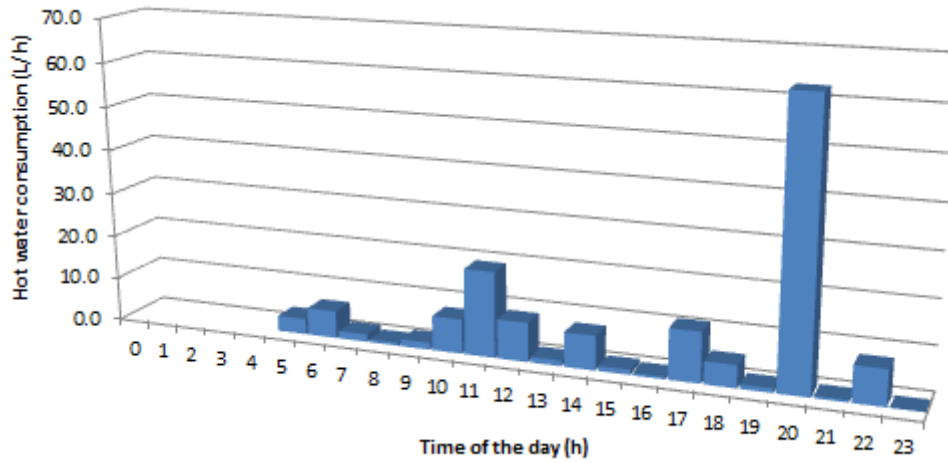


fig. 71 - Domestic hot water draw profile used in for the model of the Oban case study

For the space heating, the water flow is directed at 65% in the non-living area and 35% in the living area. The temperature is controlled in the living area and the heating system in the non-living area is dimensioned to reach a similar temperature. The whole house is indeed heated equally with an under-floor heating system. As there is no under-floor heating system model available in ESP-r, a radiator model is used with modified parameters including a higher thermal mass, a larger area and a lower heat transfer. The values chosen for these parameters are adapted to get a similar temperature profile in the house than the monitored data (paragraph 7.1.3).

	Area (m ²)	Total mass (kg)	Heat transfer coefficient (W/m ² K)	Mass weighted average specific heat (J/kgK)
Under-floor living area	15	1952	2.5	1942
Under-floor non-living area	46	5856	2.5	1942

table 13 - Parameters used for the model of the under floor heating system

In addition, the under-floor heating system induces extra losses in the ground as highlighted by Weitzmann et al. [48]. In particular, during the heating season with a U-value of the floor of 0.2W/Km², the losses to the ground are increased by 60% in comparison with no under-floor heating. To consider these extra losses, the U-value of the ground is increased by 60% (cf. appendix B for the detail of the dwelling model).

In terms of controls, the heat pump operation is commanded by the temperature both at the top of the tank and at the outlet for the under floor heating. The temperature in the living area is controlling the circulation pump operation for the heating system (fig. 70). A summary of the controls with the set points is presented on the table 14.

Sensor	Actuator	Type of control	Setpoints	Period operation
Tank top temperature	Heat Pump	ON-OFF control	50 – 53 °C	6am – 23pm
Temperature heating system outlet in the tank	Heat Pump	ON-OFF control	39 – 44 °C	6am – 23pm
Room Temperature	Pump	ON-OFF control	20 – 22 °C	7am – 23pm

table 14 - Summary of the controls used in the model of the Sanyo system

7.1.3 Comparison simulation and experimental data in March

The model is first simulated between the 14th and the 19th of March and is compared to the corresponding monitored data. The climate is taken on a period where the outside temperatures are similar. The same graph corresponding to the monitored data are drawn for the system and enable to assess the behaviour of the model.

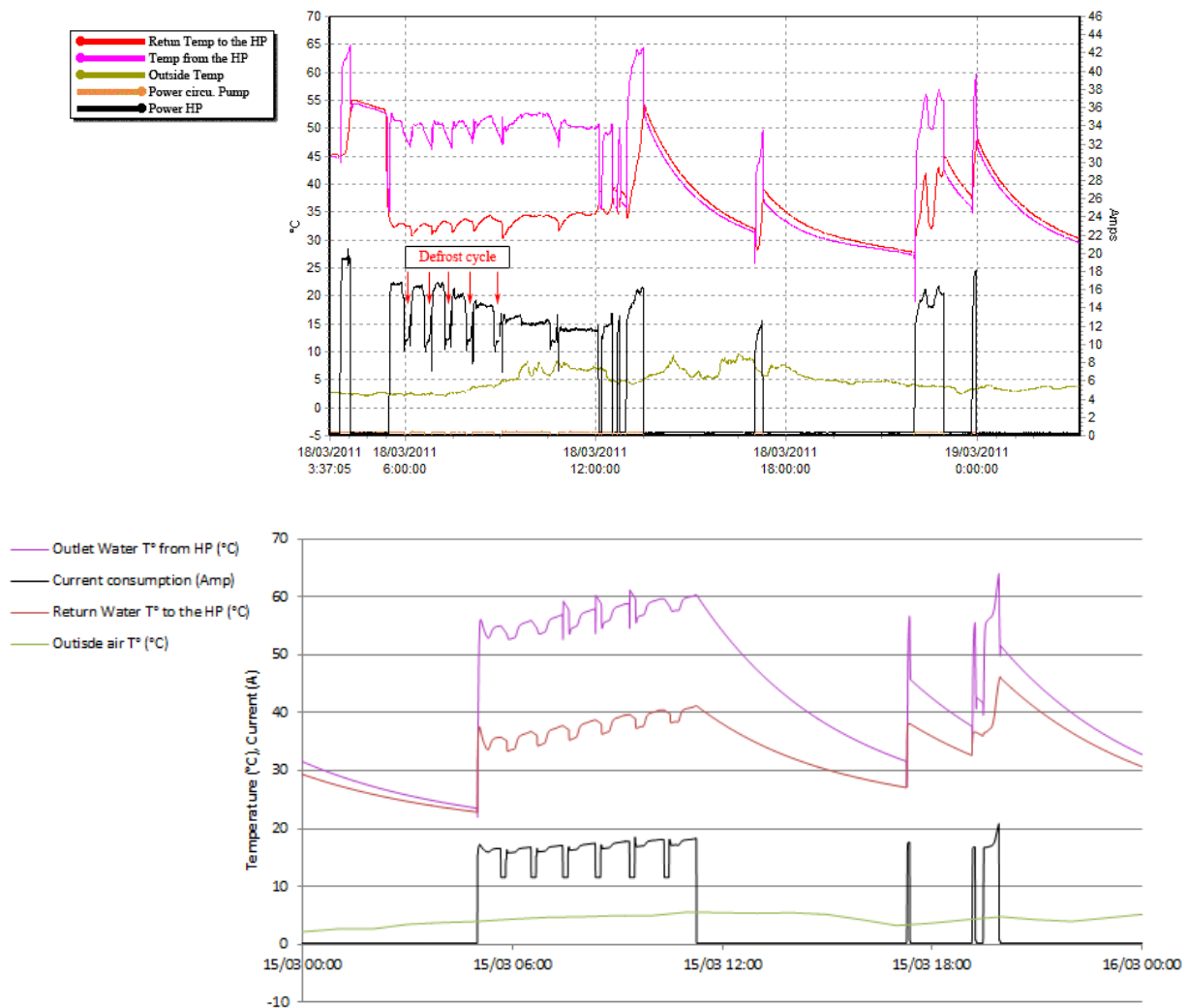


fig. 72 - Comparison of the monitoring data 18/03/2011 and the model concerning the heat pump parameters

The graphs (fig. 72) show that the behaviour of the model is very similar to the monitored data. The heat pump operates mainly in the morning from 5am and provides hot water to the tank at 50 - 55°C while the return temperature is between 30 and 40°C. In the afternoon, the heat pump operates sometimes for small periods to maintain the temperature in the tank with in general a more important operation in the evening for the bath. The bath is considered to be at 6pm but appears to be sometimes later in the monitored data.

It can be seen in fig. 73 that the outside air temperature and relative humidity are not exactly the same that in the model. However at relatively cold temperature in the morning and high relative humidity, quite a lot of defrost cycles occur similarly to the monitored data. Moreover, when the relative humidity decreases around 9am, the time of ice formation increases.

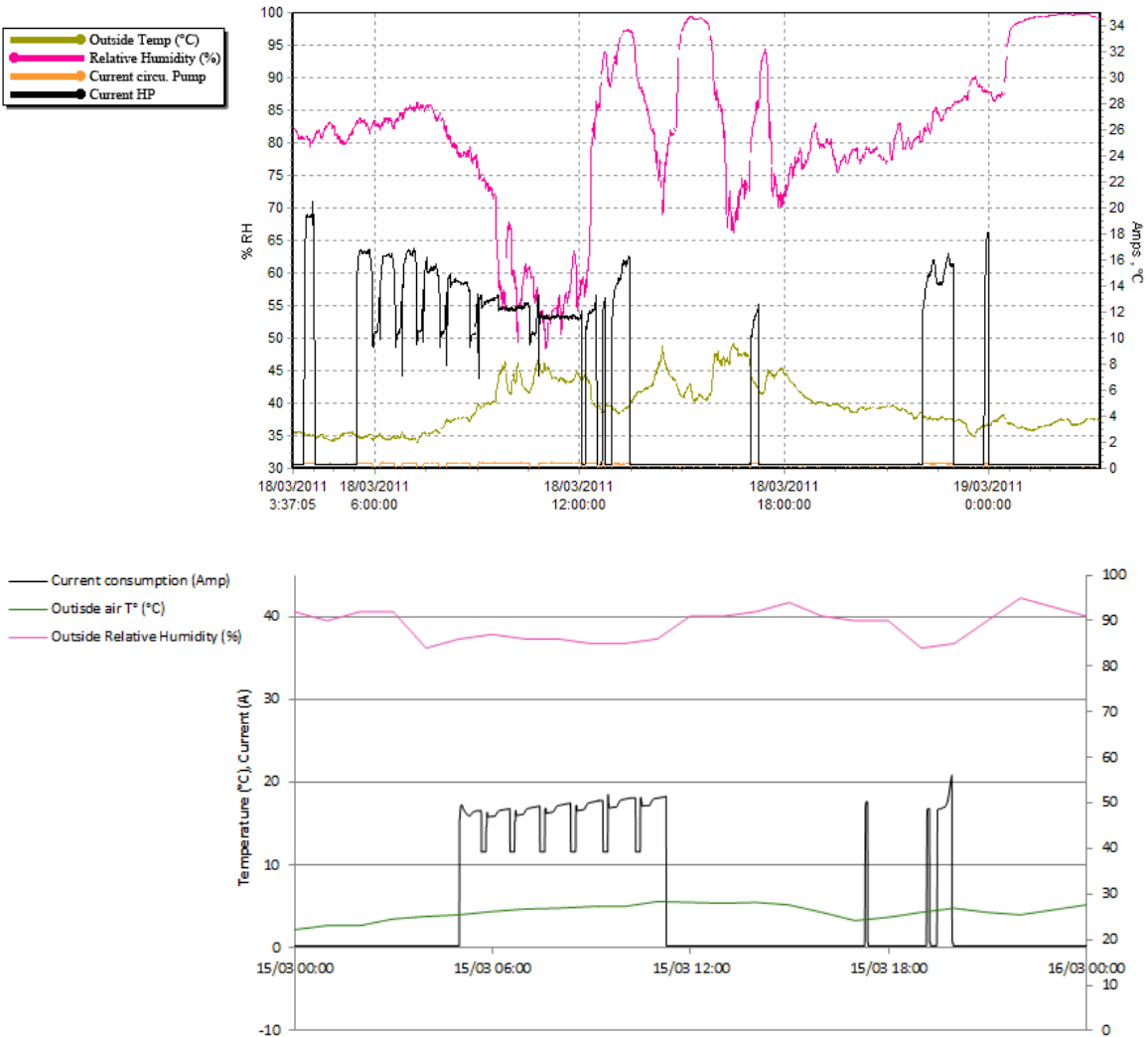


fig. 73 - Comparison of the monitoring data 18/03/2011 and the model concerning the heat pump parameters

Concerning the water feeding the heating system (fig. 74), its temperature is properly controlled in the real system by the mixing valve to reach 35 to 40°C. In the model, it can be seen that the temperature are quite similar even though it tends to increases when the tank get warmer.

Concerning the temperature in the house, it increases similarly in the whole house and stays high until 6pm before decreasing. In the monitored data, the increase in temperature is slightly slower but is quite similar to the model.

The day considered is without direct solar radiations which add a significant heat gain in the model because of all the glazing used in the house. On the monitored data, the impact of the solar radiations is less important since the sensor is located as for the heating system in a corridor at the back of the house.

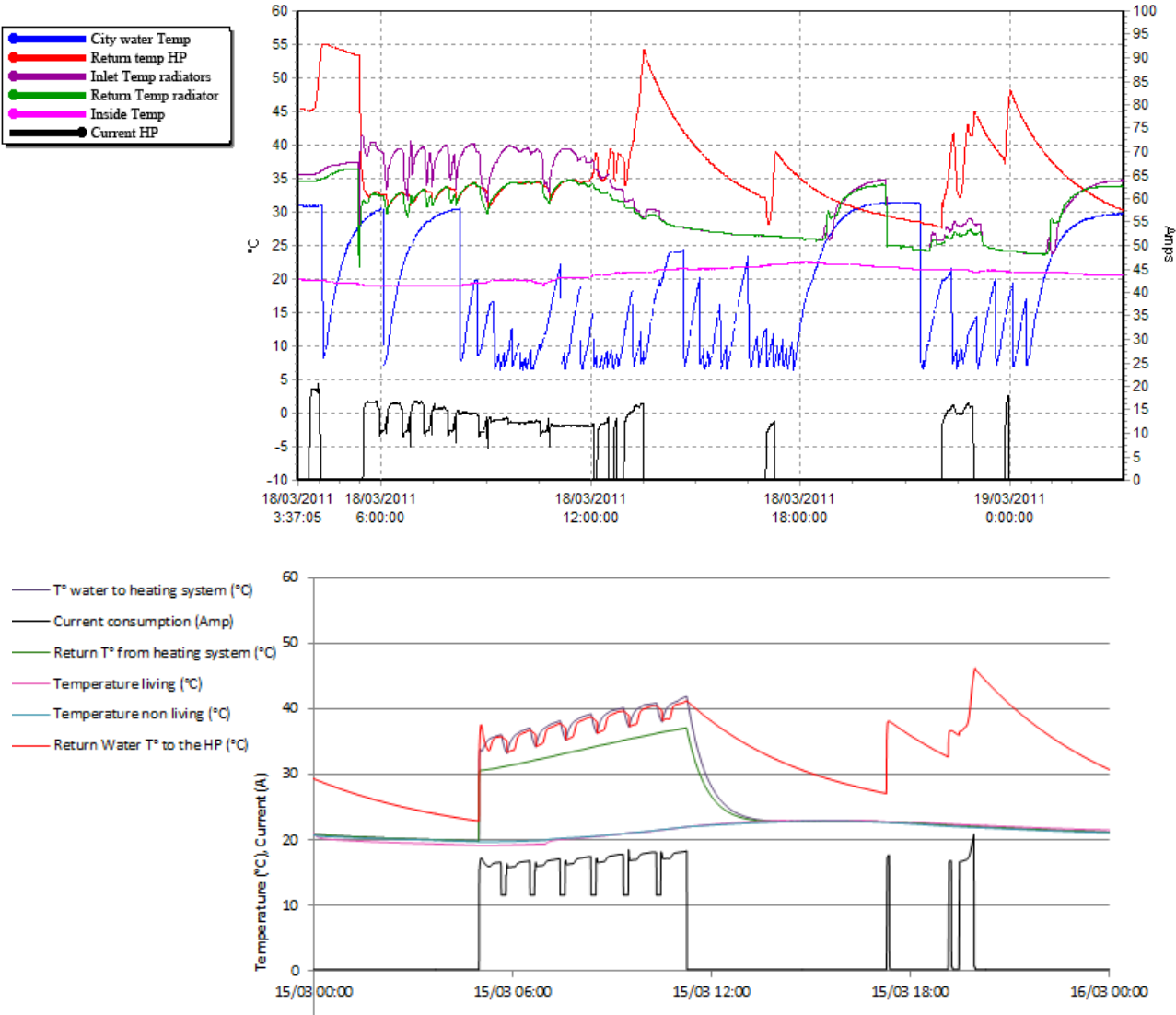


fig. 74 - Comparison of the monitoring data 18/03/2011 and the model concerning the heat pump parameters

It can also be seen on the fig. 74 that the heat flow to the under-floor heating system stops earlier even though the outside temperature is lower in the simulation. It could be explained by the house model which is quite rough (appendix B). A more detail model of the house should be realised to achieve better results. In addition the losses of the under-floor system are not properly modelled. An increase of the losses through the floor has been modelled but all the heat is assumed to be directly transferred to the room. The dynamic behaviour of the under-floor heating system must be therefore partially distorted.

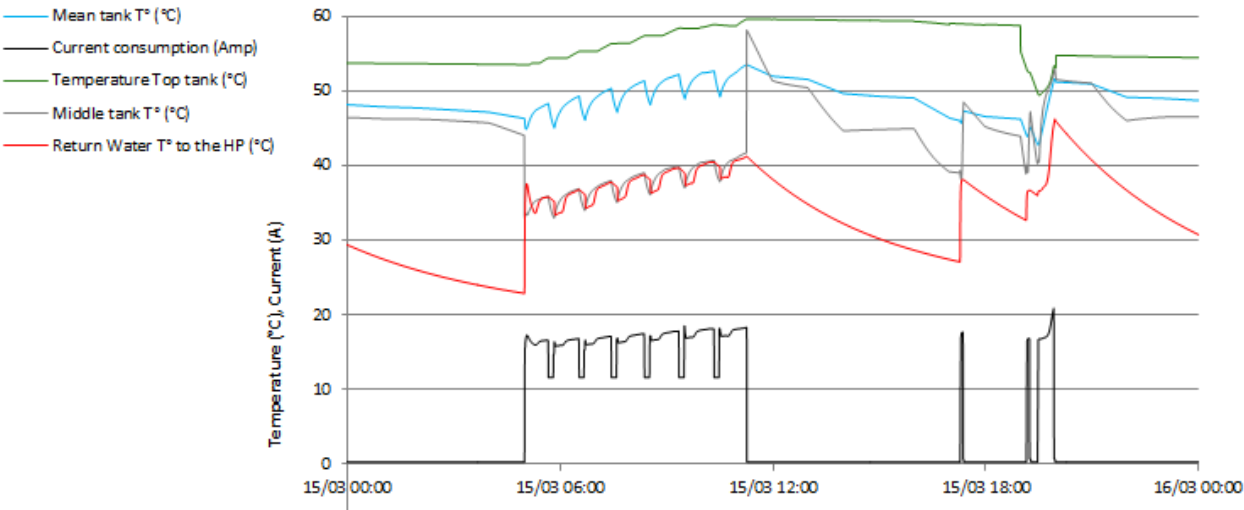


fig. 75 - Temperature distribution in the tank for the simulation

The fig. 75 shows the different temperatures in the tank. As long as the under-floor heating system operates, the temperature in the middle of the tank is raising only slightly. However, it can be noticed that the return temperature to the heat pump is very close to the water temperature going to the under floor system. The inlet water from the heat pump at 55°C tends to warm the bottom of the tank, especially because a mass flow is induced from the middle to the bottom of the tank when the heat pump operates. In addition the partitions plates are not represented in this model.

All these remarks highlight that the tank model is quite approximate and doesn't enable to model very properly the system. But the temperatures of the water flows are more or less similar with the monitored data collected.

Concerning the energy produced and consumed during this day (table 15), it can be seen that the figures for the model are globally a bit lower, probably due to the approximations in the house model. Nevertheless, the COP predicted by the model is very similar to the monitored data.

	Power Heat Pump (kWh)	Power standby Control (kWh)	Energy Defrost	Heat generated by heat pump (kWh)	COP (without back-up)
Monitored data 18/03/2011	30.3	1.52	3.29	63.7	2.10
Simulation	25.8	1.02	2.33	54.1	2.09

table 15 - Comparison of the energy used and produced for the simulation and the monitored data (one day of March)

7.1.1 Comparison simulation and experimental data in July

A simulation is also run in summer in order to check the behaviour of the model against the monitored data over this period. The comparison during one day of July with very similar outside air temperature is realised.

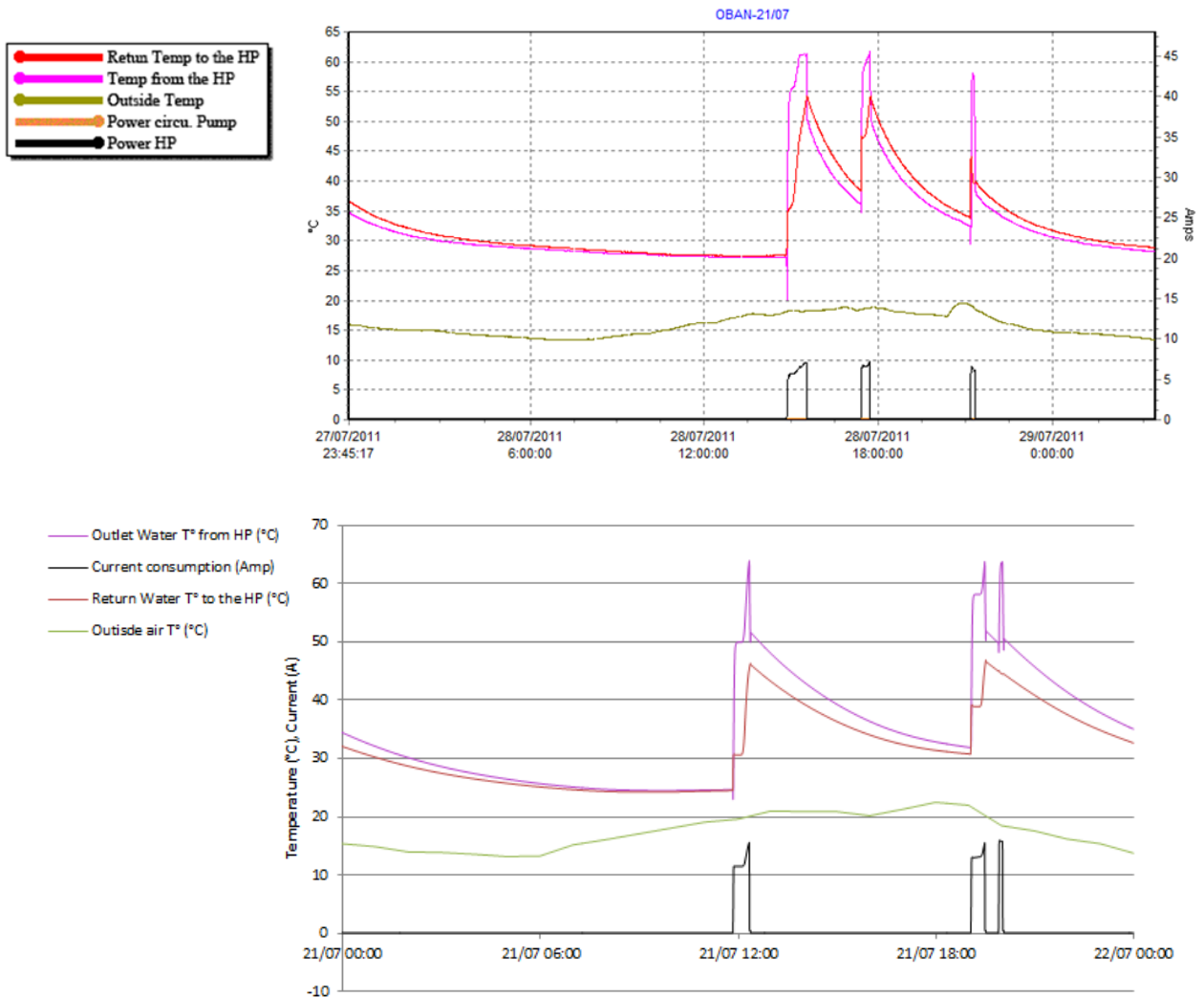


fig. 76 - Comparison of the monitoring data 18/03/2011 and the model concerning the heat pump parameters in July

During this period, the heat pump operates only a few times per day to provide the energy for the domestic hot water (fig. 76). The behaviour of the model is closed to the monitored data but in the model, the heat pump seem to work at a reduce capacity since the current draw by the heat pump is limited at 7A. This behaviour is represented in the model.

In term of energy consumed, more heat is provided in the simulation in comparison with the monitored data. It can be explained partially by a lower inlet water temperature from the city considered in the model (10°C) than it is in the monitored data for this period (19°C). In addition the day of monitoring considered is characterized by a low heat generation. Concerning the COP, it is also overestimated in the simulation. The reason could be still the colder inlet water temperature from the city which decreases the return water temperature to the heat pump.

	Power Heat Pump (kWh)	Power standby Control (kWh)	Power heat pump operation (kWh)	Heat generated (kWh)	COP
Monitored data 28/07/2011	2.21	0.77	1.54	4.01	1.8
Simulation	3.18	0.69	2.49	7.01	2.2

table 16 - Comparison of the energy used and produced for the simulation and the monitored data (one day of July)

Finally the model realized shows a quite similar behaviour than the monitored data. There is only in summer than the behaviour of the model is a bit different. A specific simulation will be therefore run to assess the impact of a higher temperature of the water coming from the city and lower domestic hot water consumption.

7.2 Estimation of the seasonal performance factor for the Sanyo System

The model previously defined and validated against the monitored data can be simulated for the whole year in order to predict the seasonal performance factor of the installation. The heat pump provides 11183kWh of heat to the house with a coefficient of performance of 2.15.

As mentioned previously, another simulation is run with a city water temperature increased to 15°C and a domestic hot water consumption reduced to 122 litres per day. With these parameters, the energy provided by the heat pump is 10299kWh with a coefficient of performance of 2.13.

The system performances are therefore not very impacted by the domestic hot water consumption and the temperature of water coming from the city with this configuration of the tank. Even though the overall amount of energy produced has been reduced of almost 8%, the COP has only decreased of

1%. It therefore increase the validity of the seasonal performances factor calculated which is not gonna be strongly affected by variations in the domestic hot water demand.

7.3 Design of a new optimized system

It is possible to do some modifications in order to optimize the performances of the CO₂ heat pump. Firstly, the energy used for the controls of the system in stand-by is particularly high and it seems reasonable to reduce them to 10W as considered in the Kelly model.

Moreover, the tank design could be improved as highlighted by the KTH report [33] and the previous group project [32]. Following the recommendations mentioned previously in the literature review, the inlet of cold water is displaced to the bottom of the tank while the outlet from the heat pump is moved to the top of the tank. In addition the tank size is increased to 500 litres with a height of 1.5 meters to enable a better stratification. The overall aim is to minimize the water temperature at the bottom of the tank.

Finally the annual simulation gives an energy production of 10997kWh for an SPF of 2.52. These modifications enable therefore to increase the seasonal performance factor of 18% while the global energy produced during the year stays very similar.

8 CONCLUSION

Heat pumps performances vary a lot according to their environment of performance and it is particularly true for CO₂ heat pumps which are very sensitive to the temperature of the water returning to the heat pump. In order to assess the performances of such systems including many varying parameters, dynamic simulations are well adapted and enable to reach high degrees of detail in the model.

With the analysis of different sources of data on a CO₂ heat pump, a dynamic model of a black box type has been developed to study the performances of the system in different environments of operation. It includes the calculation of the COP as a function of the outside temperature and the temperature of the water returning to the heat pump, and the consideration of the defrost cycles required for the system according to of the outside air temperature and relative humidity.

The comparison with the Kelly model shows that CO₂ heat pumps are really penalised when the temperature of the water returning to the heat pump is above 40°C. It justifies the fact that most of these heat pumps are used as water heaters in Japan. However, to also provide space heating with reasonably good performances, a special tank such as the one designed by Sanyo can be used.

Considering a particular Scottish installation as a case study, a complete model has been realised and validated according to monitored data of one week in March and in July. The results of the annual simulation give a seasonal performance factor of 2.15 which is in the average of the performances of air source heat pumps in the UK. However, it has been also highlighted that the current system is not perfect and that some improvements would be easily achievable. In particular, by reducing the power used for the control and optimising the tank design, the system could reach a seasonal performance factor of 2.52.

Probably because they are still quite a new technology, the CO₂ systems in operation today show some weaknesses. However in terms of environmental benefits, today they can clearly compete with conventional systems. In addition, it can be expected that a further development of the technology could bring CO₂ systems close to the performances of conventional ones which would totally justify their use.

This project also highlights the possibility offered by dynamic modelling in order to predict the performances of systems including heat pumps. The whole model achieved is quite complex but enables us to get a quite accurate representation of the system behaviour. The

level of details that these models can have, including the different elements of the plant system, the heat pump behaviour, the controls and the building make of it a powerful tool of analysis. Finally this study highlights the links between the CO₂ heat pump, the heating system and the house which have to be considered as a whole in order to achieve overall optimization of the performances.

9 FURTHER WORK

Certain elements of the model, especially in the plant, could be improved in order to achieve a higher precision in the simulations:

- ✓ There are quite a few questions about the tank model that is one of the critical elements of the installation. First it would be required to have a bit more information about the validity of the model used. And then the tank could be analysed more in detail to study how the performances could be maximized.
- ✓ The model of the under-floor heating should also be improved in order to integrate the losses to the ground. It would be useful if a proper model of an under-floor heating system was integrated in the plant library of ESP-r.

With the new heat pump model developed in ESP-r, dynamic simulations could be used to study the impact of different parameters on the seasonal performances of an installation:

- ✓ The impact of the ratio between space heating and domestic hot water could be analysed and compared with the results of Stene [21] concerning its tripartite gas cooler. This project highlighted with one simulation that a higher domestic hot water demand enables to achieve a better SPF.
- ✓ The impact of the type of heating system used could also be analysed. A new structure of the heating system could also be imagined by using the under-floor heating system or radiators for the different building zone in series more than in parallel. In general less heat is required in the non-living area which could be heated by the water from the heating system of the living area. It would enable to achieve another reduction of return temperature to the heat pump.
- ✓ The defrost cycles could also be studied more in detail. In particular, it has been shown by the previous project that long periods of operation tends to require a lot of defrost cycles. In opposition, a more staggered operation enables the system to defrost naturally when the system stops and the temperature is above 0°C which is often the case in the UK.

APPENDIX A - EXTRA MONITORED DATA

Monitored data from the Scottish Installations in Oban and Athelstaneford in March

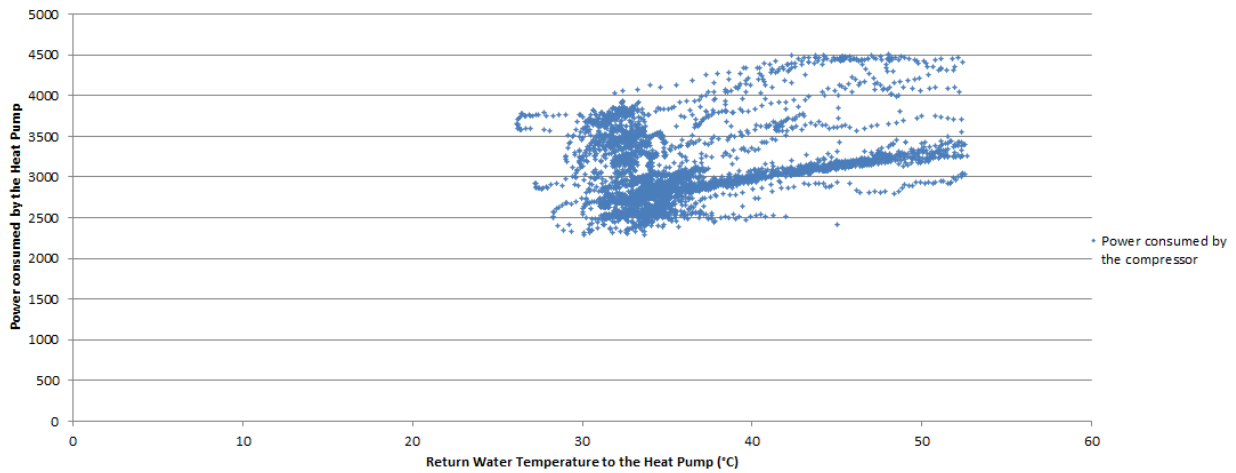


fig. 77 - Heat pump power consumption in function of the water return temperature to the heat pump for the installations monitored in Scotland

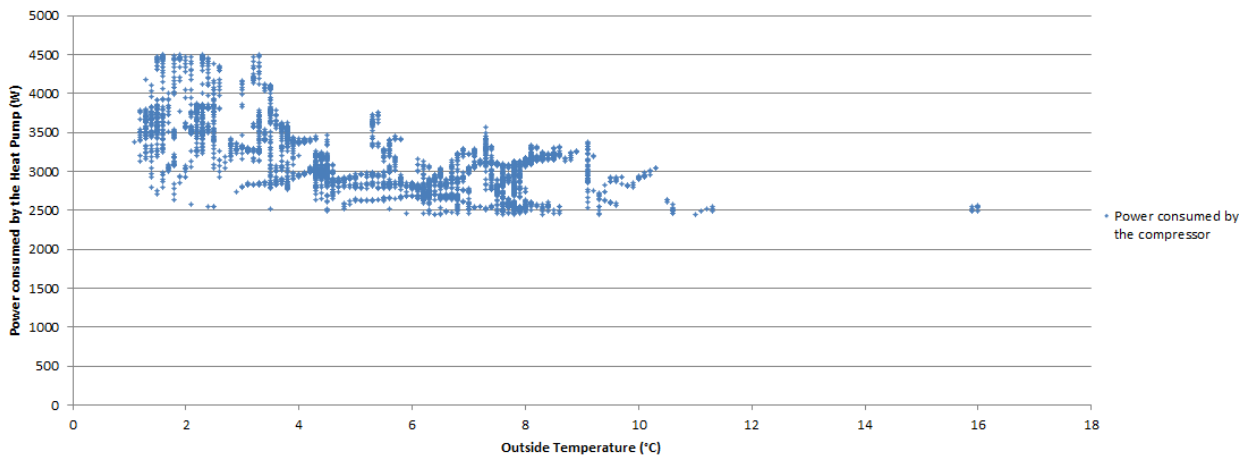


fig. 78 - Heat pump power consumption in function of the water return temperature to the heat pump for the installations monitored in Scotland

APPENDIX B - PLAN HOUSE IN OBAN

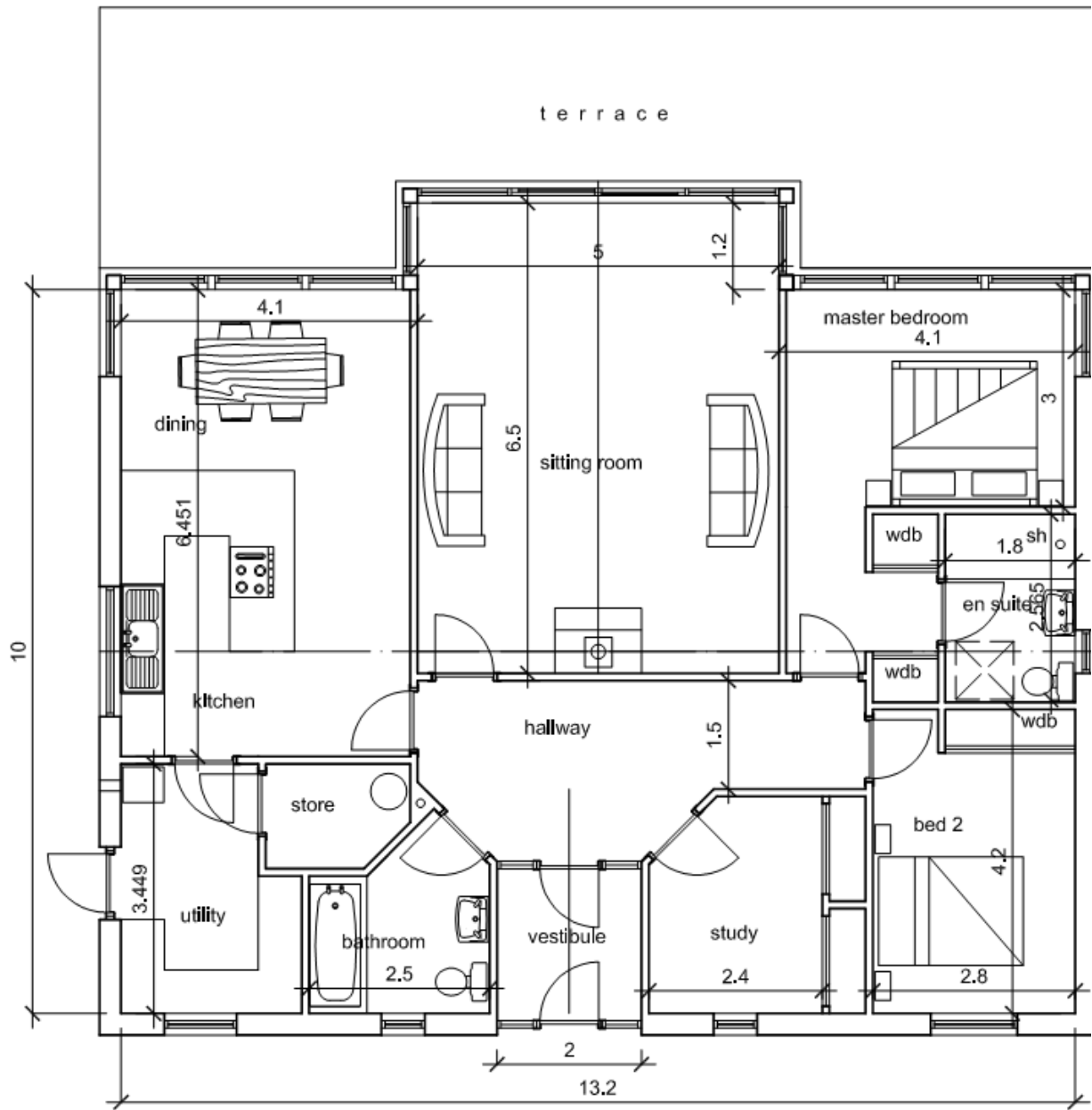


fig. 79 - Plan of the House in Oban

APPENDIX C - BUILDING MODEL

The houses considered in the models are 2 storeys detached houses with 3 zones: living, non-living and loft. The total surface area is 135m² with the living zone of 34m² and the non-living of 101m². Different house characteristics are used in this project: a model representing the average UK housing, a model representing a passive house and a modified model matching the characteristics of the case-study in Oban. The different parameters used for the models in terms of U-values, casual gains and infiltration rate are presented in this appendix.

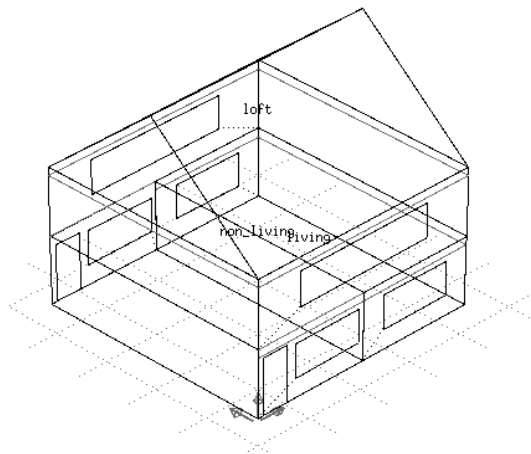


fig. 80 - Schema of the house used in Kelly's Model

Construction materials and U-values

The U-values used for the 3 different models are presented on the fig. 81. They correspond to standard values for the average UK housing and passive house. For the house in Oban, the characteristics of the insulation were given by the owner and are presented in the literature review (paragraph 4.3.1).

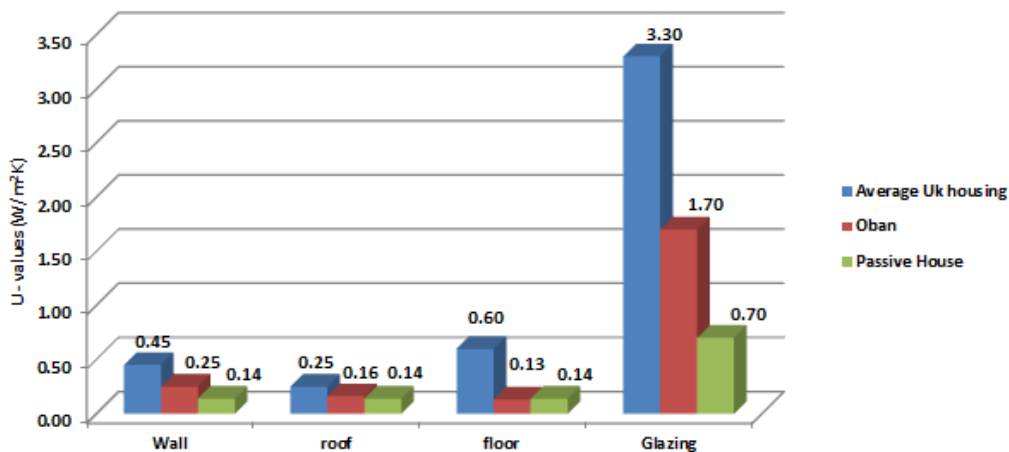


fig. 81 - Different values used in the Models

In Oban, the structure of the house is however significantly different from the Kelly model since there is only one storey. A proper model of the house is not realised but the U-values are adapted to match the case study.

Concerning the glazing, the house is characterized by large bay-windows on the front of the house and the table 17 gives the glazing area on each side of the house. Using the average UK housing as a base for this model, the area of glazing is adapted to this case study. In addition, the house facing a North-West direction is oriented of -55° from the North in ESP-r.

	West	North	South	East
Glazing Area (m ²)	20	4.26	5.8	3.6

table 17 - Distribution of the glazing area on the House in Oban

The total area of the houses is similar (135m²) but the surfaces of walls, floor and roof is different. In Oban, there is 138m² of floor and roof for only 68m² in the Kelly model. In opposition, there is 124.4 m² of wall in the Kelly model for 83.4m² in Oban (without glazing). A coefficient is therefore applied on the U-values to correct the differences of surface. The U-values for the roof and the floor are doubles and the U-values of the wall are reduced of 33%.

Moreover, the under-floor heating system induces extra losses in the ground as highlighted by Weitzmann et al. [48]. In particular, with a U-value of 0.2W/Km² for the floor during the heating season, the losses to the ground are increase of 60% in comparison with a different heating system. To consider these extra losses, the U-value of the ground is increased by 60%. The extra losses during the rest of the year shouldn't impact too much the results. The critical period concerning the losses is indeed in winter when the heating system is operating. Finally the U-values used for the model are presented in the table 18.

	Wall	Floor	Ceiling	Glazing
U-Values (W/m ² K)	0.17	0.42	0.32	1.7

table 18 - U-values finally used in the simulation to model the house in Oban

Casual gains

For the model of the average UK housing, the casual gains of Kelly’s model were used for the living and the non-living zones (fig. 82). They correspond to the heat gain of a family of 4 persons with 2 adults and 2 children considering a permanent presence in the house.

For the passive house, the same casual gains were defined in the models of Kelly. However the values used are relatively high since it corresponds to an average of 8 W/m². In the Passive House Planning Package (PHPP), it is specified that “internal heat sources of 2.1 W/m² are realistic for efficient household appliances rather than 5W/m², as frequently assumed” [49]. In the Kelly model, the casual gains seem to be therefore very high and they are scale down with a factor 0.35, to reach an average of 2.8 W/m² assuming relatively good household appliances.

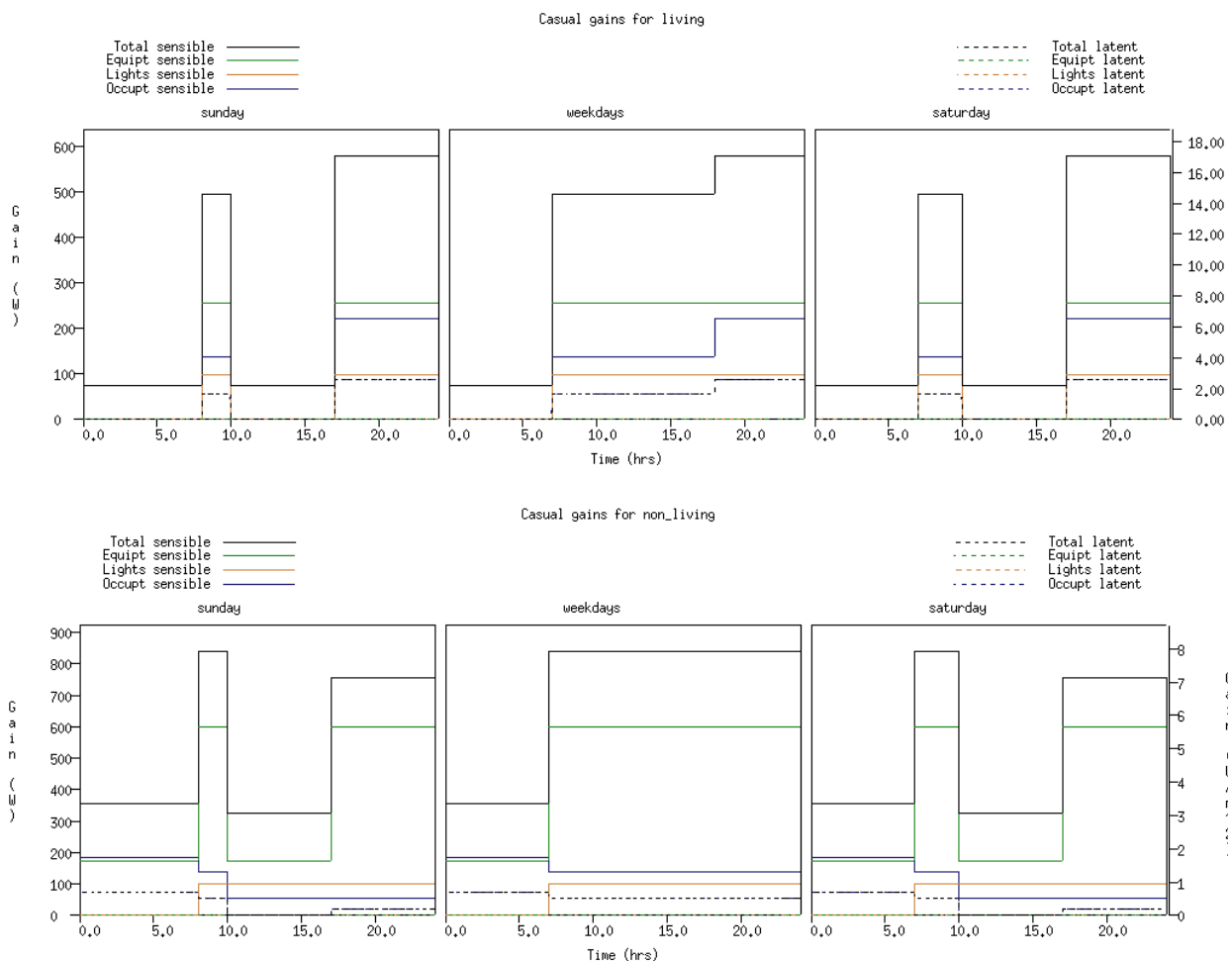


fig. 82 - Casual gains for the living (top) and non-living (bottom) zone for the Average UK housing model

For the house in Oban where 2 retiree people are living, the heat gain from the occupant is scaled down to 65% of the previous value (ratio of 2 adults over 2 adults plus 2 children). The lighting and appliances are assumed to be efficient and the corresponding casual gains are scale down by a factor 0.35, similarly to the passive house. Finally the total internal gains are around 3.6W/m².

Infiltration rate

In terms of infiltration rate, the value commonly used for the UK average house is 0.5 ac/h (air changes per hour) and for passive house, the standard is 0.07 ac/h. However, in order to simulate the windows opening when it is getting warmer inside the house, the infiltration rate is controlled in function of the temperature in the room. When the temperature reaches 23°C, an infiltration rate of 1.5 ac/h is considered and 10 ac/h when the temperature is above 25°C. For the house in Oban, the same infiltration rate than the average UK housing is considered, i.e. 0.5 ac/h.

Domestic hot water profile

The domestic hot water profile of Nick Kelly is used by default for the simulation. It corresponds to a hot water consumption of 122 litres of hot water per day with a ΔT of 35°C from the inlet water temperature to the outlet. It corresponds to the needs of hot water for a family with 2 Adults and 2 children.

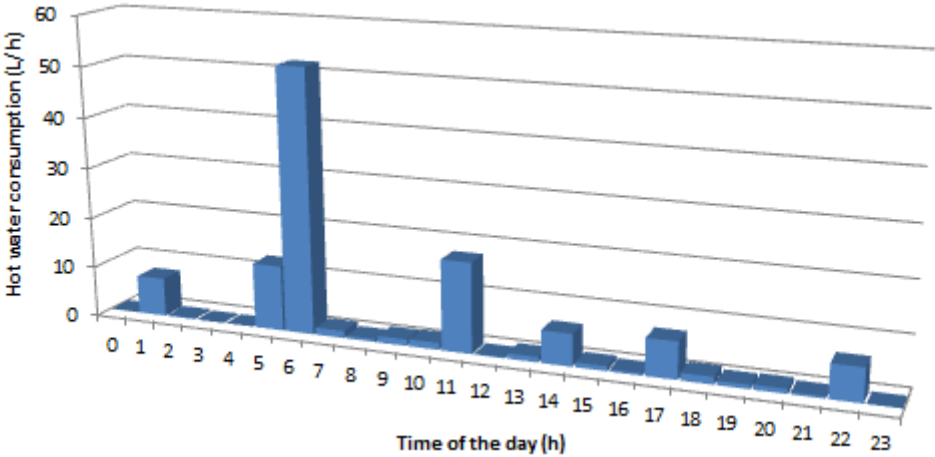


fig. 83 - Domestic hot water draw profile in the Kelly Model

In Oban the domestic hot water draw will be modified according to the monitored data (cf. paragraph 7.1.2).

APPENDIX D - SANYO TANK

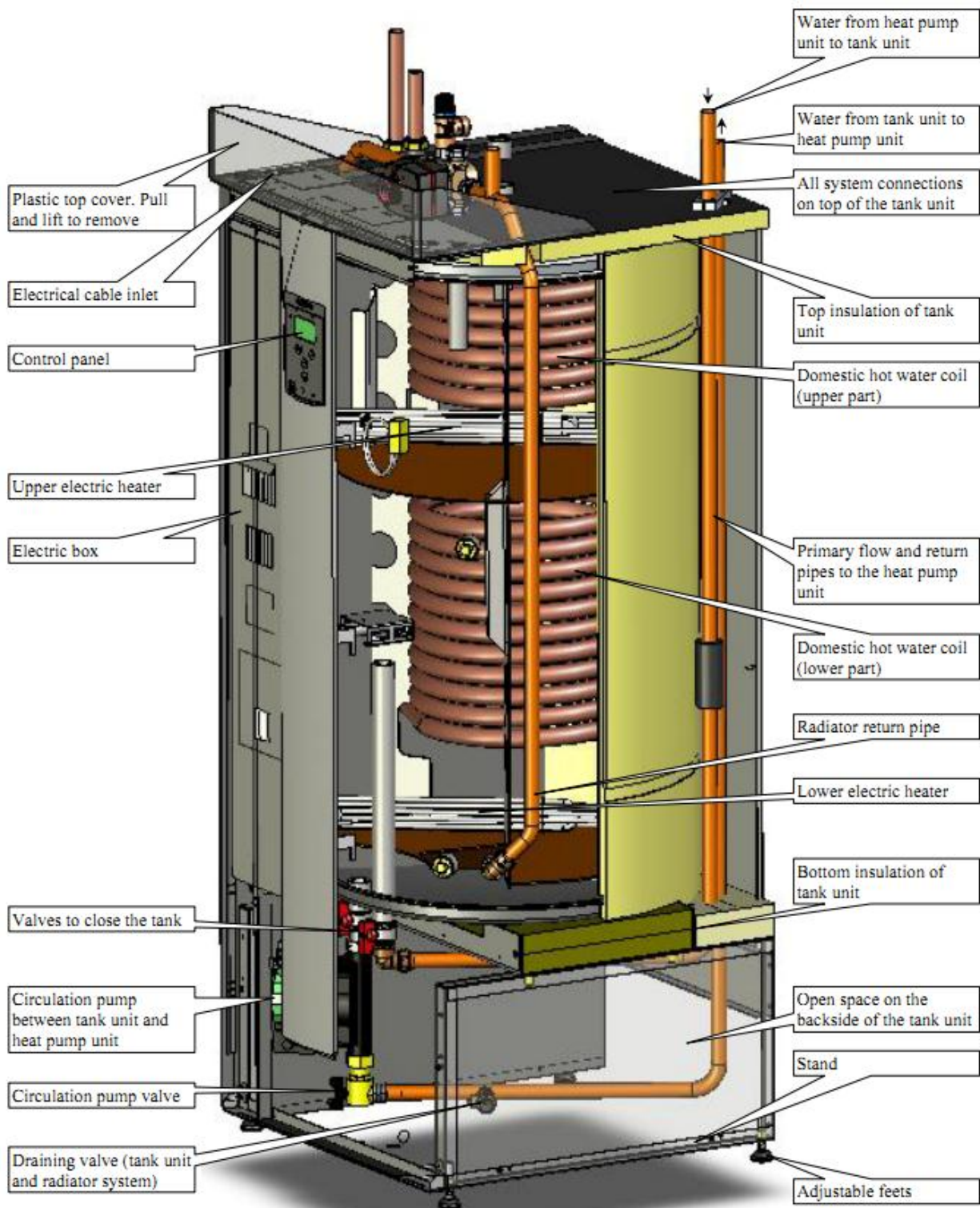


fig. 84 - Detail schema of the Sanyo tank given by the manufacturer

APPENDIX E - PLANT FILE MODEL SANYO SYSTEM

ESP-r plant file version 2 written on: Tue Aug 30 10:44:27 2011

Project title:

Total no. of specified components and simulation type

```

17      2
#-> 1, Air Source Heat Pump connecting to WCH system; 1 node model
ASHP      102
1          # Component has 1 control variable(s).
0.0000000
36      5
11.000    # 1 Component total mass (kg)
2000.0    # 2 Mass weighted average specific heat (J/kgK)
1.2000    # 3 Heat loss modulus (W/K)
5.0000    # 4 COP model [1 fixed;2 - Carnot efficiency; 3- quadratic; 3-
cubic]
3.6280    # 5 COP empirical coefficient a0 (-)
0.46900E-01 # 6 COP empirical coefficient a1 (-)
0.61100E-02 # 7 COP empirical coefficient a2 (-)
-0.34100E-01 # 8 COP empirical coefficient a3 (-)
3.0000    # 9 Compressor Model
2.6210    # 10 Compressor empirical coefficient a0 (-)
-0.28100   # 11 Compressor empirical coefficient a1 (-)
0.11400E-01 # 12 Compressor empirical coefficient a2 (-)
0.44300E-01 # 13 Compressor empirical coefficient a3 (-)
0.90000    # 14 Compressor pf (-)
90.000    # 15 Pump rating (W)
0.90000    # 16 Pump pf (-)
0.11110    # 17 Flowrate at rated pump power (l/s)
220.00    # 18 Fan power (W)
0.90000    # 19 Fan pf (-)
60.000    # 20 Controller power (W)
1.0000    # 21 Controller pf (-)
90.000    # 22 Tout max (degC)
60.000    # 23 Tin max (degC)
5.0000    # 24 Defrost cycle trigger ambient temp (degC)
3.0000    # 25 Defrost cycle time calc (0 - no defrost 1-user def 2-f(RH))
4500.0    # 26 Defrost cycle calc coefficient b0 or time (-)
0.16000    # 27 Defrost cycle calc coefficient b1 (-)
40.000    # 28 Defrost cycle lockout time (mins)
2.0000    # 29 Min defrost time (mins)
0.9000    # 30 Max defrost time (mins)
0.0000    # 31 Temp compensation on/off (0-off 1-on)
50.000    # 32 Nominal water return temperature (Deg C)
6.0000    # 33 Nominal water return deadband (Deg C)
3.0000    # 34 Temp compensation start temperature [Deg C]
17.000    # 35 Temp compensation end temperature (-)
-1.3000    # 36 Temp compensation gradient c1 (-)
# Component electrical details.
0.700 1 2.000 230.000 1

```

Rmq: The parameters for the heat pump don't have any meaning since the source has been modified and most of the parameters are implemented directly in the code.

```

#-> 2, WCH pipe; 1 node model
Buff_pump      13
0          # Component has 0 control variable(s).
6
2.0000    # 1 Component total mass (kg)
2250.0    # 2 Mass weighted average specific heat (J/kgK)
0.3000    # 3 UA modulus from wall to environment (W/K)

```

```

0.15000E-01 # 4 Hydraulic diameter of pipe (m)
5.0000 # 5 Length of pipe section (m)
0.17670E-03 # 6 Cross sectional face area (m^2)
#-> 3, WCH pipe; 1 node model
Buff_flow 13
0 # Component has 0 control variable(s).
6
2.0000 # 1 Component total mass (kg)
2250.0 # 2 Mass weighted average specific heat (J/kgK)
0.3000 # 3 UA modulus from wall to environment (W/K)
0.15000E-01 # 4 Hydraulic diameter of pipe (m)
5.0000 # 5 Length of pipe section (m)
0.17670E-03 # 6 Cross sectional face area (m^2)
#-> 4, WCH pipe; 1 node model
Buff_rtn 13
0 # Component has 0 control variable(s).
6
2.0000 # 1 Component total mass (kg)
2250.0 # 2 Mass weighted average specific heat (J/kgK)
0.3000 # 3 UA modulus from wall to environment (W/K)
0.15000E-01 # 4 Hydraulic diameter of pipe (m)
5.0000 # 5 Length of pipe section (m)
0.17670E-03 # 6 Cross sectional face area (m^2)
#-> 5, Stratified tank with 2 immersed HXs; 3 node model
Buff_S_tank 104
0 # Component has 0 control variable(s).
25
0.23000 # 1 Tank volume (m3)
1.0000 # 2 Tank height (m)
-1.0000 # 3 Tank perimeter (m; -1 if cylindrical)
0.55000 # 4 Height of flow inlet (m)
0.0000 # 5 Height of flow outlet (m)
0.10000 # 6 Tank heat loss coefficient (W/m2-K)
0.0000 # 7 Additional destratification conductivity (W/m-K)
100.00 # 8 Number of nodes
5.0000 # 9 Internal time steps per simulation time step
20.000 # 10 Initial temperature of tank (C)
100.00 # 11 Boiling temperature of fluid (C)
0.40000 # 12 Height of first immersed HX inlet (m)
1.0000 # 13 Height of first immersed HX outlet (m)
0.34000E-01 # 14 Inside diameter of first immersed HX coil (m)
0.38000E-01 # 15 Outside diameter of first immersed HX coil (m)
0.35100 # 16 Diameter of first immersed HX coil (m)
0.56000E-01 # 17 Pitch of first immersed HX coil (distance from one loop to
the n
30.000 # 18 Thermal conductivity of first immersed HX coil material
(W/m/K)
0.00000 # 19 eight of second immersed HX inlet (m)
0.50000 # 20 Height of second immersed HX outlet (m)
0.34000E-01 # 21 Inside diameter of second immersed HX coil (m)
0.38000E-01 # 22 Outside diameter of second immersed HX coil (m)
0.35100 # 23 Diameter of second immersed HX coil (m)
0.40000E-01 # 24 Pitch of second immersed HX coil (distance from one loop to
the
900.00 # 25 Thermal conductivity of second immersed HX coil material
(W/m/K)
#-> 6, variable speed domestic WCH pump; 1 node model
HW_pump 98
1 # Component has 1 control variable(s).
0.0000000
6
5.0000 # 1 Component total mass (kg)
2250.0 # 2 Mass weighted average specific heat (J/kgK)
0.20000 # 3 UA modulus from wall to environment (W/K)
45.000 # 4 Rated total absorbed power (W)
0.20000 # 5 Rated mass flow rate (m^3/s)
0.70000 # 6 Overall efficiency (-)
#-> 7, WCH pipe; 1 node model
HW_flow 13

```

```

0      # Component has 0 control variable(s).
6
2.0000 # 1 Component total mass (kg)
2250.0 # 2 Mass weighted average specific heat (J/kgK)
2.0000 # 3 UA modulus from wall to environment (W/K)
0.15000E-01 # 4 Hydraulic diameter of pipe (m)
5.0000 # 5 Length of pipe section (m)
0.17670E-03 # 6 Cross sectional face area (m^2)
#-> 8, WCH pipe; 1 node model
rad_A_suppl 13
0      # Component has 0 control variable(s).
6
2.0000 # 1 Component total mass (kg)
2250.0 # 2 Mass weighted average specific heat (J/kgK)
2.0000 # 3 UA modulus from wall to environment (W/K)
0.15000E-01 # 4 Hydraulic diameter of pipe (m)
5.0000 # 5 Length of pipe section (m)
0.17670E-03 # 6 Cross sectional face area (m^2)
#-> 9, WCH pipe; 1 node model
rad_B_suppl 13
0      # Component has 0 control variable(s).
6
2.0000 # 1 Component total mass (kg)
2250.0 # 2 Mass weighted average specific heat (J/kgK)
2.0000 # 3 UA modulus from wall to environment (W/K)
0.15000E-01 # 4 Hydraulic diameter of pipe (m)
5.0000 # 5 Length of pipe section (m)
0.17670E-03 # 6 Cross sectional face area (m^2)
#-> 10, simple domestic hot water radiator; 2 node model
RadiatorA 97
0      # Component has 0 control variable(s).
11
1952.0 # 1 Component total mass (kg)
1942.0 # 2 Mass weighted average specific heat (J/kgK)
15.000 # 3 Radiator surface area (m2)
2.5000 # 4 Radiator heat transfer coefficient (W)
20.000 # 5 Nominal environment temperature (C)
1.0000 # 6 Index of coupled building zone (-)
0.0000 # 7 Number of walls used for defining Te (-)
1.0000 # 8 Index of 1st wall for defining Te (-)
0.0000 # 9 Weighting factor 1st wall when defining Te (-)
0.0000 # 10 Index of 2nd wall for defining Te (-)
0.0000 # 11 Weighting factor 2nd wall when defining Te (-)
#-> 11, simple domestic hot water radiator; 2 node model
RadiatorB 97
0      # Component has 0 control variable(s).
11
5856.0 # 1 Component total mass (kg)
1942.0 # 2 Mass weighted average specific heat (J/kgK)
46.000 # 3 Radiator surface area (m2)
2.5000 # 4 Radiator heat transfer coefficient (W)
20.000 # 5 Nominal environment temperature (C)
2.0000 # 6 Index of coupled building zone (-)
0.0000 # 7 Number of walls used for defining Te (-)
1.000 # 8 Index of 1st wall for defining Te (-)
0.0000 # 9 Weighting factor 1st wall when defining Te (-)
0.0000 # 10 Index of 2nd wall for defining Te (-)
0.0000 # 11 Weighting factor 2nd wall when defining Te (-)
#-> 12, WCH pipe; 1 node model
rad_A_rtn 13
0      # Component has 0 control variable(s).
6
2.0000 # 1 Component total mass (kg)
2250.0 # 2 Mass weighted average specific heat (J/kgK)
2.0000 # 3 UA modulus from wall to environment (W/K)
0.15000E-01 # 4 Hydraulic diameter of pipe (m)
5.0000 # 5 Length of pipe section (m)
0.17670E-03 # 6 Cross sectional face area (m^2)
#-> 13, WCH pipe; 1 node model

```

```

rad_B_rtn          13
0 # Component has 0 control variable(s).
6
2.0000 # 1 Component total mass (kg)
2250.0 # 2 Mass weighted average specific heat (J/kgK)
2.0000 # 3 UA modulus from wall to environment (W/K)
0.15000E-01 # 4 Hydraulic diameter of pipe (m)
5.0000 # 5 Length of pipe section (m)
0.17670E-03 # 6 Cross sectional face area (m^2)
#-> 14, WCH pipe converging 2-leg junction; 1 node model
merge_B_A         14
0 # Component has 0 control variable(s).
3
0.10000 # 1 Component total mass (kg)
2250.0 # 2 Mass weighted average specific heat (J/kgK)
0.20000E-01 # 3 UA modulus from wall to environment (W/K)
#-> 15, WCH pipe; 1 node model
heating_rtn      13
0 # Component has 0 control variable(s).
6
2.0000 # 1 Component total mass (kg)
2250.0 # 2 Mass weighted average specific heat (J/kgK)
2.0000 # 3 UA modulus from wall to environment (W/K)
0.15000E-01 # 4 Hydraulic diameter of pipe (m)
5.0000 # 5 Length of pipe section (m)
0.17670E-03 # 6 Cross sectional face area (m^2)
#-> 16, 1-node water hourly draw profile
water_draw       88
0 # Component has 0 control variable(s).
24
0.0 # 1 Water draw for hour ending 1:00 a.m. (L/hr)
0.100 # 2 Water draw for hour ending 2:00 a.m. (L/hr)
0.000 # 3 Water draw for hour ending 3:00 a.m. (L/hr)
0.000 # 4 Water draw for hour ending 4:00 a.m. (L/hr)
2.924 # 5 Water draw for hour ending 5:00 a.m. (L/hr)
5.092 # 6 Water draw for hour ending 6:00 a.m. (L/hr)
1.404 # 7 Water draw for hour ending 7:00 a.m. (L/hr)
0.576 # 8 Water draw for hour ending 8:00 a.m. (L/hr)
1.296 # 9 Water draw for hour ending 9:00 a.m. (L/hr)
6.404 # 10 Water draw for hour ending 10:00 a.m. (L/hr)
15.784 # 11 Water draw for hour ending 11:00 a.m. (L/hr)
7.216 # 12 Water draw for hour ending 12:00 p.m. (L/hr)
1.044 # 13 Water draw for hour ending 1:00 p.m. (L/hr)
6.336 # 14 Water draw for hour ending 2:00 p.m. (L/hr)
0.936 # 15 Water draw for hour ending 3:00 p.m. (L/hr)
0.468 # 16 Water draw for hour ending 4:00 p.m. (L/hr)
9.272 # 17 Water draw for hour ending 5:00 p.m. (L/hr)
4.144 # 18 Water draw for hour ending 6:00 p.m. (L/hr)
0.828 # 19 Water draw for hour ending 7:00 p.m. (L/hr)
51.152 # 20 Water draw for hour ending 8:00 p.m. (L/hr)
0.468 # 21 Water draw for hour ending 9:00 p.m. (L/hr)
6.588 # 22 Water draw for hour ending 10:00 p.m. (L/hr)
0.108 # 23 Water draw for hour ending 11:00 p.m. (L/hr)
0.000 # 24 Water draw for hour ending 12:00 a.m. (L/hr)
#-> 17, WCH pipe; 1 node model
Pipe_ConstT      13
0 # Component has 0 control variable(s).
6
2.0000 # 1 Component total mass (kg)
2250.0 # 2 Mass weighted average specific heat (J/kgK)
2.0000 # 3 UA modulus from wall to environment (W/K)
0.15000E-01 # 4 Hydraulic diameter of pipe (m)
5.0000 # 5 Length of pipe section (m)
0.17670E-03 # 6 Cross sectional face area (m^2)
# The following is a list of component connections.
20 # Total number of connections
# receiving node conncn sending node diversion suppl1 suppl2
# component type component ratio
ASHP 1 3 Buff_rtn 1 1.000 # 1

```


Buff_pump	1	3	ASHP	1	1.000				# 2
Buff_flow	1	3	Buff_pump	1	1.000				# 3
Buff_S_tank	1	3	Buff_flow	1	1.000				# 4
Buff_rtn	1	3	Buff_S_tank	1	1.000				# 5
HW_pump	1	3	Buff_S_tank	3	1.000				# 6
Buff_S_tank	2	2	Pipe_ConstT	1	1.000	15.00	0.00		# 7
HW_flow	1	3	HW_pump	1	1.000				# 8
rad_A_suppl	1	3	HW_flow	1	0.350				# 9
rad_B_suppl	1	3	HW_flow	1	0.650				# 10
RadiatorA	1	3	rad_A_suppl	1	1.000				# 11
RadiatorB	1	3	rad_B_suppl	1	1.000				# 12
rad_A_rtn	1	3	RadiatorA	2	1.000				# 13
rad_B_rtn	1	3	RadiatorB	2	1.000				# 14
merge_B_A	1	3	rad_A_rtn	1	1.000				# 15
merge_B_A	1	3	rad_B_rtn	1	1.000				# 16
heating_rtn	1	3	merge_B_A	1	1.000				# 17
water_draw	1	3	Buff_S_tank	2	1.000				# 18
Buff_S_tank	3	3	heating_rtn	1	1.000				# 19
Pipe_ConstT	1	3	water_draw	1	1.000				# 20

The following is a list of containment temperatures.
14 # Total number of containments

# Component	cont	type	suppl1	suppl2	suppl3
ASHP	0		0.00000	0.00000	0.00000
Buff_S_tank	3		2.00000	0.00000	0.00000
Buff_pump	0		0.00000	0.00000	0.00000
Buff_flow	3		2.00000	0.00000	0.00000
Buff_rtn	3		2.00000	0.00000	0.00000
rad_A_suppl	3		1.00000	0.00000	0.00000
RadiatorA	3		1.00000	0.00000	0.00000
rad_A_rtn	3		1.00000	0.00000	0.00000
rad_B_suppl	3		2.00000	0.00000	0.00000
RadiatorB	3		2.00000	0.00000	0.00000
rad_B_rtn	3		2.00000	0.00000	0.00000
HW_pump	3		2.00000	0.00000	0.00000
HW_flow	3		2.00000	0.00000	0.00000
heating_rtn	3		2.00000	0.00000	0.00000

No mass flow network defined.
0

BIBLIOGRAPHY

- [1] Department of Energy & Climate Change. *Energy consumption in the United Kingdom*. 2011. Available: <http://www.decc.gov.uk/en/content/cms/statistics/publications/ecuk/ecuk.aspx> [Accessed 10/08/2010]
- [2] Office of Public Sector Information (OPSI): UK Statute Law Database. *Climate Change Act 2008*. 2008. Available: <http://www.legislation.gov.uk/ukpga/2008/27/contents> [Accessed 10/08/2011]
- [3] Department of Energy & Climate Change. *Climate Change Act 2008, Impact Assessment*. 2009. Available: http://www.decc.gov.uk/assets/decc/85_20090310164124_e_@@_climatechangeactia.pdf [Accessed 10/08/2011]
- [4] Renewable Heat Incentive Ltd. *Renewable Heat Incentive - The information site or the forthcoming guaranteed payment for renewable heat*. 2011. Available: <http://www.rhincensive.co.uk/> [Accessed 12.08.2011]
- [5] Energy Saving Trust. *Getting warmer: a field trial of heat pumps*. 2010. Available: http://www.energysavingtrust.org.uk/Media/node_1422/Getting-warmer-a-field-trial-of-heat-pumps-PDF [Accessed 09/09/2011]
- [6] Delta Energy & Environment. *Heat pumps in the UK: How Hot Can They Get*. 2011. Available: http://www.sepemo.eu/fileadmin/red/Publications/Delta_Heat_Pump_Trials_Whitepaper_January_2011.pdf [Accessed 09/09/2011]
- [7] Fujitsu General. *liveheatpump - Six Waterstage heat pumps continuously measured and compared to gas heating*. 2011. Available: <http://www.liveheatpump.com/t/en> [Accessed 2011]
- [8] European Heat Pump Association. *Welcome to EHPA*. Available: <http://www.ehpa.org/> [Accessed 09/09/2011]
- [9] Department of Energy & Climate Change (DECC) and Department for Environment Food and Rural Affairs (Defra). *Guidelines to Defra / DECC's GHG Conversion Factors for Company Reporting*. 2011. Available: <http://www.defra.gov.uk/environment/economy/business-efficiency/reporting/> [Accessed 01/08/2011]
- [10] Department of Energy & Climate Change. *Quarterly Energy Prices - Juin 2011*. 2011. Available: <http://www.decc.gov.uk/en/content/cms/statistics/publications/prices/prices.aspx> [Accessed 01/08/2011]
- [11] BRECSU. *Boiler Efficiency Database*. 2011. Available: <http://www.sedbuk.com/> [Accessed 02/08/2011]
- [12] European Committee for Standardization, *Heating systems in buildings - Method for calculation of system energy requirements and system efficiencies, in Part 4-2: Space heating generation systems, heat pump systems*. 2008: EN 15316-4-2.
- [13] European Committee for Standardization, *Air conditioners, liquid chilling packages and heat pumps with electrically driven compressors for space heating and cooling, in Part 2: Test conditions*. 2007: EN 14511-2.
- [14] European Committee for Standardization, *Air conditioners, liquid chilling packages and heat pumps with electrically driven compressors for space heating and cooling, in Part 3: Test methods*. 2007: EN 14511-3.

- [15] Kelly, N.J. and J. Cockroft, *Analysis of retrofit air source heat pump performance: Results from detailed simulations and comparison to field trial data*. Energy and Buildings, 2011. **43**(1): p. 239-245.
- [16] Calm, J.M. and G.C. Hourahan, *Refrigerant Data Summary*. Engineering Systems 18, 2001: p. pp. 74-88.
- [17] Madani, H., J. Claesson, and P. Lundqvist, *Capacity control in ground source heat pump systems: Part I: modeling and simulation*. International Journal of Refrigeration, 2011. **In Press, Corrected Proof**.
- [18] Levine, M., et al., *Residential and commercial buildings*, in *In Climate Change 2007: Mitigation*. 2007, Cambridge University Press, Cambridge, United Kingdom and New York, NY, USA: Contribution of Working Group III to the Fourth Assessment Report of the Intergovernmental Panel on Climate Change [B. Metz, O.R. Davidson, P.R. Bosch, R. Dave, L.A. Meyer (eds)].
- [19] Johnson, E.P., *Air-source heat pump carbon footprints: HFC impacts and comparison to other heat sources*. Energy Policy, 2011. **39**(3): p. 1369-1381.
- [20] Stene, J., *Integrated CO₂ Heat Pump Systems for Space Heating and Hot Water Heating in Low Energy Houses and Passive Houses*. International Energy Agency (IEA) Heat Pump Programme - Annex 32, 2007.
- [21] Stene, J., *Residential CO₂ Heat Pump System for Combined Space Heating and Hot Water Heating*, in *Department of Energy and Process Engineering*. 2004, NTNU, Norwegian University of Science and Technology
- [22] Lorentzen, G., *Revival of carbon dioxide as a refrigerant*. International Journal of Refrigeration, 1994. **17**(5): p. 292-301.
- [23] Neksa, P., *CO₂ heat pump systems*. International Journal of Refrigeration, 2002. **25**(4): p. 421-427.
- [24] IEA Heat Pump Center, *Energy Efficient Buildings: Heating and Cooling Technology Roadmap*. Newsletter, 2011. **Volume 29 - No. 2/2011**.
- [25] Sarkar, J., S. Bhattacharyya, and M.R. Gopal, *Optimization of a transcritical CO₂ heat pump cycle for simultaneous cooling and heating applications*. International Journal of Refrigeration, 2004. **27**(8): p. 830-838.
- [26] Fornazieri, E., et al., *Handbook - Natural refrigerant CO₂ - Master Module 1 THERMODYNAMIC TOPICS*. 2009.
- [27] Agrawal, N. and S. Bhattacharyya, *Studies on a two-stage transcritical carbon dioxide heat pump cycle with flash intercooling*. Applied Thermal Engineering, 2007. **27**(2-3): p. 299-305.
- [28] Sarkar, J., S. Bhattacharyya, and M. Ram Gopal, *Transcritical CO₂ heat pump systems: exergy analysis including heat transfer and fluid flow effects*. Energy Conversion and Management, 2005. **46**(13-14): p. 2053-2067.
- [29] Staffell, I. *A Review of Domestic Heat Pump Coefficient of Performance*. 2009. Available: http://wogone.com/iq/review_of_domestic_heat_pump_cop.pdf [Accessed 09/09/2011]
- [30] *Everything R744*. Available: <http://www.r744.com/> [Accessed 08/09/2011]
- [31] Sanyo. *CO₂ ECO Heating System*. 2011. Available: <http://uk.sanyo.com/en/aircon/Products/CO2-ECO-Heating-System/> [Accessed 21/08/2011]
- [32] Petinot, R., et al. *CO₂ Air Source Heat Pump*. 2011. Available: http://www.esru.strath.ac.uk/EandE/Web_sites/10-11/ASHP_CO2/index.html [Accessed 2011]
- [33] Chen, Y., et al., *Effsys2 - project report CO₂ heat pumps for the Swedish market Test and analysis of the SANYO ECOCUTE heat pump modified for Swedish conditions*.

- 2007, KTH, Energy Technology, lab of Division of Applied Thermodynamics and Refrigeration.
- [34] Hakari, T. *How good is a Sanyo Heat Pump*. 2009. Available: <http://www.elisanet.fi/sanyoco2log/> [Accessed 04/08/2011]
- [35] Hermes, C.J.L., et al., *A study of frost growth and densification on flat surfaces*. Experimental Thermal and Fluid Science, 2009. **33**(2): p. 371-379.
- [36] Seker, D., H. Karatas, and N. Egrican, *Frost formation on fin-and-tube heat exchangers. Part I--Modeling of frost formation on fin-and-tube heat exchangers*. International Journal of Refrigeration, 2004. **27**(4): p. 367-374.
- [37] da Silva, D.L., C.J.L. Hermes, and C. Melo, *First-principles modeling of frost accumulation on fan-supplied tube-fin evaporators*. Applied Thermal Engineering, 2011. **In Press, Corrected Proof**.
- [38] Cui, J., et al., *A new time- and space-dependent model for predicting frost formation*. Applied Thermal Engineering, 2011. **31**(4): p. 447-457.
- [39] Qu, K., S. Komori, and Y. Jiang, *Local variation of frost layer thickness and morphology*. International Journal of Thermal Sciences, 2006. **45**(2): p. 116-123.
- [40] Wu, X., et al., *Mesoscale investigation of frost formation on a cold surface*. Experimental Thermal and Fluid Science, 2007. **31**(8): p. 1043-1048.
- [41] Guo, X.-M., et al., *Experimental study on frost growth and dynamic performance of air source heat pump system*. Applied Thermal Engineering, 2008. **28**(17-18): p. 2267-2278.
- [42] Tassou, S.A. and C.J. Marquand, *Effects of evaporator frosting and defrosting on the performance of air-to-water heat pumps*. Applied Energy, 1987. **28**(1): p. 19-33.
- [43] Wang, W., et al., *Field test investigation of the characteristics for the air source heat pump under two typical mal-defrost phenomena*. Applied Energy, 2011. **In Press, Corrected Proof**.
- [44] Chen, Y.-g. and X.-m. Guo, *Dynamic defrosting characteristics of air source heat pump and effects of outdoor air parameters on defrost cycle performance*. Applied Thermal Engineering, 2009. **29**(13): p. 2701-2707.
- [45] Finnish Meteorological Institute. *Helsinki Testbed*. 2011. Available: <http://testbed.fmi.fi/> [Accessed 16/08/2011]
- [46] Liu, Z., H. Zhu, and H. Wang, *Study on Transient Distributed Model of Frost on Heat Pump Evaporator*. JAABE val.4 no.1, 2005.
- [47] Han, Y.M., R.Z. Wang, and Y.J. Dai, *Thermal stratification within the water tank*. Renewable and Sustainable Energy Reviews, 2009. **13**(5): p. 1014-1026.
- [48] Weitzmann, P., et al., *Modelling floor heating systems using a validated two-dimensional ground-coupled numerical model*. Building and Environment, 2005. **40**(2): p. 153-163.
- [49] International Passive House Association. *PHPP - the Passive House Planning Package*. Available: http://passipedia.passiv.de/passipedia_en/planning/calculating_energy_efficiency/php_p_-_the_passive_house_planning_package [Accessed 02/09/2011]